



**Universidade de Aveiro** Departamento de Ambiente e  
Ano 2010 Ordenamento

**Carlos Eduardo  
Salgueiro e Silva  
Monteiro**

**Mercúrio e Metilmercúrio em cores de  
sedimento do Estuário do Tejo**

**Mercury and Methylmercury in sediment  
cores from the Tagus Estuary**





**Universidade de Aveiro**  
**Ano 2010**

Departamento de Ambiente e  
Ordenamento

**Mercúrio e Metilmercúrio em cores de  
sedimento do Estuário do Tejo**

**Carlos Eduardo  
Salgueiro e Silva  
Monteiro**

**Mercury and Methylmercury in sediment cores  
from the Tagus Estuary**

Dissertação apresentada à Universidade de Aveiro para cumprimento dos requisitos necessários à obtenção do grau de Mestre em Ciências do Mar e das Zonas Costeiras, realizada sob a orientação científica da Doutora Mónica Susana Gonçalves de Almeida Válega, Estagiária de Pós-Doutoramento do Departamento de Química da Universidade de Aveiro e Doutor João Alfredo Vieira Canário, Investigador Auxiliar do Departamento de Ambiente Aquático e Biodiversidade do INRB - IPIMAR.



*À minha Família, pelo incansável apoio...*



## **o júri**

presidente

### **Doutora Filomena Maria Cardoso Pedrosa Ferreira Martins**

Professora associada do Departamento de Ambiente e Ordenamento da Universidade de Aveiro

### **Doutor Miguel Ângelo do Carmo Pardal**

Professor Associado do Departamento de Zoologia da Universidade de Coimbra

### **Doutora Mónica Susana Gonçalves de Almeida Válega**

Estagiária de Pós-Doutoramento do Departamento de Química da Universidade de Aveiro

### **Doutor João Alfredo Vieira Canário**

Investigador Auxiliar do Departamento de Ambiente Aquático e Biodiversidade do INRB - IPIMAR





## **agradecimentos**

Certamente que a muitos gostaria de prestar o meu reconhecido agradecimento. Embora nem o tempo nem o espaço o permitam, a todos aqueles que me impulsionaram, me acompanharam, me apoiaram, me ajudaram e me 'aturaram' nos momentos mais difíceis, o meu MUITO OBRIGADO!

Especialmente agradeço,

Aos meus orientadores, Doutora Mónica Válega e Doutor João Canário, pela paciência e orientação, sem eles nunca seria possível.

À Universidade de Aveiro por me ter recebido neste mestrado.

Ao INRB/IPIMAR, pela oportunidade de realização deste trabalho e pelo excelente acolhimento que prestou.

Ao projecto PROFLUX – Processos e fluxos de mercúrio e metilmercúrio num ecossistema contaminado (Estuário do Tejo, Portugal) (Refª PTDC/MAR/102748/2008) pelo financiamento necessário, e a toda a equipa do projecto que me acolheu e apoiou.

Ao Doutor Nelson O'Driscoll pelas análises do metilmercúrio, à Doutora Marta Nogueira pela análise do carbono orgânico e ao Doutor Miguel Caetano e Drª. Rute Cesário pela preciosa colaboração nas saídas de campo. O meu muito obrigado a todos!

Ao Pentágono de Oceanografia que aqui encerra mais um ciclo.

À Prof. Doutora Eduarda Pereira, por todo o apoio e 'tempo' que me disponibilizou. Muito Obrigado!

Aos meus amigos e toda a minha família... Distantes mas tão próximos!



**palavras-chave**

Mercúrio, metilmercúrio, sedimentos, águas intersticiais, Estuário do Tejo.

**resumo**

O mercúrio é actualmente considerado um dos metais mais nocivos para o ambiente. O presente trabalho incide sobre os factores que actuam sobre o mercúrio, influenciando a sua distribuição em ambientes estuarinos. Dado o histórico de contaminação no Estuário do Tejo, foram recolhidos cores de sedimentos e separadas as águas intersticiais em dois locais distintos: um fortemente contaminado, Cala do Norte, e outro não contaminado, Ponta da Erva. Os cores foram seccionados em camadas, tendo-se posteriormente analisado os teores de mercúrio total ( $Hg_T$ ) e metilmercúrio (MeHg) na fracção sólida dos sedimentos e  $Hg_T$  e  $Hg_R$ , bem como MeHg dissolvidos nas águas intersticiais. As concentrações de  $Hg_T$  e MeHg foram relacionadas com outros parâmetros obtidos na fracção sólida e nas águas intersticiais, nomeadamente pH, Eh,  $O_2$  dissolvido, humidade, e as concentrações de LOI, Al, Si, Fe, Mn,  $C_{org}$ , DOC,  $Cl^-$ ,  $SO_4^{2-}$  e  $HS^-$ .

Na Cala do Norte, a concentração de mercúrio total nos sedimentos variou entre 1 e 18  $\mu g/g$  enquanto na Ponta da Erva foram determinados valores mais baixos, entre 0.4 e 0.5  $\mu g/g$ . Em relação às concentrações de metilmercúrio, os valores variaram entre os não detectáveis ( $< 0.1$  ng/g) e 87 ng/g na Cala do Norte e 0.54 ng/g na Ponta da Erva. Nos dois locais, apesar da diferença de concentrações, o  $Hg_T$  e MeHg mostraram-se encontrar-se em equilíbrio entre a fracção sólida e águas intersticiais. Os fluxos difusivos foram calculados na interface sedimento/água de modo a estimar a mobilidade das espécies de Hg e avaliar se existem trocas entre o sedimento e a coluna de água, considerando a toxicidade do MeHg. O fluxo estimado na Cala do Norte foi de 0.30  $ng/m^2d$  para o MeHg e 0.50  $ng/m^2d$  para  $Hg_R$ . Na Ponta da Erva, o fluxo de MeHg foi inferior ao calculado para a Cala do Norte, 0.19  $ng/m^2d$ , enquanto para o  $Hg_R$  foi maior, 1.13  $ng/m^2d$ . Estes fluxos evidenciam o transporte difusivo de Hg das águas intersticiais para a coluna de água em ambos os locais, reflectindo a importância das características do sedimento que potenciam os processos de metilação do Hg.



**keywords**

Mercury, methylmercury, sediments, porewaters, Tagus Estuary.

**abstract**

Mercury is currently considered one of the most harmful metals to the environment. This study focuses on factors that influence mercury distribution and its bioavailability in estuarine environments. Given the history of contamination in the Tagus estuary, sediment cores were collected and pore waters were separated from two sites: one heavily contaminated, Cala do Norte, and a non-contaminated, Ponta da Erva. In the laboratory, the levels of total mercury (Hg) and methylmercury (MeHg) in solid sediments and dissolved Hg ( $Hg_R$  and  $Hg_T$ ) and MeHg in the pore waters were analyzed. Obtained Hg data were then compared to other parameters, namely the pH, Eh, dissolved  $O_2$ , water content, as well the concentrations of LOI, Al, Si, Fe, Mn,  $C_{org}$ , DOC,  $Cl^-$ ,  $SO_4^{2-}$  and  $HS^-$ .

In Cala do Norte, total mercury concentrations in sediments ranged between 1 and 18  $\mu g/g$  while in Ponta da Erva, lower values were determined, ranging between 0.4 and 0.5  $\mu g/g$ . Concentrations of methylmercury ranged between detection limit ( $< 0.1$  ng/g) up to 87 ng/g in Cala do Norte and up to 0.54 ng/g in Ponta da Erva. In both places, despite the differences in concentrations,  $Hg_T$  and MeHg were in equilibrium between the pore waters and the solid fractions. The diffusive fluxes were calculated across the sediment/water interface in order to estimate the mobility of Hg species and assess whether there are exchanges between the sediment and water column, considering the MeHg toxicity. The estimated flux in Cala do Norte was 0.30 ng/m<sup>2</sup>d for MeHg and 0.50 ng/m<sup>2</sup>d for  $Hg_R$ . Conversely, in Ponta da Erva MeHg flux was lower than in Cala do Norte, 0.19 ng/m<sup>2</sup>d, while for  $Hg_R$  was higher, 1.13 ng/m<sup>2</sup>d. These fluxes evidence the diffusive transport of Hg from the pore waters to the overlying water in both sites reflecting the importance of sediment characteristics that enhance the Hg methylation processes.



# Contents

|   |           |
|---|-----------|
| Index of Figures .....                                      | iii       |
| Index of Tables .....                                       | vi        |
| <b>1. INTRODUCTION .....</b>                                | <b>1</b>  |
| 1.1. Physico-chemical properties of Mercury .....           | 3         |
| 1.2. The biogeochemical cycle of mercury.....               | 4         |
| 1.3. Mercury in the aquatic environment.....                | 7         |
| 1.3.1. Mercury in natural waters.....                       | 8         |
| 1.3.2. Mercury in sediments.....                            | 9         |
| 1.4. Mercury methylation .....                              | 13        |
| 1.5. Study area .....                                       | 17        |
| 1.5.1. Cala do Norte.....                                   | 18        |
| 1.5.2. Ponta da Erva .....                                  | 19        |
| 1.6. Objectives.....  | 20        |
| <b>2. MATERIAL and METHODS.....</b>                         | <b>21</b> |
| 2.1. Decontamination procedures .....                       | 23        |
| 2.2. Field work.....  | 23        |
| 2.3. Sample processing.....                                 | 25        |
| 2.4. Analytical methods.....                                | 25        |
| 2.4.1. Solid fraction .....                                 | 25        |
| 2.4.1.1. Water content .....                                | 25        |
| 2.4.1.2. Lost On Ignition (LOI).....                        | 25        |
| 2.4.1.3. Total mercury and methylmercury in sediments.....  | 26        |
| 2.4.1.4. Total iron, manganese, aluminum and silicium ..... | 27        |
| 2.4.1.5. Organic carbon .....                               | 27        |
| 2.4.2. Pore waters .....                                    | 28        |
| 2.4.2.1. Reactive dissolved mercury.....                    | 28        |
| 2.4.2.2. Total dissolved mercury and methylmercury.....     | 28        |

|           |  |           |
|-----------|--|-----------|
| 2.4.2.3.  | Total dissolved iron and manganese .....   | 29        |
| 2.4.2.4.  | Dissolved chloride .....   | 29        |
| 2.4.2.5.  | Dissolved sulphate.....  | 30        |
| 2.4.2.6.  | Dissolved inorganic sulfides .....   | 30        |
| 2.4.2.7.  | Dissolved organic carbon.....  | 30        |
| 2.5.      | Quality control.....   | 31        |
| <b>3.</b> | <b>RESULTS .....</b>   | <b>33</b> |
| 3.1.      | Sediment characteristics .....   | 35        |
| 3.2.      | Total concentrations of Al, Si, Fe and Mn in sediments.....  | 37        |
| 3.3.      | Organic carbon in sediments.....   | 38        |
| 3.4.      | Total dissolved concentrations of $\text{SO}_4^{2-}$ , $\text{HS}^-$ and $\text{Cl}^-$ in pore waters..... | 39        |
| 3.5.      | Total dissolved concentrations of Fe and Mn in pore waters.....  | 40        |
| 3.6.      | Dissolved organic carbon .....   | 42        |
| 3.7.      | Mercury .....  | 42        |
| 3.7.1.    | Total Hg and MeHg in sediments .....   | 42        |
| 3.7.2.    | Hg and MeHg in pore waters.....  | 43        |
| <b>4.</b> | <b>DISCUSSION .....</b>  | <b>47</b> |
| 4.1.      | Sediment characteristics .....   | 49        |
| 4.1.1.    | Solid sediments .....  | 49        |
| 4.1.2.    | Pore waters .....  | 52        |
| 4.2.      | Mercury in sediments.....  | 55        |
| 4.3.      | Mercury in pore waters.....  | 60        |
| 4.4.      | Methylmercury diagenesis.....  | 65        |
| 4.5.      | Mercury fluxes.....  | 68        |
| 4.6.      | Contamination impacts and legal figure .....   | 69        |
| <b>5.</b> | <b>CONCLUSIONS.....</b>  | <b>73</b> |
| <b>6.</b> | <b>REFERENCES.....</b>   | <b>77</b> |



## **Index of Figures**

|  |    |
|--|----|
| <b>Figure 1</b> – The biogeochemical cycle of mercury. Principal Hg forms in the different compartments, adapted from Pereira (1996); Valega (2003) and Canario (2004).....  | 6  |
| <b>Figure 2</b> – Locations of the sampling sites in Tagus Estuary. (A) Cala do Norte and (B) Ponta da Erva.....   | 19 |
| <b>Figure 3</b> – Schematic representation of the cores sampled in Cala do Norte and Ponta da Erva and their slicing intervals. ....   | 24 |
| <b>Figure 4</b> – Picture of one of the cores collected in Cala do Norte, Tagus estuary.....   | 35 |
| <b>Figure 5</b> – Vertical profiles of pH, Eh (mV), water content (%) and Lost On Ignition (%) both in sediment cores collected in Cala do Norte and Ponta da Erva. The black circles correspond to the Cala do Norte core and the red triangles to the core collected in Ponta da Erva. ....  | 36 |
| <b>Figure 6</b> – Vertical profiles of Al, Si, Fe (%) and Mn ( $\mu\text{g/g}$ ) concentrations both in sediment cores collected in Cala do Norte and Ponta da Erva. The black circles correspond to the Cala do Norte core and the red triangles to the core collected in Ponta da Erva. ....                                       | 38 |
| <b>Figure 7</b> – Vertical profiles of organic carbon (%) both in sediment cores collected in Cala do Norte and Ponta da Erva. The black circles correspond to Cala do Norte core and the red triangles to the core collected in Ponta da Erva.....  | 39 |
| <b>Figure 8</b> – Vertical profiles of $\text{SO}_4^{2-}$ (mM), $\text{HS}^-$ ( $\mu\text{M}$ ) and $\text{Cl}^-$ (mM) both in pore waters of the sediment cores collected in Cala do Norte and Ponta da Erva. The black circles correspond to Cala do Norte core and the red triangles to the core collected in Ponta da Erva. .... | 40 |
| <b>Figure 9</b> – Vertical profiles of Fe and Mn ( $\mu\text{g/L}$ ) both in pore waters of the sediment cores collected in Cala do Norte and Ponta da Erva. The black circles correspond to Cala do Norte core and the red triangles to the core collected in Ponta da Erva.....  | 41 |
| <b>Figure 10</b> – Vertical profiles of dissolved organic carbon (mg/L) both in pore waters of the sediment cores collected in Cala do Norte and Ponta da Erva. The black circles correspond to Cala do Norte core and the red triangles to the core collected in Ponta da Erva. ....  | 42 |
| <b>Figure 11</b> – Vertical profiles of $\text{Hg}_T$ ( $\mu\text{g/g}$ ) and MeHg (ng/g) both in sediment cores collected in Cala do Norte and Ponta da Erva. The black circles correspond to Cala do Norte core and the red triangles to the core collected in Ponta da Erva. ....   | 43 |
| <b>Figure 12</b> – Vertical profiles of $\text{Hg}_T$ ( $\mu\text{g/L}$ ) and MeHg (ng/g) both in pore waters of the sediment cores collected in Cala do Norte and Ponta da Erva. The black circles correspond to Cala do Norte core and the red triangles to the core collected in Ponta da Erva. ....                              | 44 |

|  |    |
|--|----|
| <b>Figure 13</b> – Vertical profiles of Si, Fe and Mn normalized to Al both in sediment cores collected in Cala do Norte and Ponta da Erva. The black circles correspond to Cala do Norte core and the red triangles to the core collected in Ponta da Erva. ....  | 52 |
| <b>Figure 14</b> - Vertical profiles of $\text{SO}_4^{2-}$ (mM) and $\text{HS}^-$ ( $\mu\text{M}$ ) both in pore waters of the sediment cores collected in Cala do Norte (CN) and Ponta da Erva (PE). The black circles correspond to $\text{SO}_4^{2-}$ vertical distribution and the red triangles to $\text{HS}^-$ vertical distribution.....                           | 54 |
| <b>Figure 15</b> – Vertical profiles of Hg and MeHg normalized to Al both in sediment cores collected in Cala do Norte and Ponta da Erva. The black circles correspond to Cala do Norte core and the red triangles to the core collected in Ponta da Erva. ....  | 58 |
| <b>Figure 16</b> - Vertical profiles of Hg and MeHg normalized to $\text{C}_{\text{org}}$ both in sediment cores collected in Cala do Norte and Ponta da Erva. The black circles correspond to Cala do Norte core and the red triangles to the core collected in Ponta da Erva. ....   | 59 |
| <b>Figure 17</b> – Vertical profiles of Hg concentrations ( $\mu\text{g/g}$ ) and MeHg ( $\text{ng/g}$ ) both in sediment cores collected in Cala do Norte (CN) and Ponta da Erva (PE). The black circles correspond to Hg vertical distribution and the red triangles to MeHg vertical distribution.....  | 60 |
| <b>Figure 18</b> – Vertical profiles of Hg concentrations in sediments ( $\mu\text{g/g}$ ) and $\text{Hg}_T$ ( $\text{ng/L}$ ) in pore waters both in cores collected in Cala do Norte (CN) and Ponta da Erva (PE). The black circles correspond to Hg vertical distribution in sediments and the red triangles to $\text{Hg}_T$ vertical distribution in pore waters..... | 62 |
| <b>Figure 19</b> – Vertical profiles of MeHg concentrations in sediments ( $\text{ng/g}$ ) and dissolved MeHg ( $\text{ng/L}$ ) in pore waters both in cores collected in Cala do Norte (CN) and Ponta da Erva (PE). The black circles correspond to MeHg vertical distribution in sediments and the red triangles to MeHg vertical distribution in pore waters.....       | 63 |
| <b>Figure 20</b> – Vertical profiles of $\text{Hg}_T$ and $\text{Hg}_R$ ( $\text{ng/L}$ ) in pore waters both in sediment cores collected in Cala do Norte (CN) and Ponta da Erva (PE). The black circles correspond to $\text{Hg}_T$ vertical distribution and the red triangles to $\text{Hg}_R$ vertical distributions in pore waters. ....                             | 64 |
| <b>Figure 21</b> – Vertical profiles of $\text{Hg}_R$ and MeHg ( $\text{ng/L}$ ) in pore waters both in sediment cores collected in Cala do Norte (CN) and Ponta da Erva (PE). The black circles correspond to $\text{Hg}_R$ vertical distribution and the red triangles to MeHg vertical distributions in pore waters. ....   | 65 |
| <b>Figure 22</b> - Correlation between total MeHg ( $\text{ng/L}$ ) in pore waters (x axis) and MeHg ( $\mu\text{g/g}$ ) in sediment cores (y axis) both in Cala do Norte and Ponta da Erva. ....  | 66 |
| <b>Figure 23</b> – Vertical profiles of MeHg concentrations ( $\text{ng/L}$ ) versus $\text{HS}^-$ ( $\mu\text{M}$ ) both in pore waters of the sediment cores collected in Cala do Norte (CN) and Ponta da Erva (PE). The black circles   |    |

correspond to MeHg vertical distribution, respectively, and the red triangles to HS<sup>-</sup> vertical distribution..... 68

## **Index of Tables**

|   |    |
|---|----|
| <b>Table 1</b> – Principal Hg species present in solid phase and pore waters of the sediments (from Canário, 2004). .....   | 10 |
| <b>Table 2</b> – Operating conditions used in the analysis of Fe, Mn, Al and Si with FA-AAS.....  | 27 |
| <b>Table 3</b> – Detection limits, error and precision of $\text{Cl}^-$ and $\text{SO}_4^{2-}$ (mM), $\text{HS}^-$ ( $\mu\text{M}$ ), Fe and Mn ( $\mu\text{g/L}$ ), Hg and MeHg (ng/L) analysed in pore waters both in Cala do Norte and Ponta da Erva. .... | 31 |
| <b>Table 4</b> – Concentrations and average deviation of Hg ( $\mu\text{g/g}$ ), MeHg (ng/g), Fe (%), Mn ( $\mu\text{g/g}$ ), Al (%) and Si (%) of the certified materials PACS-2, MESS-3, BCR-580, IAEA-405, MESS-1 and standard rock AGV-1.....             | 32 |
| <b>Table 5</b> – Comparison of total mercury (Hg) and methylmercury (MeHg) concentrations in sediments from Tagus Estuary with other national estuarine / coastal systems. ....   | 56 |
| <b>Table 6</b> – Comparison of total mercury (Hg) and methylmercury (MeHg) concentrations in sediments from international estuarine / coastal systems (modified from Oh <i>et al.</i> , 2010). ....   | 57 |
| <b>Table 7</b> - Comparison of total mercury ( $\text{Hg}_T$ ) and methylmercury (MeHg) concentrations in sediments from Tagus Estuary with other national and international estuarine / coastal systems (modified from Wang <i>et al.</i> , 2009).....       | 61 |
| <b>Table 8</b> – Classification of Hg contamination levels in dredged sediment materials, according to “Portaria nº 1450/2007, de 12 de Novembro” .....   | 70 |

# **1. INTRODUCTION**



## 1.1. Physico-chemical properties of Mercury

A series of magical properties have been attributed to mercury since ancient times. Mercury is considered a heavy metal due to its density, higher than  $5 \text{ g/cm}^3$  and is the only liquid metal at room temperature, with a melting point of  $-38.89 \text{ }^\circ\text{C}$  and boiling temperature of  $357.25 \text{ }^\circ\text{C}$ . Mercury has also low electric resistance, high superficial tension and high thermal conductivity. Its volume expansion along the liquid range is uniform and vapor pressure is temperature depending, varying between  $5.5 \text{ mg/m}^3$  at  $10 \text{ }^\circ\text{C}$  and  $72 \text{ mg/m}^3$  at  $100 \text{ }^\circ\text{C}$  (Canário, 2004). Mercury presents strong affinity to form stable complexes through covalent metal-ligand bonds such as carbon compounds (Jackson, 1998).

The emissions of mercury into the environment can be natural or anthropogenic. The most important natural input of mercury in biosphere is volcanic activity. Anthropogenic emissions can derive from coal combustion, solid waste incineration and chlor-alkali plants, which are considered the biggest polluters due to their use, in the past, of Hg in the production of chlorine and caustic soda (Wiener *et al.*, 2003). Mercury was used in navigation devices and generally in instruments for temperature and pressure measures. Amalgamation with other metals is another feature to its high industrial value in the past. It also had a variety of utilities due to its ability to conduct electricity and was frequently used in electrical industry (e.g., switches, batteries and lamps). Other applications for mercury compounds could be found in wood processing (as anti fungal), vaccines (as preservative) and as a solvent for reactive and precious metals, such as in gold mining (Clark, 2001).

Depending on the chemical form, mercury can have strong ecotoxicological effects. The major concern of mercury pollution is the transformation of inorganic Hg into organic species, which are the most toxic to aquatic organisms (e.g., Jonnalagadda and Rao, 1993; Ullrich *et al.*, 2001). Methylmercury (MeHg) is the most common form of organic mercury species and is a strong neurotoxin with lipophilic and protein-binding properties, being readily bioaccumulated by aquatic biota and biomagnified through the food chain (Ullrich *et al.*, 2001). Consequently, MeHg can have strong implications in human health, causing damages in cerebellum and sensory pathways with lesions in the cerebral cortex (Burbacher *et al.*, 1990; Crespo-Lopéz *et al.*, 2007). The most important and incidents with

large human health repercussions occurred in the 1950's and 1960's in Japan (e.g., at the Minamata Bay) and Iraq. Since then, mercury has been considered one of the highest hazard environmental contaminant and of crucial interest to study (Forstner and Wittmann, 1981; Ullrich *et al.*, 2001).

## 1.2. The biogeochemical cycle of mercury

Mercury biogeochemical cycle is very complex (Figure 1), therefore the prediction of its chemical forms and environmental circulation is very difficult. Several sources can be pointed out as major contributors of this metal into the environment, as already mentioned before, and depending on physical, chemical and biological conditions Hg compounds can be transformed into other forms and travel between the different compartments (Farago, 2000). Briefly, Hg can be released from the sediments to the water phase, taken up by aquatic biota, be lost to the atmosphere or transported through the atmosphere particulate matter to new locations previously uncontaminated (Ullrich *et al.*, 2001), such as the Arctic (Poissant *et al.*, 2008).

In a simplified view, Hg biogeochemical cycling gathers the transformation reactions involving the following species:



Mercury (II) ( $\text{Hg}^{2+}$ ) can be found in soils, sediments and natural waters as simple chemical compounds (e.g., as cinnabar,  $\text{HgS}$ ) or in more complex forms as the ones found with the organic matter. Mercury (II) may be:

- reduced to  $\text{Hg}^0$  by photoreduction processes (e.g., Amyot *et al.*, 1997) or microbial reduction (e.g., Mason *et al.*, 1995), being found as dissolved gas in waters or mercury vapor in the atmosphere;
- biologically methylated to  $\text{CH}_3\text{Hg}^+$  by microorganisms (e.g., Baldi, 1997) to methylmercury, the most toxic Hg form for living organisms, particularly the aquatic (e.g., Bloom, 1992).



The concentrations of Hg species in an ecosystem (reaction 1) will depend on the chemical equilibrium between those species and the particular physico-chemical properties of the ecosystems (e.g., Jackson, 1998).

Despite of the different mercury species that occur in the environment, Hg biogeochemical cycle is dominated by the atmospheric transport, due to the high vapor pressure of elemental mercury ( $\text{Hg}^0$ ) and to the low residence time of this element in the atmosphere, around 1 year (Butcher *et al.*, 1992; Covelli *et al.*, 1999). Thus, elemental mercury is transported over long distances and represents approximately 99 % of the total Hg in the atmosphere. The remaining Hg is present in particulate or dissolved form (Pereira, 1996). These Hg forms are then deposited on the continents, rivers and oceans through wet and dry deposition (Fitzgerald *et al.*, 1994; Lamborg *et al.*, 1994).

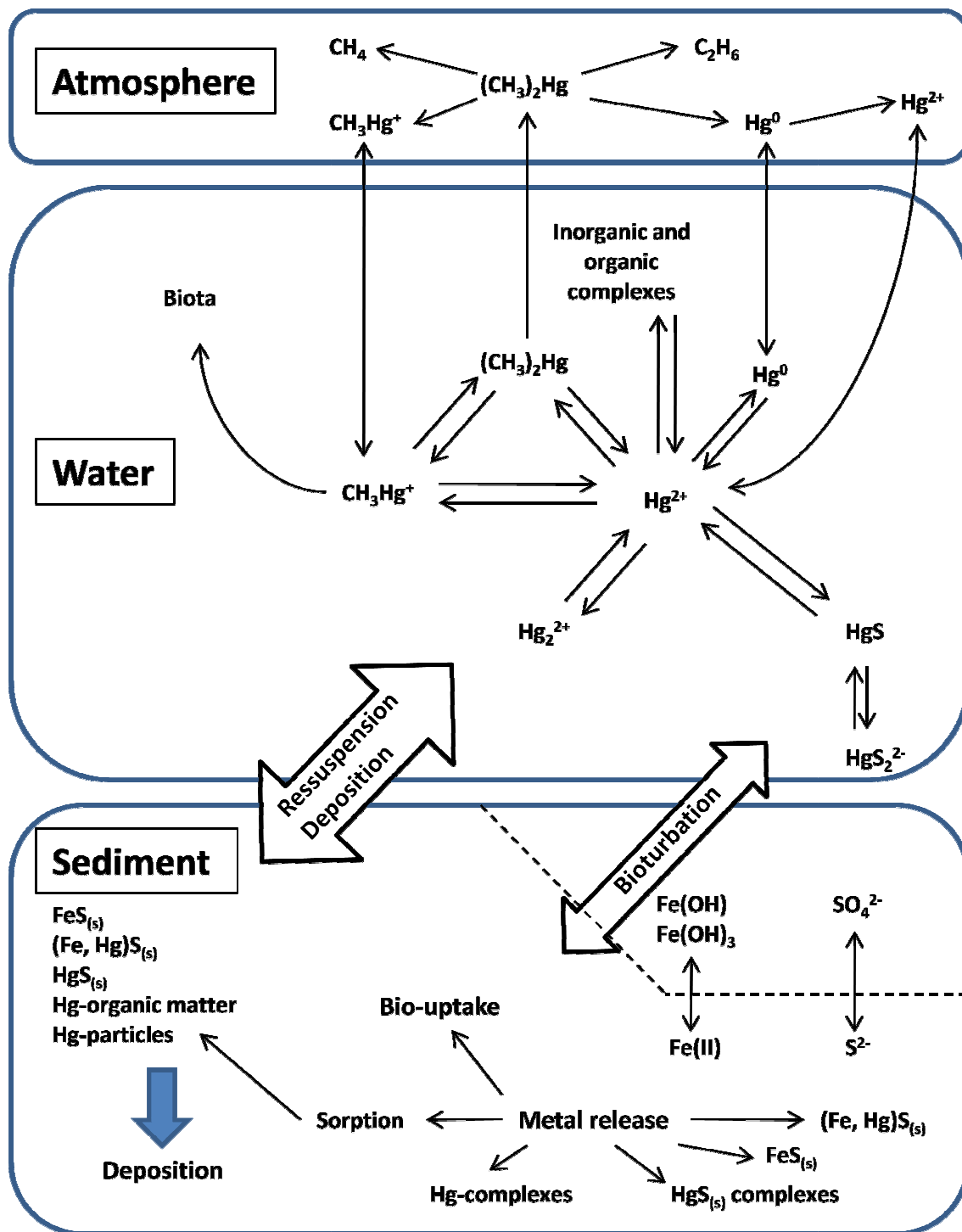


**Figure 1** – The biogeochemical cycle of mercury. Principal Hg forms in the different compartments, adapted from Pereira (1996); Válega (2003) and Canário (2004).

### 1.3. Mercury in the aquatic environment

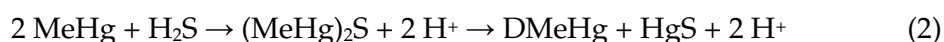
One of the most important aquatic systems involved in Hg biogeochemical processes are the estuaries and other transitional water systems. This is due to strong horizontal and vertical geochemical gradients that can be found in these systems, controlling trace mercury speciation and distribution (Mason *et al.*, 1993; Chiffoleau *et al.*, 1994; Leermakers *et al.*, 1995; Laurier *et al.*, 2003; Turner *et al.*, 2004; Schafer *et al.*, 2010). These environments play an important role in transformation reactions and may be considered a pathway before transferring toxic components, such as methylmercury, to the coastal/oceanic ecosystems (Schafer *et al.*, 2010). Primary producers are the base of the estuarine/marine trophic webs and may, therefore, also represent an important pathway for mercury transportation (Monterroso *et al.*, 2003) and incorporation into biota higher trophic levels (Coelho *et al.*, 2005). Consequently, mercury bioaccumulation and biomagnification in aquatic biota is of major interest, considering the food chains in these environments (Ullrich *et al.*, 2001; Heyes *et al.*, 2004; Kim *et al.*, 2004).

The understanding of Hg behavior in aquatic environments is also not easy due to the variety of species that can be formed, as well as the specific characteristics of each group. Elemental mercury presents high vapor tension, low solubility and a partition coefficient octanol/water ( $K_{ow}$ ) of 4.15 and together with dimethylmercury,  $(CH_3)_2Hg$ , (an organic mercury species extremely volatile) exist as dissolved gases. Ionic mercury ( $Hg^{2+}$ ) and methylmercury may exist either in dissolved or particulate forms (NOAA, 1996).

In natural waters  $Hg^{2+}$  can be methylated or reduced and associated with organic or inorganic ligands, especially those containing sulphur, to form stable complexes (e.g., Ullrich *et al.*, 2001).

Most important than inorganic mercury compounds/complexes in natural environments, is the presence of organic mercury species, once total metal levels alone do not allow assessing short term environmental risks since they do not reflect the mobility, reactivity, or bioavailability of potentially toxic trace elements (Ullrich *et al.*, 2001). Even in ecosystems with low Hg concentrations in water and/or sediments can represent a remarkable source of MeHg to bioaccumulation in aquatic organisms, particularly observed in fishes (Covelli *et al.*, 2001; Hammerschmidt and Fitzgerald, 2004) or phyto and zooplankton (Kehrig *et al.*, 2009).

Methylmercury in aquatic systems is mostly synthesized by microorganisms, which may occur in sediments, water column or possibly inside the aquatic organisms (NOAA, 1996). Among them, sulphate-reducing bacteria are known to be the main Hg methylators (Barkay and Wagner-Dobler, 2005). Associated with methylation processes and resulting in a detoxification process from organisms (Merrit and Amirbahman, 2009) dimethylmercury may be formed (reaction 2). In anoxic environments, degradation of MeHg can produce dimethylmercury which is highly volatile and therefore removed from the sediment (Baldi, 1997):



### 1.3.1. Mercury in natural waters

Mercury enters the water via anthropogenic discharges, atmospheric deposition and natural processes such as river runoff. In water it may be present in dissolved or particulate phase, depending on the salinity, concentration and nature of organic matter (particulate and dissolved) and suspended particulate matter, among other factors (Canário et al., 2008).

The dissolved fraction can be defined as the fraction where all forms of an element pass through a 0.45  $\mu\text{m}$  porosity filter (Strodel *et al.*, 1996). In this fraction Hg is found as hydrated ions, ionic pairs, chelates, metal oxyhydroxides and colloidal particles (Ramalhosa, 2002).

In surface waters,  $\text{Hg}^0$  is produced from the reduction of Hg(II) by microorganisms or from abiotic reduction by humic substances, with a strong relation with photoreduction mechanism mediated by humic material (Ullrich *et al.*, 2001). Mercury(I), another mercury ion, is only stable as a dimer ( $\text{Hg}_2^{2+}$ ) in aqueous solution and is easily transformed into  $\text{Hg}^0$  and  $\text{Hg}^{2+}$ , the most stable forms in water, whereas  $\text{Hg}^{2+}$  is the mainly oxidation state that can be found (Jackson, 1998, Ullrich *et al.*, 2001).

In natural waters,  $\text{Hg}^{2+}$  does not exist as a free ion, but usually it complexes with hydroxide or chloride, forming species such as  $\text{HgX}_2$ ;  $\text{HgX}_3^-$ ;  $\text{HgX}_4^{2-}$  (where X can be OH<sup>-</sup>, Cl<sup>-</sup>). The existence of these species depends mainly on pH and chloride concentrations (Issaro *et al.*, 2009). Mercury complexes with chloride predominantly at pH 8, whereas is

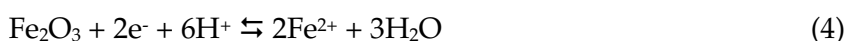
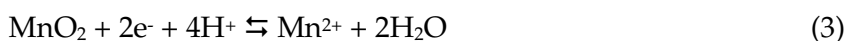
the estuarine and marine environment characteristic value (e.g., Ullrich *et al.*, 2001). As salinity decreases, the formation of HgCl<sub>2</sub> is more favorable than HgCl<sub>3</sub> and HgCl<sub>4</sub>, mostly present in seawater (Morel *et al.*, 1998). In the presence of sulphide (S<sup>2-</sup>, HS<sup>-</sup> and S<sub>x</sub><sup>2-</sup>) the reactive mercury forms complexes, which may increase Hg concentrations in dissolved fraction (Benoit *et al.*, 2001). Mercury can also be associated with dissolved organic matter (DOM), bond through covalent bonds to the acidic groups such as thiol and carboxylic groups (e.g., Ravichandran, 2004).

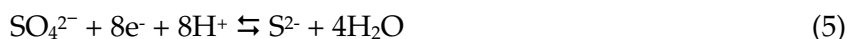
In dissolved fraction Hg can be also found as organometallic species, such as MeHg associated with hydroxide or chloride, forming CH<sub>3</sub>HgOH or CH<sub>3</sub>HgCl, or dimethylmercury (DMHg), which is thermodynamically stable due to the covalent bonds that it can establish (Gagnon *et al.*, 1997; Ullrich *et al.*, 2001). In anoxic waters, such as pore waters, enriched in sulphide, MeHg can form polysulphides, such as CH<sub>3</sub>HgSH. Though, competition between sulphide and humic matter can exist, once the humic matter also has high affinity to bond with MeHg (Lepine, 1995; Gagnon *et al.*, 1997; Ullrich *et al.*, 2001).

In the water column, a large amount of Hg is associated to suspended matter (Lu and Jaffe, 2001). Methylmercury is strongly adsorbed onto particles although to a less extent than the inorganic Hg (Ullrich *et al.*, 2001). Consequently, suspended solids have a major role on the distribution of Hg forms in aquatic systems (Pato *et al.*, 2010).

### 1.3.2. Mercury in sediments

Sediments are constituted by a solid fraction, pore waters and dissolved gases resulting from the diagenetic processes that occur within. The behavior of trace elements is, to a large extent, determined by their chemical forms of occurrence. As a result, metals fate in sediments is governed by numerous processes, including sorption/desorption, precipitation/dissolution and complexation/ decomplexation. Major reactions include denitrification, manganese [Mn (IV)] reduction, ferric iron [Fe (III)] reduction, sulphate (SO<sub>4</sub><sup>2-</sup>) reduction, and methanogenesis (Froelich *et al.*, 1979; Du Laing *et al.*, 2009). Some are represented by the following reactions and can be of major importance regarding the mobility of metals as Hg (Du Laing *et al.*, 2009):





These processes are catalyzed by microorganisms and have been extensively studied and reviewed (e.g., Du Laing *et al.*, 2009).

Sediments are the main reservoir of mercury in estuaries (Benoit *et al.*, 1998; Ullrich *et al.*, 2001) and can be a significant source to the overlying water column via processes that include diffusion, resuspension and/or bioturbation (Gagnon *et al.*, 1997; Bloom *et al.*, 1999; Mason and Lawrence, 1999; Ullrich *et al.*, 2001). Sediments can act both as sinks and potential sources of Hg (Covelli *et al.*, 1999; Ullrich *et al.*, 2001) and constitute the main reservoir of Hg in freshwater and estuarine systems. The sediments once contaminated, may pose a risk to aquatic environments for many years.

Accordingly to Gambrell (1994), general chemical forms of mercury in sediments include, the water-soluble Hg species, as free ions; inorganic or organic complexes; exchangeable metals; metals precipitated as inorganic compounds, including insoluble sulphides; metals complexed with large molecular-weight humic materials; metals adsorbed or occluded to precipitated hydrous oxides; metals bond within the crystalline lattice structure of primary minerals, as presented in Table 1.

**Table 1** – Principal Hg species present in solid phase and pore waters of the sediments (from Canário, 2004).

|                                   | <b>Solid fraction</b>               | <b>Pore waters</b>   |
|-----------------------------------|-------------------------------------|--|
| <b>Oxic / Sub-oxic conditions</b> | Hg associated with Fe oxyhydroxides | Hg <sup>0</sup>  |
|                                   | Hg associated with Mn oxyhydroxides | HgCl <sub>2</sub> , HgCl <sub>3</sub> <sup>-</sup> , HgCl <sub>4</sub> <sup>2-</sup> |
|                                   | Hg associated with organic matter   | Hg(OH) <sub>2</sub>  |
| <b>Anoxic conditions</b>          | HgS                                 | HgHS <sub>2</sub> <sup>-</sup> , HgS <sub>2</sub> <sup>2-</sup>                      |
|                                   | Adsorb to mineral sulphides         | Complexed with organic ligands   |

The Hg chemical forms in sediments are strongly influenced by redox (Eh) and pH conditions, which control adsorption and retention in the sedimentary column, as well as the concentration of inorganic and organic complexing agents. Hg<sup>2+</sup> and CH<sub>3</sub>Hg<sup>+</sup> forms have high tendency to form complexes, particularly with soft ligands such as sulphur, by covalent and ionic bonds (Jackson, 1998).

Therefore, mobility and bioavailability of Hg and MeHg depends on its nature and concentration. Generally, Hg associates primarily with particulate organic matter and iron/manganese oxides through adsorption and coprecipitation reactions in oxidized sediments (Gagnon *et al.*, 1997), with organic matter typically being the overriding controlling solid phase (Miller, 2006). In anoxic sediments, Hg is adsorbed onto and/or co-precipitated with sulphide minerals (Gobeil and Cossa, 1993; Gagnon *et al.*, 1997; Ullrich *et al.*, 2001).

Iron and manganese oxyhydroxides play an important and particular role in the cycling and transport of Hg and MeHg in aquatic systems, due to their large surface areas and high capacity to adsorb and co-precipitate Hg (e.g., Gagnon *et al.*, 1997). When Fe and Mn oxides are reduced in the solid phase, Hg can potentially be released into pore waters, which can be eventually released to the overlying water via diffusion (Canário *et al.*, 2007). The degradation of organic matter as well as the Fe hydroxides transformation to Fe sulphides in anoxic layers of the sediment reduces the capacity of adsorption of trace metals in solid phase (Du Laing *et al.*, 2009).

Mercury can also be released by chemical dissolution of sulphides due to redox changes during diagenesis, once it can form highly insoluble sulphide minerals and adsorb/coprecipitate with pyrite and acid volatile sulphides (AVS) (Miller, 2006), making them less bioavailable to aquatic organisms (Allen, 1980). Bloom *et al.* (1999) reported that the mobility of MeHg in estuarine surface sediments was linked to the Fe redox cycle, while the mobility of Hg(II) was controlled by the formation of polysulphide or organic complexes (Ullrich *et al.*, 2001).

Although the proportion of dissolved Hg may sometimes decrease under anoxic conditions due to the formation of reduced species (such as cinnabar, HgS), anoxic conditions favor the release of Hg from the solid phase of the sediment, due to the dissolution of oxyhydroxides and subsequent release of any associated Hg (Ullrich *et al.*, 2001). This mechanism is thought to be one reason for the seasonal variability observed in Hg and MeHg enrichment in anoxic waters (Ullrich *et al.*, 2001) and is linked with redox changes effects (Du Laing *et al.*, 2009).

Usually, metal concentrations in pore waters reflect its concentrations in sediments (Bufflap and Allen, 1995) and organic colloids, that are present in pore waters, can contain

a substantial proportion of the traditionally defined dissolved Hg fraction ( $< 0.45 \mu\text{m}$ ) in freshwater, estuarine and marine environments (Ullrich *et al.*, 2001). Mercury remobilization may also occur from sediments to pore waters due to interactions with microorganisms, where sulphate-reducing bacteria (SRBs) play an important role during these transformation processes involving the sulfur cycling (Du Laing *et al.*, 2009). At high pH, the oxidation of metal sulphides is expected to happen. Metals co-precipitated with or adsorbed to FeS and MnS are rapidly oxidized, due to their relative solubility in oxic conditions (Du Laing *et al.*, 2009). However, more stable sulphide-bound metals (such as pyrite) are unlikely to be oxidized in the short term due to their slower oxidation kinetics (Caetano *et al.*, 2002). After sulphide oxidation, the released Fe and Mn can be rapidly re-precipitated and deposition of insoluble oxides/hydroxides can remove from solution the newly released metals, becoming adsorbed (Caetano *et al.*, 2002; Eggleton and Thomas, 2004) and thereby recycling Hg concentration available in pore waters for methylation activity.

Mercury easily adsorbs onto particles surface and therefore, it is mostly bound to sediments (Ullrich *et al.*, 2001). Mercury concentrations in sediments and suspended particles are also closely associated to the organic content and in interstitial waters are often significantly correlated with dissolved organic matter (DOM) (Ullrich *et al.*, 2001). Despite that, partitioning of Hg and MeHg may also be related to changes in particulate matter. If oxyhydroxides form labile complexes with organic matter and clay minerals, which may further increase their metal scavenging capacity, thereby the organic matter content influences methylation, by controlling the availability of inorganic Hg (Ullrich *et al.*, 2001). Kim *et al.* (2006) suggested that sediment resuspension plays a role in Hg methylation by changing the association of Hg with sediment binding phases. In addition, sediment resuspension can play a large role in transferring sediment MeHg to organisms in shallow water systems (e.g., Heyes *et al.*, 2004).

The sediment/water interface is pointed as the main site for methylation processes and therefore the deposition and settling of particulate matter is an important mechanism in these areas (Heyes *et al.*, 2004). Total Hg concentrations tend to be higher in pore waters than in the overlying water column and the proportion of MeHg can reach between 30 to 85% (Ullrich *et al.*, 2001). Hg appears to be more strongly sorbed by humic substances



than MeHg, which may be the reason why it is less easily mobilized from sediments than MeHg (Ullrich *et al.*, 2001).

#### **1.4. Mercury methylation**

After the release in the environment, elements may be subjected to biotic (e.g. methylation, oxidation, reduction) and abiotic reactions (e.g. dissolution, precipitation, hydrolysis), generating new chemical species that affect their bioavailability (Clark, 2001; Gailer, 2007). Over the years, it became clear that toxicity effects of Hg are due essentially to its methylated form in spite of its total concentrations in the environment (Ullrich *et al.*, 2001).

As mentioned before, some of the sources of mercury in aquatic environments are considered to be atmospheric deposition (Hall *et al.*, 1995; Munthe *et al.*, 1995), terrestrial runoff and especially wetlands (Louis *et al.*, 1996; Driscoll *et al.*, 1998); however, the relatively high levels of MeHg found in sediments, biota and water require that other sources of methylmercury need to be identified, namely the potential methylation route within the aquatic environment. Mercury methylation is dependent of several factors that can be grouped as those affecting the bioavailability of Hg and those affecting the activity of the methylating bacteria (Choi *et al.*, 1994, Benoit *et al.*, 2003). The factors controlling the bioavailability of Hg for methylation depend on the dissolved and solid phase speciation and partitioning of Hg (Benoit *et al.*, 1999, 2001; Ravichandran, 2004).

In estuarine sediments, processes such as methylation/demethylation and volatilization determine the state and overall toxicity of mercury pollutants (Ullrich *et al.*, 2001; Mason and Benoit, 2003). Mercury speciation, and therefore its bioavailability, is a primary factor governing the methylation potential in a system and sediments are widely recognized as a major site for Hg methylation (Gilmour *et al.*, 1992; Ullrich *et al.*, 2001; Hammerschmidt and Fitzgerald, 2004; Hines *et al.*, 2004). Though, methylation processes in the water column shouldn't be excluded, considering the volume typically higher than the volume of superficial sediments, which can account for a potential increase in methylation (Ullrich *et al.*, 2001).

Mercury contaminated sediments may exhibit extremely high total concentrations, reaching over 300 µg/g (e.g., Pereira *et al.*, 1998; Válega *et al.*, 2008a); however, MeHg concentrations in sediments are typically only about 1 to 1,5% of total Hg content and tend to be lower (typically < 0,5%) in estuarine and marine environments (Válega *et al.*, 2008a), reflecting the equilibrium between methylation and demethylation rates (Ullrich *et al.*, 2001; Mason and Benoit, 2003). Though, the complexity of factors acting in methylation processes may increase MeHg production in sediments, over than 30 % (Canário *et al.*, 2007). Usually, maximum methylation rates are observed at the redox boundary, decreasing with increasing sediment depth, and are often coincident with the sediment/water interface, which in turn can result in seasonal variability of methylation rates (Ullrich *et al.*, 2001; Benoit and Mason, 2003).

Despite of most methylation studies report strong dependence on SRB activity, some researchers indicate that SRB activity is not only responsible for Hg speciation (Flemming *et al.*, 2006) but also abiotic methylation in one important factor which needs to be taken into account regarding methylation processes (Celo *et al.*, 2006). The rates and mechanisms of chemical methylation are also expected to be affected by the parameters that influence the mercury speciation, including pH, temperature and the presence of complexing agents such as chloride, also reflecting the saline matrix effects (Celo *et al.*, 2006).

Purely chemical methylation of mercury is possible only if suitable methyl donors are present. The presence of proper methyl donors is required and in aquatic environments a large variety of potential donor molecules are present, most of them biologically synthesized (Ullrich *et al.*, 2001).

Although the methyl donors available in aqueous, particulate or sediment environments may themselves be products of biological processes, mercury methylation by these compounds is considered to be abiotic (Krishnamurthy, 1992; Falter and Wilken, 1998). The factors thought to cause abiotic methylmercury formation include small organic molecules such as methyl iodide and dimethylsulphide, and larger organic components of dissolved organic matter such as fulvic and humic acids (Weber, 1993; Celo *et al.*, 2006). Transmethylation reactions involving organometallic complexes such as methylcobalamin, methyllead or methyltin compounds have also been considered as

possible pathways for chemical methylation of mercury in the aquatic environment (Celo *et al.*, 2006). Yet, the contribution of abiotic mercury methylation is still unresolved.

An important factor controlling methylation/demethylation processes is temperature (Ullrich *et al.*, 2001). This is probably related with the effect that temperature has on microbial activity instead of a direct influence. Therefore, higher methylation rates were observed during summer, whereas demethylation rates appear to be related with lower temperatures, resulting in seasonal variations linked with primary productivity as well as changes in redox conditions (Ullrich *et al.*, 2001; Mason and Benoit, 2003; Canário *et al.*, 2007).

Among the factors affecting methylation rates, pH has been considered to affect MeHg concentrations in aquatic systems, once both Hg and MeHg mobility and solubility are influenced by pH (Ullrich *et al.*, 2001). Low pH leads to an easy release of mercury from the sediments and organic matter. However, data are still contradictory (Ullrich *et al.*, 2001; Benoit and Mason, 2003; Du Laing *et al.*, 2009). Yet, no evidence of pH direct influence on methylation is recognized (Ullrich *et al.*, 2001), i.e., relations between methylation and pH appear to be related with bioavailability of  $\text{Hg}^{2+}$ . This is also related with higher volatilization and demethylation rates as long as pH increases, therefore, decreasing the amount of reactive mercury available for the formation of MeHg (Du Laing *et al.*, 2009). At low pH, demethylation is less affected than methylation and thereby, MeHg concentrations appear to increase (Ullrich *et al.*, 2001; Mason and Benoit, 2003).

Redox conditions of the sediments are another factor governing methylation rates (Du Laing *et al.*, 2009). As well as observed with low pH values, low redox potential enhances methylation rates and therefore, increases MeHg concentrations in sediments, which are usually high at the redox boundary, i.e., between the oxic and anoxic layers of the sediment (Ullrich *et al.*, 2001). Compeau and Bartha (1984) found that Hg methylation in estuarine sediments was strongly favored at low Eh (-220 mV) (Ullrich *et al.*, 2001). At higher Eh values, mostly in oxic conditions, Hg demethylation is favored, which result in lower MeHg concentrations (Du Laing *et al.*, 2009). This could be also related with degradation of organic matter, which is known to be faster in the oxic layers of the sediment (Ullrich *et al.*, 2001; Mason and Benoit, 2003).

As mentioned before, a large number of studies indicate that SRBs are the primary mercury methylators in freshwater and estuarine anoxic sediments (e.g., Gilmour *et al.*, 1992; King *et al.*, 1999, 2000, 2001; Holloway *et al.*, 2009, Schafer *et al.*, 2010) and thus, factors that affect the activity of SRB will have effects on Hg biotic methylation (Gilmour *et al.*, 1992; Choi *et al.*, 1994). The optimum sulphate concentration in which sulphate-reducers efficiently produce methylmercury is 0.3 mM (Gilmour *et al.*, 1992). Methylation stops completely at sulphate concentrations exceeding 5 mM (Weber, 1993). Though, King *et al.* (2000), observed methylating activity in four species of SRBs (*Desulfovibrio desulfuricans*, *Desulfobulbus propionicus*, *Desulfobacter sp.* and *Desulfococcus multivorans*) in the presence of both sulphate and sulphide concentrations within the same range (< 30 mM).

Despite methylation reactions being inhibited by the presence of sulphide, which reacts with inorganic Hg decreasing its concentration in solution available for methylation (King *et al.*, 2000), some authors (Ullrich *et al.*, 2001) regarded that the solubility of Hg is actually increased in the presence of excess sulphide, most likely due to the formation of soluble sulphide complexes (Gagnon *et al.*, 1997). Moreover, the lack of a relationship between dissolved Hg(II) concentrations in pore waters and MeHg production suggests that  $\text{Hg}^{2+}$  may not be the main species that is methylated (Benoit *et al.*, 1998). However, although MeHg production is generally greatly reduced at high sulphide concentrations, it is not usually completely inhibited (Ullrich *et al.*, 2001). On the other hand, in estuarine environments, which are not  $\text{SO}_4^{2-}$  limited systems, sulphide enrichment can vary with organic matter enrichment resulting in increased Hg methylation at higher sulphide concentration (Sunderland *et al.*, 2006). As biological Hg methylation takes place within microorganisms, cellular uptake of Hg plays a key role in methylation process (Ullrich *et al.*, 2001). The biotic pathway for mercury methylation requires that a significant amount of mercury must be uncomplexed, i.e., existing as free  $\text{Hg}^{2+}$  (Choi *et al.*, 1994). However, despite mercury being the heavy metal with the highest toxicity to bacteria, it is not clear why the SRB population is resistant to mercury while other bacteria are highly vulnerable. Reviewing, the biogeochemical processes that control Hg methylation are still poorly understood (Goulet *et al.*, 2007). If by one hand some authors indicate that high dissolved sulphide concentrations inhibit MeHg production (Sunderland *et al.*, 2006; Gilmour *et al.*, 1998), the sorption/desorption events and precipitation reactions are also likely to affect

Hg bioavailability and need to be taken into account when estimating rates of MeHg production in natural environments (Ullrich *et al.*, 2001; Mason and Benoit, 2003).

Macro fauna abundance may be also as important as physical mixing in controlling conditions that favor Hg methylation. Demethylation rate constants were found to be similar between the redox and non-redox systems, suggesting that continual Hg methylation was required to maintain the MeHg pool in sediments (Ullrich *et al.*, 2001).

### **1.5. Study area**

The Tagus Estuary is ~80 km longitudinally distance and the margins distance varies between 0.7 km upstream, 15 km at the central area and 2 km at the outflow channel (Figure 2). The Tagus river is the main source of freshwater into the Estuary. Average annual flows are in the order of 400 m<sup>3</sup>/s. Other freshwater inputs to the estuary are small, the average annual flow in the Sorraia river amounts to about 35 m<sup>3</sup>/s (Fortunato *et al.*, 1997).

With approximately 325 km<sup>2</sup> of total area and with an intertidal area of about 120 km<sup>2</sup>, this mesotidal system (mean tidal range of 2.2 m) stratification conditions vary strongly with river flow and tidal conditions. The estuary is vertically well mixed for spring tides and low river flows (Fortunato *et al.*, 1997; Alvera-Azcárate *et al.*, 2003), partially stratified for average conditions and strongly stratified under extreme conditions (Fortunato *et al.*, 1997).

The tidal phase difference between Cascais and V. F. Xira is about 1 h and 20 min (Fortunato *et al.*, 1997). Channels and pools are formed in intertidal areas during the ebb tide and are persistent for a part of the tidal cycle. In these pools, suspended particulate matter sediments quickly resuspends with the wind forcing and rising tide and water exchange with the main channels (Alvera-Azcárate *et al.*, 2003). These are important aspects on the dynamics of particle settling regarding the close relations between Hg and suspended particulate matter. The intertidal area is repeatedly exposed to the atmosphere and therefore chemical reactions occur directly within the sediment surface layer and atmosphere (Canário and Vale, 2004).

Since the last century, the Tagus Estuary have been traditionally a local region of several activities, whether industrial or agricultural, linked to fisheries, salt extraction and others. Consequently, was an important region for exportation of these products. With the increase of these activities and the increasing population, the Tagus margins have been overloaded with pollutants over the years, being identified around 600 pollution sources associated with the referred activities and other anthropogenic pressures, as well as river runoff and atmospheric deposition (Dias and Marques, 1999). Nowadays the river still receives discharges from industrial and agricultural effluents and the estuary is historically contaminated by mercury from two major industrial sources (Figuères *et al.*, 1985), being the “Cala do Norte” and “Barreiro” considered the ‘hotspots’ of mercury environmental pollution in the Tagus Estuary (Canário, 2000, 2004).

Recent works from Canário *et al.* (2005, 2007) regarding total Hg and MeHg concentrations in sediments of the Tagus Estuary report that the proportion of MeHg to the total Hg varies in the entire estuary from 0.02 to 0.4%, which is in agreement with values reported in other published literature (Ramalhosa, 2002). By analyzing 80 surface sediments samples covering all the Estuary, Canário *et al.* (2005) reported an estimation of 23 tons of Hg stored in the first 5-cm of sediments, whereas 24 kg in the form of methylmercury. Moreover, in a work published in 2007, Canário *et al.* found that MeHg concentrations were higher in summer than in winter, with estimations around 37 % over total Hg, reflecting the warmer and reducing properties of the surface sediments during the summer period. These results enhance the seasonal variability that affected methylation in this estuarine system.

### **1.5.1. Cala do Norte**

‘Cala do Norte’ of the Tagus Estuary has approximately 15 km of extension and is 750 meters wide and its depth varies until a maximum of 2 m. This area is considered a high mercury contaminated area, some high levels of contamination have been recorded in sediments, water and organisms by several authors (Figuères *et al.*, 1985; Ferreira *et al.*, 1997; Canário, 2000, 2004). This contamination was mainly due to high industrial activity in the channel margins and particularly by waste water discharges from a chlor-alkali plant. The Cala do Norte has low hydrodynamics and therefore the water residence time

is relatively high in this channel. Thus, high contamination levels have been found in the southward sediments of this channel (Canário, 2004).

### 1.5.2. Ponta da Erva

Conversely to the Cala do Norte, 'Ponta da Erva' is considered a low contaminated area. No industrial inputs have been identified in this area. In this side of the estuary Hg can enter the system via the surrounding agricultural activities, where the Sorraia river may contribute and somehow influence the accumulation of Hg in the adjoining areas, though its annual freshwater contribution to the estuary is considered low.

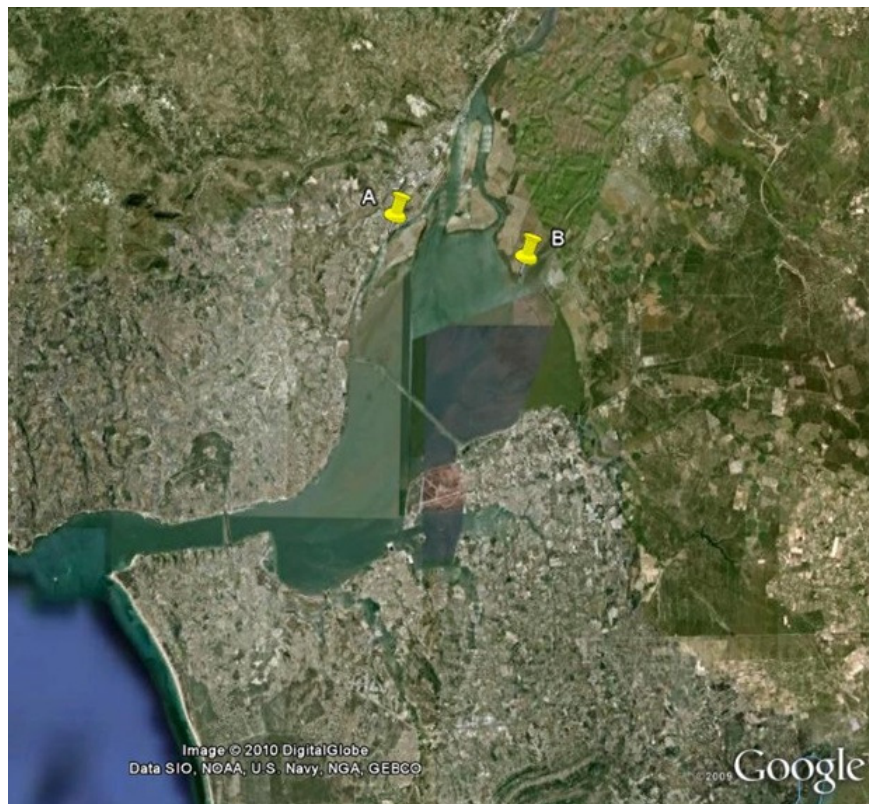


**Figure 2** – Locations of the sampling sites in Tagus Estuary. (A) Cala do Norte and (B) Ponta da Erva.

## **1.6. Objectives**

The aim of this work is to understand the Hg dynamics in sediments of two different areas of the Tagus Estuary characterized by different degrees of Hg contamination. In order to achieve this goal, several objectives have been proposed:

- Evaluate Hg and MeHg concentrations in sediment cores of two different areas of the Tagus Estuary;
- Study the main processes involved in mobility, partitioning and speciation in those sediments;
- Classify the degree of Hg contamination in these important areas of the Tagus Estuary.

It also should be invoked that for the first time MeHg levels in pore waters are quantified in sediment cores collected in Portuguese water systems, addressing this issue of major interest.



## **2. MATERIAL and METHODS**



## 2.1. Decontamination procedures

All material used on field and in the laboratory was previously decontaminated to avoid cross contamination of the samples. This crucial step employs several stages as exposed in the next sequence:

- 1 – Rinsing twice with distilled water;
- 2 – Minimum 2 days in 20% HNO<sub>3</sub>;
- 3 – Rinsing twice with distilled water;
- 4 – Minimum 2 days in 30% HCl;
- 5 – Rinsing twice with Milli-Q water;
- 6 – Drying in a laminar flux chamber in a clean room;
- 7 – Storage in clean plastic bags until usage.

## 2.2. Field work

Field work was developed in the Tagus Estuary in two sampling periods. The first sampling campaign took place in May 2010 in Cala do Norte (Figure 2-A). The second sampling took place in June 2010 in Ponta da Erva, on the east part of the estuary (Figure 2-B). According to Canário (2005), locations A and B were regarded as mercury contaminated and uncontaminated sites, respectively.

Several sediment cores were collected at each location using a PVC decontaminated corer. Cores were sliced into sections (Figure 3) of 1-cm thick in the top 10 cm, and in sections of 2 cm from 10 to 20 cm depth. Below 20 cm depth sediment slices were sampled in every 5 cm until the end of the core (40 cm in Cala do Norte and 25 cm depth in Ponta da Erva).

Sections from one of the cores were placed in plastic bags and kept inside a cooler until being processed in the laboratory. Sections from a second core were stored in polycarbonate leak proof tubes (50-250 mL) and hermetic sealed, for later separation of the pore water content and dissolved sulfide. One last core was also sectioned to measure pH, Eh (mV), temperature (°C) and dissolved oxygen. The pH was measured *in situ* using a portable device Crison mod. 507 with temperature control and a combined electrode to measure pH, Mettler-Toledo, calibrated with two buffers (4.00 and 7.00 ± 0.02 at 20 °C).

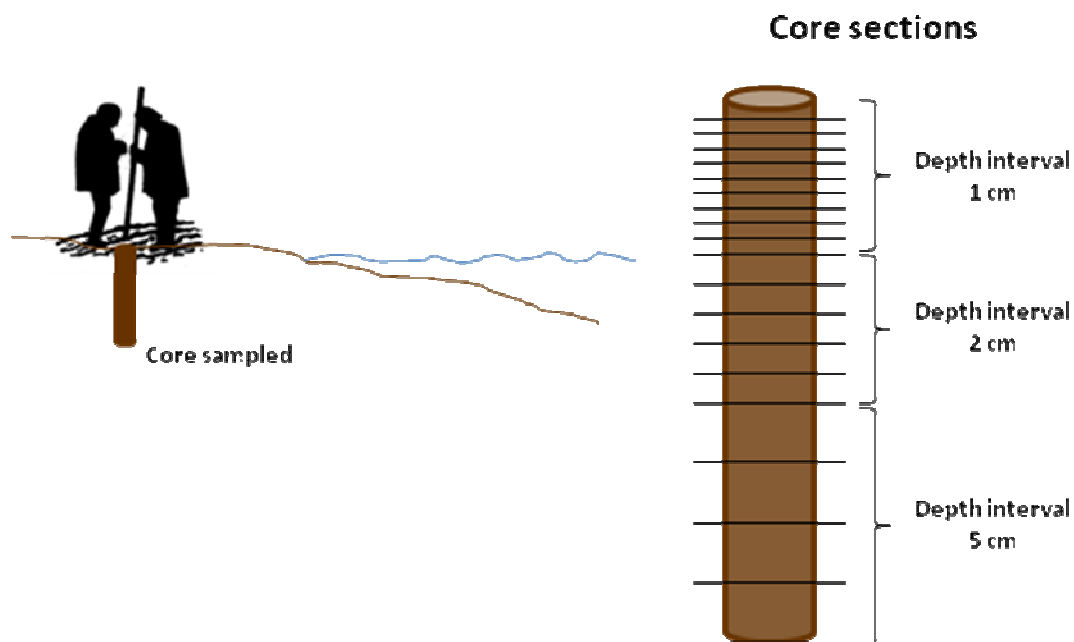


**Figure 3** – Schematic representation of the cores sampled in Cala do Norte and Ponta da Erva and their slicing intervals.

Redox potential (Eh) was also measured with a combined electrode Ag/AgCl-Platinum, Mettler-Toledo, calibrated with a buffer for  $220 \text{ mV} \pm 0.05 \text{ mV}$  vs. Ag/AgCl at  $25 \text{ }^\circ\text{C}$ . Dissolved oxygen was measured in the first cm layer and overlying water using a Diamond Electro-Tech Inc. needle electrode following the method described by Brotas *et al.* (1990).

Overlying water (1cm thick) was sampled at each site in the sediment/water interface. This water was collected using a decontaminated syringe and was immediately filtrated with  $0.45 \text{ }\mu\text{m}$  *Whatmann* cellulose acetate syringe filters. Samples were separated into three flasks: a glass flask for reactive dissolved mercury determination in which the water was immediately acidified to  $\text{pH} < 2$  with concentrated  $\text{HNO}_3$  (Hg free), a Teflon flask, acidified with concentrated HCl (Hg free) for total Hg and MeHg analysis, and polypropylene tubes acidified with bi distilled  $\text{HNO}_3$  for total dissolved metals, chloride and sulphate determinations.

## 2.3. Sample processing

In the laboratory, all samples were processed in order to determine physical and chemical parameters. Fresh sediments were used to determine the water content and organic matter lost on ignition (LOI). Another portion was oven dried at 40 °C to avoid Hg volatilization (Pereira, 1996), desegregated in a agate mortar and homogenized for later analysis.

Fresh sediments samples previously collected into polycarbonate leak proof tubes were centrifuged at 8000 rpm for 30 minutes, in order to extract pore waters content from the solid fraction. Pore waters were then immediately filtrated through 0.45 µm *Whatmann* cellulose acetate syringe filters using syringes and separated into different containers, using the same separation and acidification procedure previously described for overlying waters *in situ*.

## 2.4. Analytical methods

### 2.4.1. Solid fraction

#### 2.4.1.1. Water content

Sediment water content (%) was determined using a small portion of fresh sediment that was carefully weighed in a porcelain crucible. Sample was then placed in an oven at 105 °C, until constant weight. Samples were cooled in a desiccator and re-weighed. Sediment water content was calculated by weights loss before and after the oven step, using the expression in Canário (2004):

$$\%H = \frac{m_{H_2O}(105\text{ }^{\circ}\text{C})}{m_{sed}(105\text{ }^{\circ}\text{C})} \times 100 \quad (6)$$

where %H is the sediment water content and is given as the reason between the water mass lost at 105 °C ( $m_{H_2O}(105\text{ }^{\circ}\text{C})$ ) and the sediment mass at the same temperature ( $m_{H_2O}(105\text{ }^{\circ}\text{C})$ ).

#### 2.4.1.2. Lost On Ignition (LOI)

This parameter was estimated by using the samples previously dried at 105 °C. For this purpose these sediments were placed inside a muffle furnace at 450 °C for two hours. The

amount of sedimentary organic matter was calculated using the difference of the weights in this interval, expressed by:

$$\%LOI = \frac{m_{sed}(105\text{ }^{\circ}C) - m_{sed}(450\text{ }^{\circ}C)}{m_{sed}(105\text{ }^{\circ}C)} \times 100 \quad (7)$$

where %LOI is the percentage of weight Lost On Ignition and is given by the reason between the difference of the weights at 105 °C and 450 °C ( $m_{sed}(105\text{ }^{\circ}C)$ ) and ( $m_{sed}(450\text{ }^{\circ}C)$ ), respectively, and the weight of sediment at 105 °C.

#### **2.4.1.3. Total mercury and methylmercury in sediments**

Total mercury content was quantified using a LECO 254 Advanced Mercury Analyzer. As described by Costley *et al.* (2000), this method works with a structure system in which a known amount of the dried solid sample is placed on a nickel boat that is introduced into a quartz combustion tube containing a catalyst. The solid sample is first dried followed by combustion at 750 °C in an oxygen atmosphere. The released mercury vapor ( $Hg^0$ ) is trapped on the surface of a gold amalgamator and after a pre-specified time interval, the amalgamator is heated to 900 °C to quantitatively release the mercury which is transported to a heated cuvette (120 °C) prior to analysis by AAS using a silicon diode detector at 253.7 nm.

Between 10 to 20 mg of dried sediments was accurately weighed and analysis was made using the typical operating conditions: drying time, 10 s; decomposition time, 150 s; waiting time, 45 s. Before the analysis and between samples several blank readings were performed with empty nickel boats and at the end the system was cleaned using tap water. A certified reference material of marine sediment (PACS-2 and MESS-3) was analyzed between samples and detection limit was calculated based on blank replicates.

Methylmercury was determined in dry sediments as described by Canário *et al.* (2004). Briefly, 200 mg of sediment were subject to alkaline digestion (KOH/MeOH) followed by organic extraction with dichloromethane (DCM), pre-concentration in aqueous sulfide solution, back-extraction into DCM and quantification by GC-AFS in an Agilent Chromatograph coupled with a pyrolyser unit and a PSA fluorescence detector. Recoveries and the possible MeHg artifact formation were evaluated by spiking several samples with  $Hg(II)$  and MeHg standard solutions at different concentrations. Recoveries were higher

than 97 %. International certified standards (IAEA-405 and BCR-580) were used to ensure the accuracy of the procedure.

#### **2.4.1.4. Total iron, manganese, aluminum and silicium**

Total Fe, Mn, Al and Si concentrations in sediments were determined using the method described by Rantala and Loring (1975). Briefly, 100 mg of dried sediments were accurately weighed in a Teflon autoclave and 1 mL of aqua-regia (HCl/HNO<sub>3</sub> (3:1)) and 6 mL of concentrated HF were added. The autoclaves were heated in an oven at 100 °C for one hour and after, the content was transferred to leak proof 50 mL Falcon tubes containing 2.3 g of boric acid. After homogenization, the volume of the digested solutions was adjusted to 50 mL. Reagent blanks and certified reference materials (MESS-1, BCSS-1 and AGV-1) were also processed along with the samples.

The quantification of Fe, Mn, Al and Si total concentrations in the digested sediments was made by atomic absorption spectrophotometry (Perkin-Elmer AAnalyst 100) with flame atomization (FA-AAS). Operating conditions are summarized in Table 2. The concentrations of these elements were calculated based on the standard addition method, using Titrisol Merck 1000 ppm FeCl<sub>3</sub>, MnCl<sub>2</sub>, AlCl<sub>3</sub> and SiCl<sub>4</sub> standard solutions and detection limits were calculated based on blank replicates.

**Table 2** – Operating conditions used in the analysis of Fe, Mn, Al and Si with FA-AAS.

| <b>Element</b> | <b>Wavelength (nm)</b> | <b>Slit (nm)</b> | <b>Type of flame (Comb./Ox.)</b>                |
|----------------|------------------------|------------------|---|
| <b>Fe</b>      | 248.3                  | 0.2              | C <sub>2</sub> H <sub>2</sub> /Air              |
| <b>Mn</b>      | 279.5                  | 0.2              | C <sub>2</sub> H <sub>2</sub> /Air              |
| <b>Al</b>      | 309.3                  | 0.7              | C <sub>2</sub> H <sub>2</sub> /N <sub>2</sub> O |
| <b>Si</b>      | 251.6                  | 0.2              | C <sub>2</sub> H <sub>2</sub> /N <sub>2</sub> O |

#### **2.4.1.5. Organic carbon**

Total carbon determinations were performed in a CHN Fissons NA 1500 Analyzer using homogenized and dried sediment samples. The calibration standard was sulphanilamide. Blanks were made using several empty ashed Sn capsules. Detection limit was 0.001 % based on the analysis of replicates. Organic carbon was estimated by the difference

between total carbon and inorganic carbon which was measured after heating samples at 450 °C during 2 hours in order to remove the organic carbon.

## **2.4.2. Pore waters**

### **2.4.2.1. Reactive dissolved mercury**

Reactive dissolved mercury concentrations ( $Hg_R$ ) was directly determined in the filtered samples using cold vapor atomic fluorescence spectrometry (CV-AFS) on a PSA Merlin atomic fluorescence mercury system. This mercury fraction includes forms such as inorganic-complexes and weakly bound organic-complexes easily reducible by  $SnCl_2$  (NOAA, 1996).

During this procedure reactive mercury is reduced to elemental mercury ( $Hg^0$ ) by a  $SnCl_2$  2 % in a 10 % HCl solution ( $Hg$  free) and  $Hg^0$  is then purged from solution by an Argon flux. For the quantification of  $Hg_R$  levels peak height corresponding to the maximum absorption peak is converted to concentration from a calibration curve built with  $Hg^{2+}$  standards (range from 0 to 100 ng/L). Detection limit was calculated based on replicate blanks.

### **2.4.2.2. Total dissolved mercury and methylmercury**

Total Hg was determined using the EPA method 1631 B (EPA 1631B, 2001). Samples were previously fixed using bromine monochloride ( $BrCl$ ) in order to oxidize all forms of mercury to  $Hg^{2+}$ . Before analyses 20  $\mu$ L of hydroxylamine ( $NH_2OH.HCl$ ) were added to each sample to destroy free halogens, and then reduced with  $SnCl_2$  to convert  $Hg^{2+}$  to volatile  $Hg^0$ . Total mercury was then determined in a PSA Merlin system by CV-AFS. Mercury concentrations were determined by using a calibration curve made with 0 to 100 ng/L standards prepared by the same procedure as the samples. Analytical quality of the results was assured through calibration and by reagent blanks.

Methylmercury concentrations in pore waters were determined by GC-CV-AFS using automatic MERX equipment manufactured by Brooks Rand Labs, by distillation, aqueous phase ethylation, purge and trap and separation by gas chromatography (GC). For this analysis, 40 mL of the sample were placed in a Teflon distillation vessel and 35 mL of this



sample was distilled into the receiving vessel at 125 °C under N<sub>2</sub> flow. The distilled water was transferred to Teflon vials, buffered to pH 4.9 with an acetate buffer and ethylated in a closed purge vessel by the addition of sodium tetraethylborate (NaBEt<sub>4</sub>). The resultant solution was topped with Milli-Q water, capped and loaded into the auto-sampler. As each vial is pierced, the liquid is automatically transferred via gas pressure to a purge vessel where N<sub>2</sub> gas volatilizes mercury species to a Tenax® trap. This trap is then heated to thermally release mercury species in an Argon carrier gas stream, into a GC separation column in which mercury species are separated. Finally, these species are thermally reduced to Hg<sup>0</sup>, which is detected by an AFS detector.

MERX software integrates the detector signal and calculates MeHg concentrations based on calibration and sample volume information. For quality control, reagent blanks and analytical recoveries were performed. Calibration was made using MeHgCl standard solutions with a range of concentrations within the real samples. This last procedure was performed daily.

#### ***2.4.2.3. Total dissolved iron and manganese***

The determination of total dissolved Fe and Mn in pore waters was made using the atomic absorption spectrophotometer (Perkin-Elmer AAnalyst 100) with flame atomization method (FA-AAS). The measurement was made directly in pore waters acidified samples, using the same operating conditions as described before for sediment analysis. The quantification of Fe and Mn in the samples was done by the standard addition method, adding the corresponding amount of a 10 ppm solution for both Fe and Mn in order to obtain an added amount of 0.5, 1.0 and 2.0 µg of Fe or Mn.

#### ***2.4.2.4. Dissolved chloride***

Chloride (Cl<sup>-</sup>) levels in pore waters were determined using an argentometric method described in APHA (1995). An AgNO<sub>3</sub> (0.05 M) solution was prepared and standardized with a NaCl (0.05 M) solution. The NaCl salt was previously dried at 200 °C. For Cl<sup>-</sup> quantification, to 1 mL of each sample it was added approximately 5 mL of Milli-Q water and 6 drops of K<sub>2</sub>CrO<sub>4</sub>, used as indicator for the reaction. AgNO<sub>3</sub> was added until it was observed a change in the color (red-brown) characteristic of AgCr precipitation. Detection limit was quantified using the methodology proposed by Gonçalves (1996).

#### **2.4.2.5. Dissolved sulphate**

The determination of the ion  $\text{SO}_4^{2-}$  was made using a turbidimetric method described in APHA (1995). A solution of 50 mL of glycerol, 30 mL of concentrated HCl, 300 mL of deionised water, 100 mL of ethylic alcohol at 90 % and 75 g of NaCl was firstly prepared. To each pore waters sample, 5 mL of this mixture were added under constant stirring after which  $\text{BaCl}_2$  was added until the saturation point. Turbidity was measured using a spectrophotometer Hitachi U-2000 in cells of 5 cm length. Standard solutions (1 to 150 mM) were made using  $\text{Na}_2\text{SO}_4$  and diluted to obtain the same concentration range of the samples. Sulphate concentrations were calculated using the calibration curve (0 to 50 mM). Detection limit was quantified using the methodology previously referred.

#### **2.4.2.6. Dissolved inorganic sulfides**

To analyze total dissolved inorganic sulfides concentrations,  $[\text{HS}^-]_t$  ( $\Sigma [\text{H}_2\text{S}]+[\text{HS}^-]+[\text{S}^{2-}]+[\text{SX}^{2-}]$ ), an aliquot of 100 – 1000  $\mu\text{L}$  of pore waters was transferred to a polarographic cell containing 9 – 9.9 mL of a NaCl solution with 36 g/L and pH 10 – 12 (adjusted with NaOH 1M), previously deaerated. The concentration of total dissolved sulfides was determined by differential pulse with cathodic stripping voltammetry (DPCSV) (Luther *et al.*, 1985; Luther and Tsamakis, 1989). Analyses were made using a Metrohm station VA 694 and a processor VA 693, using a hanging mercury dropping electrode (HMDE). Ag/AgCl (NaCl) was used as the reference electrode and a platinum electrode was used as auxiliar. After a deposition time of 60 s, the cathodic sweep was made between -400 and -900 mV with constant velocity 6.0 mV/s.  $\text{HS}^-$  peak was at -700 mV. The standard addition method was used, using 100 and 200  $\mu\text{L}$  of a sulfide solution previously standardized to 500 mg/L with  $\text{Na}_2\text{S}\cdot\text{H}_2\text{O}$  by iodometry with Milli-Q water. The quantification of the signal was made in relation with the peak observed at the mentioned potential.

#### **2.4.2.7. Dissolved organic carbon**

Dissolved organic carbon (DOC) analyses were performed using a commercial Shimadzu TOC-5000A analyzer by high temperature catalytic oxidation (HTCO). The system was previously calibrated in the range of 0 – 500  $\mu\text{M}$  with potassium hydrogen phthalate in Milli-Q water. The coefficient of variation for the slope of the calibration curves was 1.6 %. Initially, carbonate was removed from the samples by bubbling during 15 minutes with

pure air (CO<sub>2</sub> free). Then, 100 µL aliquots were injected in the system furnace, filled with Shimadzu catalyst (Al<sub>2</sub>O<sub>3</sub> impregnated with 0.5 % Pt) at 680 °C. Blanks were made before and after analysis by injecting Milli-Q water, until the blank was low and stable (Benner and Strom, 1993).

## 2.5. Quality control

The analytical quality control of the results was a key issue during the analytical procedures in order to maintain precision and accuracy of the applied methods and it was done using sample or blank replicates. Detection limits were frequently calculated, as well as each error associated. Detection limits (*DL*) were calculated using the expression (Gonçalves, 1996):

$$DL = \sigma_{n-1} \times t \quad (8)$$

where  $\sigma_{n-1}$  is average standard deviation and  $t$  is the t-student parameter for ( $n-1$ ) freedom degrees. The average standard deviation was calculated after replicate analysis of blanks and certified materials. The error associated to each method was calculated using the expression (Gonçalves, 1996):

$$Error = \frac{\sigma_{n-1}}{\sqrt{n}} \times t \quad (9)$$

where  $n$  is the number of replicates used in each analysis.

Table 3 presents the detection limits calculated for the parameters determined in pore waters, as well as the error and precision for each method used.

**Table 3** – Detection limits, error and precision of Cl<sup>-</sup> and SO<sub>4</sub><sup>2-</sup> (mM), HS<sup>-</sup> (µM), Fe and Mn (µg/L), Hg and MeHg (ng/L) analysed in pore waters both in Cala do Norte and Ponta da Erva.

|                                    | <i>Detection Limit</i> | <i>Error (%)</i> | <i>Precision (%)</i> |
|------------------------------------|------------------------|------------------|----------------------|
| Cl <sup>-</sup> (mM)               | 0,02                   | 6,5              | 3,6                  |
| SO <sub>4</sub> <sup>2-</sup> (mM) | 0,17                   | 7,9              | 10                   |
| HS <sup>-</sup> (µM)               | 0,22                   | 1,5              | 5,2                  |
| Fe (µg/L)                          | 11,5                   | 4,3              | 2,3                  |
| Mn (µg/L)                          | 6,3                    | 2,9              | 5                    |
| Hg (ng/L)                          | 0,86                   | 1,8              | 5                    |
| MeHg (ng/L)                        | 0,02                   | 3,9              | 4,4                  |

Table 4 presents the average of concentrations determined with the certified materials for total Hg ( $\mu\text{g/g}$ ) with PACS-2 and MESS-3, MeHg ( $\text{ng/g}$ ) with BCR-580 and IAEA-405, Fe (%), Mn ( $\mu\text{g/g}$ ), Al (%) and Si (%) with MESS-1, BCSS-1 and AGV-1, quantified in sediments.

**Table 4** – Concentrations and average deviation of Hg ( $\mu\text{g/g}$ ), MeHg ( $\text{ng/g}$ ), Fe (%), Mn ( $\mu\text{g/g}$ ), Al (%) and Si (%) of the certified materials PACS-2, MESS-3, BCR-580, IAEA-405, MESS-1 and standard rock AGV-1.

| Certified material | Hg ( $\mu\text{g/g}$ ) | MeHg ( $\text{ng/g}$ ) | Fe (%)          | Mn ( $\mu\text{g/g}$ ) | Al (%)          | Si (%)          |
|--------------------|------------------------|------------------------|-----------------|------------------------|-----------------|-----------------|
| PACS-2*            | $3.04 \pm 0.20$        |                        |                 |                        |                 |                 |
| PACS-2**           | $2.84 \pm 0.07$        |                        |                 |                        |                 |                 |
| MESS-3*            | $0.091 \pm 0.009$      |                        |                 |                        |                 |                 |
| MESS-3**           | $0.083 \pm 0.003$      |                        |                 |                        |                 |                 |
| BCR-580*           |                        | $75.5 \pm 3.7$         |                 |                        |                 |                 |
| BCR-580**          |                        | $76.2 \pm 0.8$         |                 |                        |                 |                 |
| IAEA-405*          |                        | $54.9 \pm 5.3$         |                 |                        |                 |                 |
| IAEA-405**         |                        | $55.9 \pm 0.5$         |                 |                        |                 |                 |
| MESS-1*            |                        |                        | $3.05 \pm 0.17$ | $513 \pm 25$           | $5.84 \pm 0.20$ | $31.6 \pm 0.89$ |
| MESS-1**           |                        |                        | $3.08 \pm 0.04$ | $510 \pm 4$            | $5.83 \pm 0.03$ | $31.9 \pm 1.26$ |
| BCSS-1*            |                        |                        | $3.29 \pm 0.10$ | $229 \pm 15$           | $6.26 \pm 0.22$ | $30.9 \pm 0.47$ |
| BCSS-1**           |                        |                        | $3.20 \pm 0.11$ | $230 \pm 11$           | $6.35 \pm 0.10$ | $29.7 \pm 0.29$ |
| AGV-1*             |                        |                        | 4.73            | 750                    | 9.13            | 27.6            |
| AGV-1**            |                        |                        | $4.11 \pm 0.22$ | $746 \pm 21$           | $9.20 \pm 0.19$ | $28.7 \pm 2.34$ |
| Detection Limits   | 0.007                  | 0.100                  |                 |                        |                 |                 |

\* Values certified by NRCC, Canada 1998. \*\* Values obtained in the present study.

## **3. RESULTS**



### 3.1.Sediment characteristics

Visual inspection of the sediment slices in Cala do Norte and Ponta da Erva showed that samples appeared to be mostly constituted by mud and silt particles with exception at surface samples (Figure 4), where the sediment appeared to have coarser material. Sedimentary columns also presented a compact distribution.



**Figure 4** – Picture of one of the cores collected in Cala do Norte.

Oxygen levels in both sites in overlying water were around 240 mM and its concentrations decreased sharply in the sediment/water interface (121 mM), becoming undetectable below the first layer of the core.

Vertical profiles of pH, Eh (mV), water content and *LOI* (%) are presented in Figure 5. In Cala do Norte, pH ranged between 6.6 and 8.2. This vertical profile was characterized by an increasing pH to its maximum (8.2) at 3 cm depth and below decreased to 6.6, around 30 cm depth. Conversely, in Ponta da Erva, pH variations were not as notorious as observed in Cala do Norte. In Ponta da Erva profile pH varied irregularly between 6.9 at 7 cm depth and 7.3 at 2 and 6 cm depth.

Redox potential, Eh (mV) (Figure 5), varied markedly in Cala do Norte, from +39 mV in the sediment/water interface, decreasing to -377 mV at 35 cm depth. The pronounced variation and decrease in Eh was observed near the surface, as observed in the top of the

profile. In Ponta da Erva, Eh was negative in the first layer of the core and variation was not so markedly as in Cala do Norte, decreasing from -57 mV in sediment/water interface until -253 mV near 20 cm of sediment depth.

Higher water content (%) (Figure 5) was observed in the top sediment layers both in Cala do Norte and Ponta da Erva. In Cala do Norte water content was 66 % at the surface, decreasing to 50 % at the bottom of the core. In Ponta da Erva, the water content decreased from 65 % at surface reaching a minimum of 53 % at the bottom of the core.

In Cala do Norte, organic matter lost on ignition (LOI) profile, in %, varied mostly in sediment/water interface, decreasing between its maximum 8.8 % at surface to 3.6 % at 17 cm depth. In Ponta da Erva, LOI varied irregularly along the sedimentary column, between a minimum 4.0 % at 10 cm depth and maximum of 5.5 % at 7 cm depth.

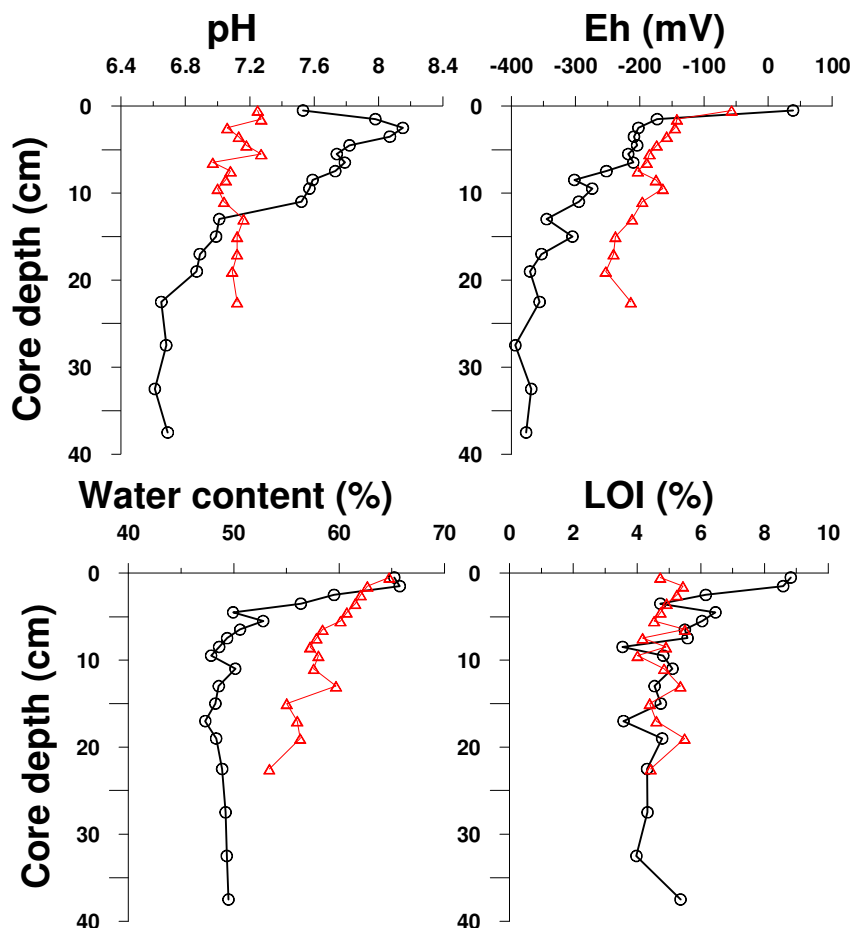


**Figure 5** – Vertical profiles of pH, Eh (mV), water content (%) and Lost On Ignition (%) both in sediment cores collected in Cala do Norte and Ponta da Erva. The black circles correspond to the Cala do Norte core and the red triangles to the core collected in Ponta da Erva.



### 3.2. Total concentrations of Al, Si, Fe and Mn in sediments

Vertical profiles of Al, Si, Fe (%) and Mn ( $\mu\text{g/g}$ ) concentrations for the sediment cores collected in Cala do Norte and Ponta da Erva are presented in Figure 6.

Aluminum concentrations (%) in Cala do Norte varied widely within a range between 5.6 and 9.9 %. At deepest layers these variations were less dense than the variations observed at surface layers. In Ponta da Erva an increment to 9.3 % at 5 cm depth was evidenced, the highest concentration observed in this core. The lowest concentration was 7.7 % at 13 cm depth.

Vertical profile of Si concentrations (%) in Cala do Norte varied irregularly between the lowest concentration 17 % at 6 cm depth and a maximum 30 % at 10 cm depth. In Ponta da Erva, despite presenting a similar irregularity as in Cala do Norte, the range of Si concentrations was slightly higher, varying between 27 % at 10 cm depth and 33 % at 5 cm depth.

Iron concentrations (%) in Cala do Norte varied irregularly between a minimum 2.4 % at sediment/water interface and a maximum at 13 cm depth (4.1 %). In Ponta da Erva the range of Fe concentrations was higher than in Cala do Norte, presenting a different shaped vertical profile. Iron concentrations varied between 4.6 % at 13 cm depth and 5.1 % at 7 cm depth.

Manganese concentrations ( $\mu\text{g/g}$ ) in Cala do Norte varied irregularly, showing the highest concentration at surface sediment reaching its maximum (614  $\mu\text{g/g}$ ) at 2 cm depth and decreasing to its minimum (312  $\mu\text{g/g}$ ) at 6 cm depth but variations in this profile, generally, were mostly around 400  $\mu\text{g/g}$ . In Ponta da Erva, sediments presented higher Mn concentrations than in Cala do Norte and a different shaped profile. It varied between its maximum concentration (1030  $\mu\text{g/g}$ ) at surface sediment and a minimum concentration (692  $\mu\text{g/g}$ ) at 9 cm depth. At the end of the core, Mn concentrations slightly increased.

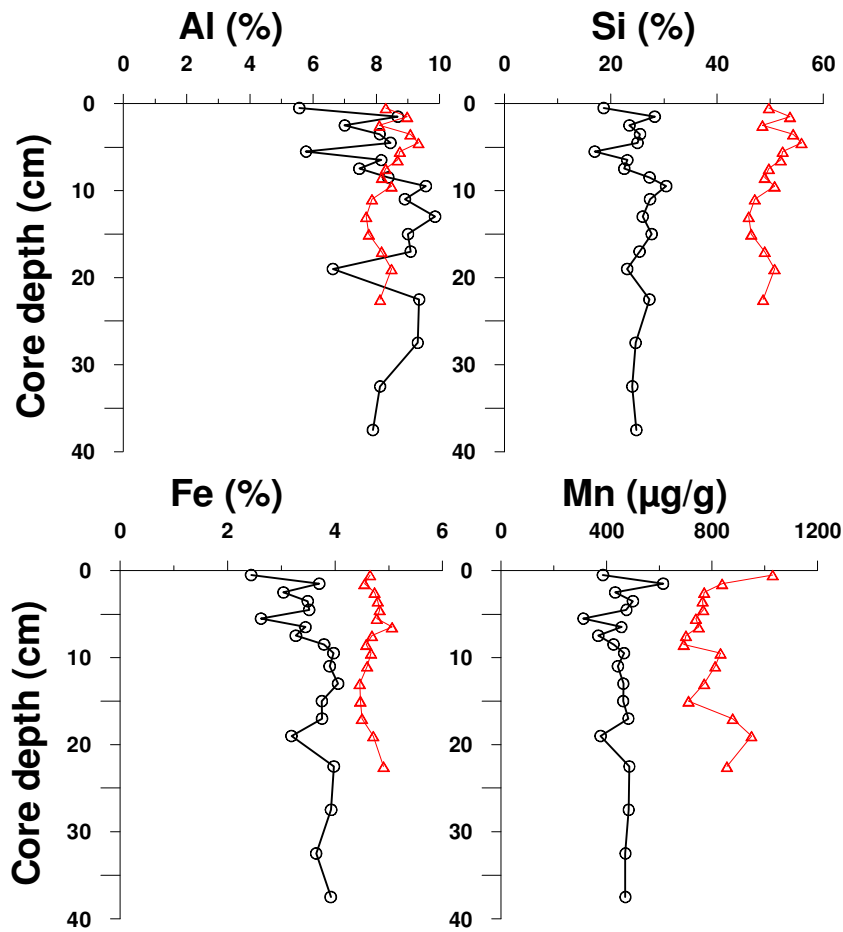


**Figure 6** – Vertical profiles of Al, Si, Fe (%) and Mn ( $\mu\text{g/g}$ ) concentrations both in sediment cores collected in Cala do Norte and Ponta da Erva. The black circles correspond to the Cala do Norte core and the red triangles to the core collected in Ponta da Erva.

### 3.3. Organic carbon in sediments

Vertical profiles of organic carbon,  $C_{\text{org}}$  (%), in Cala do Norte and Ponta da Erva are presented in Figure 7. In Cala do Norte,  $C_{\text{org}}$  varied irregularly showing the highest concentration (2.3 %) in the top layers and its lowest concentration (1.4 %) was observed at 22.5 cm depth. In Ponta da Erva, the same irregular shape was observed and concentrations varied between 1.9 % at 3 cm depth and 2.5 % at 15 cm depth.

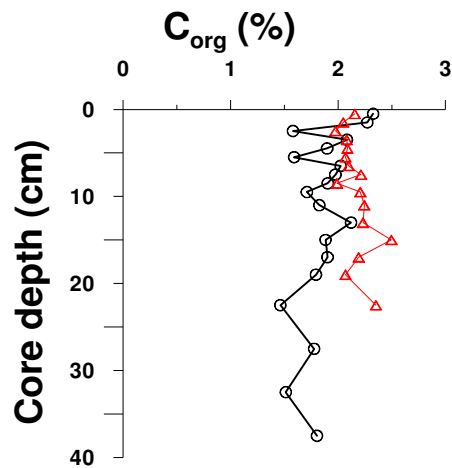


**Figure 7** – Vertical profiles of organic carbon (%) both in sediment cores collected in Cala do Norte and Ponta da Erva. The black circles correspond to Cala do Norte core and the red triangles to the core collected in Ponta da Erva.

### 3.4. Total dissolved concentrations of $\text{SO}_4^{2-}$ , $\text{HS}^-$ and $\text{Cl}^-$ in pore waters

Vertical distributions of  $\text{SO}_4^{2-}$  (mM),  $\text{Cl}^-$  (mM) and  $\text{HS}^-$  ( $\mu\text{M}$ ) concentrations measured in Cala do Norte and Ponta da Erva are presented in Figure 8.

In Cala do Norte,  $\text{SO}_4^{2-}$  concentrations ranged between its maximum concentration 18 mM at 2 cm depth, decreasing to its minimum concentration 7.3 mM at the end of the core (20 cm). In Ponta da Erva,  $\text{SO}_4^{2-}$  increased in top layers (0 – 3 cm) to its maximum concentration 16 mM. In subsequent layers concentrations decreased to the range of non detectable, below 13 cm depth.

In Cala do Norte  $\text{HS}^-$  ( $\mu\text{M}$ ) concentrations varied from the lowest values (5  $\mu\text{M}$ ) at top sediment (0 – 6 cm depth), rapidly increasing to its maximum concentration 122  $\mu\text{M}$  at 11 cm depth. Below this depth concentrations decreased to 45  $\mu\text{M}$  nearly the end of the core (20 cm). In Ponta da Erva,  $\text{HS}^-$  lowest concentrations (1.1  $\mu\text{M}$ ) were also evidenced at surface sediment (0 – 3 cm), increasing rapidly to the highest concentration 36  $\mu\text{M}$  at 6 cm depth. Below this depth concentrations varied irregularly around 20  $\mu\text{M}$ .

Chloride concentrations in Cala do Norte varied between a minimum 170 mM in sediment/water interface, increasing markedly to 380 mM in the first cm of the core. Below,  $\text{Cl}^-$  concentrations decreased to 330 mM at 10 cm depth, increasing again to 400 mM at 20 cm depth. Conversely, in Ponta da Erva profile, the highest  $\text{Cl}^-$  concentration

(360 mM) was observed in sediment/water interface. Then, concentrations decreased to 235 mM at the bottom (22.5 cm).

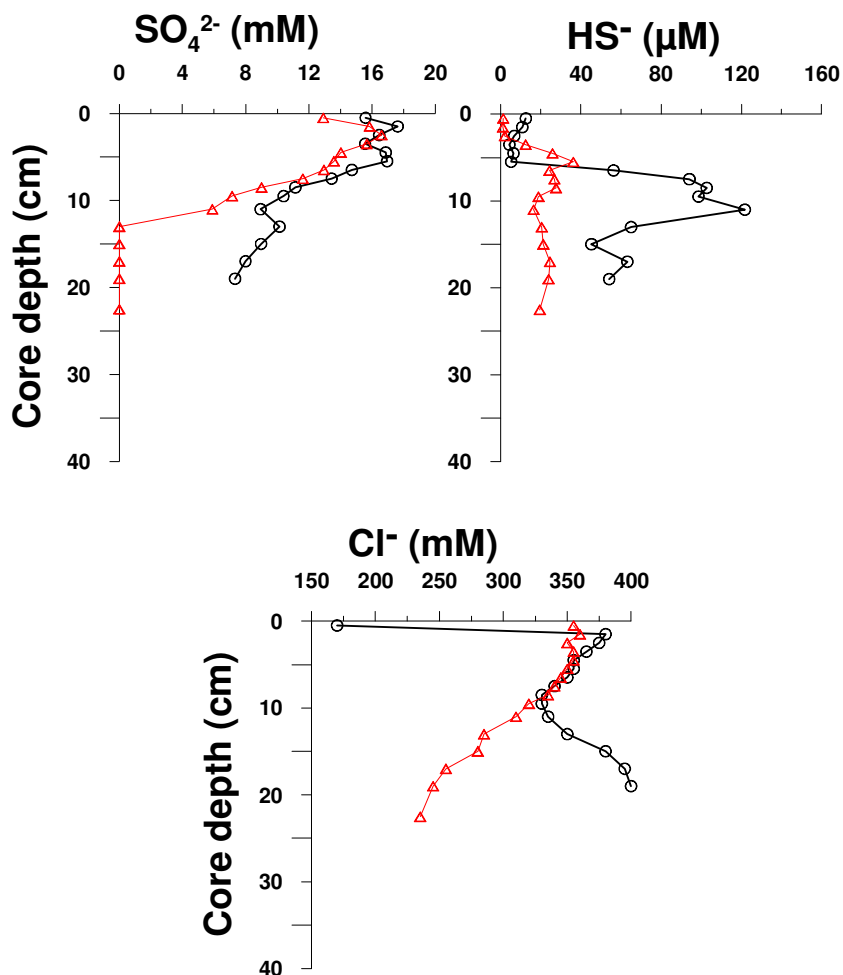


**Figure 8** – Vertical profiles of  $\text{SO}_4^{2-}$  (mM),  $\text{HS}^-$  ( $\mu\text{M}$ ) and  $\text{Cl}^-$  (mM) both in pore waters of the sediment cores collected in Cala do Norte and Ponta da Erva. The black circles correspond to Cala do Norte core and the red triangles to the core collected in Ponta da Erva.

### 3.5. Total dissolved concentrations of Fe and Mn in pore waters

Total concentrations of dissolved Fe ( $\mu\text{g/L}$ ) both in Cala do Norte and Ponta da Erva are presented in Figure 9. In Cala do Norte, Fe increased in the first cm to its maximum (371  $\mu\text{g/L}$ ), decreasing until 11 cm depth where was observed the lowest Fe concentration (53  $\mu\text{g/L}$ ). Below this depth a markedly increase was observed to 265  $\mu\text{g/L}$  between 15 and 17 cm depth, decreasing again in the last layer. In Ponta da Erva profile was observed a

different shaped profile and the range of Fe concentrations was much higher, varying between 98 and 8451  $\mu\text{g/L}$ , rapidly increasing to its maximum in top layers (0 – 8 cm). Below this depth concentrations varied irregularly until the end of the core, where concentration increased again to 7841  $\mu\text{g/L}$ .

Dissolved manganese concentrations ( $\mu\text{g/L}$ ) both in Cala do Norte and Ponta da Erva are also presented in Figure 9. In Cala do Norte, profile clearly showed its highest concentration (842  $\mu\text{g/L}$ ) at sediment/water interface, decreasing to the lowest concentrations observed (79  $\mu\text{g/L}$ ) at 17 cm depth. In Ponta da Erva, the range of Mn concentrations was much higher than in Cala do Norte but the vertical profile was similar. The highest concentration (7350  $\mu\text{g/L}$ ) was also observed at sediment/water interface, rapidly diminishing to the lowest concentration (50  $\mu\text{g/L}$ ) at 9 cm depth. Then the concentrations increase in the deepest 3 layers.

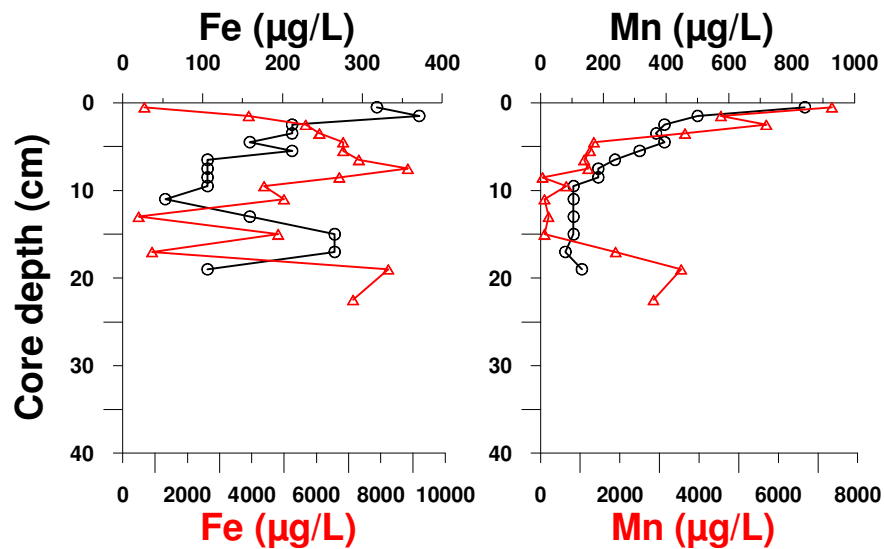


**Figure 9** – Vertical profiles of Fe and Mn ( $\mu\text{g/L}$ ) both in pore waters of the sediment cores collected in Cala do Norte and Ponta da Erva. The black circles correspond to Cala do Norte core and the red triangles to the core collected in Ponta da Erva.

### 3.6. Dissolved organic carbon

Dissolved organic carbon (mg/L) profiles are presented in Figure 10 both in sediment cores of Cala do Norte and Ponta da Erva. In Cala do Norte, DOC varied irregularly between the lowest concentration (8.6 mg/L) at 3 cm depth and the highest (42 mg/L) at 17 cm depth. In Ponta da Erva, the same irregular profile was observed and varied between the lowest concentration (6.8 mg/L) at 3 cm depth and the highest (60 mg/L) at 19 cm depth.

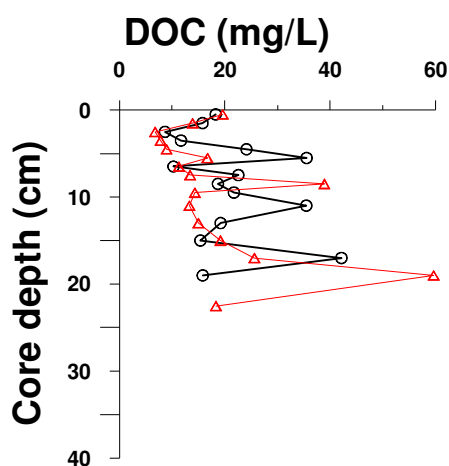


**Figure 10** – Vertical profiles of dissolved organic carbon (mg/L) both in pore waters of the sediment cores collected in Cala do Norte and Ponta da Erva. The black circles correspond to Cala do Norte core and the red triangles to the core collected in Ponta da Erva.

### 3.7. Mercury

#### 3.7.1. Total Hg and MeHg in sediments

Total mercury ( $Hg_T$ ) concentrations ( $\mu\text{g/g}$ ) both in Cala do Norte and Ponta da Erva are presented in Figure 11. In Cala do Norte,  $Hg_T$  concentrations were considerably higher compared to the values obtained in Ponta da Erva. The lowest concentrations in Cala do Norte core were observed at sediment/water interface ( $1 \mu\text{g/g}$ ) and increased rapidly to its maximum ( $18 \mu\text{g/g}$ ) at 15 cm depth. Below this depth, concentrations slightly decreased. Conversely, in Ponta da Erva the range of  $Hg_T$  concentrations was much smaller and varied between 0.4 and 0.5  $\mu\text{g/g}$ . Generally, concentrations decreased until 13 cm depth, increasing after this depth.

The vertical profiles for MeHg (ng/g) both in Cala do Norte and Ponta da Erva are also presented in Figure 11. In Cala do Norte, MeHg varied between the lowest concentration (1 ng/g) at the sediment/water interface, increasing markedly to the highest concentration (87 ng/g) at 7 cm depth. Below this depth, it rapidly decreased until not detectable concentrations at the bottom of the core. In Ponta da Erva, MeHg concentrations were much smaller than in Cala do Norte and ranged between not detectable below 5 cm depth and 0.54 ng/g at 3 cm depth.

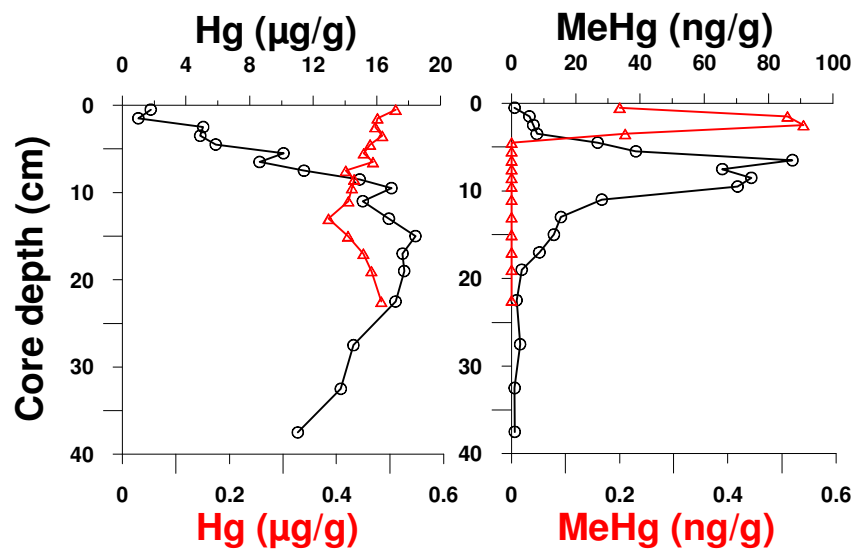


**Figure 11** – Vertical profiles of Hg<sub>T</sub> (µg/g) and MeHg (ng/g) both in sediment cores collected in Cala do Norte and Ponta da Erva. The black circles correspond to Cala do Norte core and the red triangles to the core collected in Ponta da Erva.

### 3.7.2. Hg and MeHg in pore waters

Vertical profiles of total dissolved mercury (Hg<sub>T</sub>), reactive dissolved mercury (Hg<sub>R</sub>) and dissolved methylmercury (MeHg) concentrations (ng/L) for both Cala do Norte and Ponta da Erva are presented in Figure 12.

In Cala do Norte, Hg<sub>R</sub> varied irregularly between a range between detection limit (0.02 ng/L) to 29 ng/L with the highest concentration at 13 cm depth. Conversely, in Ponta da Erva, Hg<sub>R</sub> vertical profile varied irregularly between the range of 6.5 to 15 ng/L and concentrations were higher than those found in Cala do Norte in upper sediment layers (0 – 11 cm depth).

In Cala do Norte,  $Hg_T$  varied irregularly between the lowest concentration (6.8 ng/L) at the bottom of the core (19 cm depth) and the highest concentration (166 ng/L) at 13 cm depth. In Ponta da Erva,  $Hg_T$  concentrations also varied irregularly and were considerably lower. The minimum concentration (34 ng/L) was observed at 13 cm depth and the highest concentration (60 ng/L) was observed at 8 cm depth.

With respect to MeHg concentrations in Cala do Norte, MeHg varied between the lowest concentration (0.9 ng/L) observed at the sediment/water interface, increasing to its maximum (26 ng/L) at 9 cm depth. Below this depth, MeHg decreased gradually until the end of the core. Conversely, in Ponta da Erva, MeHg concentrations are lower than in Cala do Norte and varied between the range of non detectable at the bottom of the core and 3.4 ng/L observed at 5 cm depth.

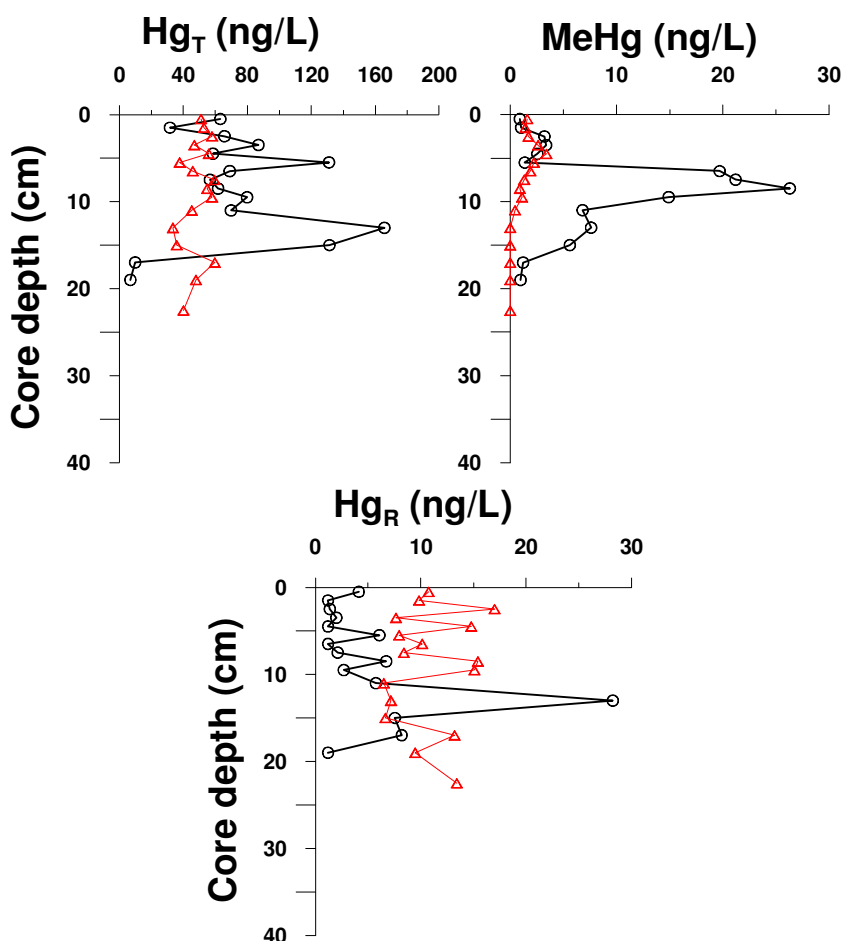


**Figure 12** – Vertical profiles of  $Hg_T$  ( $\mu\text{g/L}$ ) and MeHg (ng/g) both in pore waters of the sediment cores collected in Cala do Norte and Ponta da Erva. The black circles correspond to Cala do Norte core and the red triangles to the core collected in Ponta da Erva.



Methylmercury in overlying water of Cala do Norte was 2.6 ng/L while in Ponta da Erva was 1.3 ng/L. Total and reactive Hg in overlying water of Cala do Norte were, respectively, 37.9 and 22 ng/L while in Ponta da Erva the observed concentrations were 16.9 ng/L for Hg<sub>T</sub> and Hg<sub>R</sub> was below the detection limit (0.02 ng/L).



## **4. DISCUSSION**



## 4.1. Sediment characteristics

### 4.1.1. Solid sediments

Visual inspection of the cores collected, in Cala do Norte (Figure 2-A and Figure 4) and in Ponta da Erva (Figure 2-B), showed that their sediments were mostly constituted by mud and silt particles with exception of the topmost layers, where sediment appeared to be constituted by coarser material. Sediments in Cala do Norte also seemed to be more compact in comparison to the sediments collected in Ponta da Erva. This observation was corroborated with the higher water content (%) determined for the Cala do Norte core. Moreover, in both sites the water content was always higher in the topmost layers decreasing downwards.

Oxygen penetration occurred only in the first millimeters near the sediment/water interface. Dissolved O<sub>2</sub> measurements along the core samples confirmed its depletion immediately below the first 2-mm, in agreement with the field observations of its brown color indicating that the sediment had sub-oxic/anoxic characteristics. Despite the existence of macrofauna (such as polychaetes) in both locations, there was no evidence that these organisms significantly influenced the penetration of dissolved oxygen into the sedimentary column, as it was observed in some areas by other authors, namely Cardoso *et al.* (2008).

It was notorious that vertical profiles of the sediment core collected in Cala do Norte presented higher fluctuations of pH, Eh, water content and *LOI* in the topmost layers, compared to the one collected in Ponta da Erva. These variations may be attributed to the nearby effluent discharges from the chlor-alkali plant located in Cala do Norte, near the sampling area, altering the sediment characteristics. On the contrary, variations on pH and redox conditions were markedly different in Ponta da Erva (see Figure 5), which showed to vary less in depth compared to the Cala do Norte core. Moreover, the increase on pH in surface layers of Cala do Norte (higher than in Ponta da Erva) may be related with the addition of calcium carbonate to the effluent, once this procedure is usual in treatments of industrial effluents, in order to reduce acidity in waste waters (Canário, 2004). On the other hand, these variations in Cala do Norte sediments may be linked with the availability of H<sup>+</sup> concentrations and related with organic matter degradation (Froelich *et al.*, 1979; Du Laing *et al.*, 2009; Lesven *et al.*, 2010), whereas in Ponta da Erva

the sediments showed to be more acidic in topmost layers than in Cala do Norte. Once metabolic  $H^+$  is released during organic matter degradation, it may increase the acidity in pore waters (Lesven *et al.*, 2010). Even,  $H^+$  ions in pore waters are partially consumed through reactions with Mn and Fe oxides/hydroxides (Lesven *et al.*, 2010), which may reflect pH variations at surface layers where sediment is oxic/sub-oxic. These changes in pH associated with variations in redox potential, reinforces the existence of oxic/sub-oxic conditions. Thus, a sharp decrease in Eh was observed at both places but was more pronounced in Cala do Norte core, as a result of microbial consumption of  $O_2$  in the first millimeters of the surface sediment, followed by successive diagenetic processes involving other oxidants (e.g., Lesven *et al.*, 2010).

Organic matter content in sediments, measured as lost on ignition, was more pronounced in Cala do Norte core than in Ponta da Erva, both in range (3.5 to 6 %) and variations in surface layers, almost certainly due to the low hydrodynamics of the channel, which may induce higher deposition rates of organic matter probably due to anthropogenic inputs. This may result from deposition and resuspension processes as a consequence of higher adsorption of organic matter in the water column (Canário *et al.*, 2003a).

The vertical profiles of Si, Fe and Mn were normalized to Al and are presented in Figure 13. Aluminum is a good proxy for fine grain size particles and the normalization to this element is the attempt to compensate the natural variability of trace metals in sediments of different areas, so that any anthropogenic metal contributions may be detected and quantified (Loring *et al.*, 1991). As an example, high concentrations of Al associated with low concentrations of Si suggests that the sediment is mainly composed with aluminum-silicates (Stumm and Morgan, 1996).

In Cala do Norte site, variations on Si/Al ratios (Figure 13) occurred mostly between the 2.0 and 3.7. In Ponta da Erva, the range of values was slightly higher, varying between a minimum 3.3 at 11 cm depth and a maximum 4.0 at 5 cm depth. Sediments from the Tagus Estuary show a wide range of Si/Al ratios (0.82–52) reflecting the different mixtures of coarse and fine-grained material (Canário *et al.*, 2005). These data confirms that sediments were composed by fine grain size particles such as mud and silt, probably being constituted by aluminum-silicates particles (Stumm and Morgan, 1996).

In Cala do Norte, Fe/Al ratios (Figure 13) were marked by small variations in the upper 15 cm. Below variations were more spaced reaching the highest values at 20 and 40 cm depth. Normalization to Al changes significantly the Fe profile shape (compare with Figure 6), suggesting that Fe distribution along the sediment core was not only influenced by the sediment composition but also by Fe diagenetic reactions such as the precipitation and/or dissolution of Fe oxyhydroxides (4) in the sub-oxic layers (Du Laing *et al.*, 2009). In Ponta da Erva, variations were spaced along the vertical profile and ratios had a slightly higher range, compared to Cala do Norte. The highest ratio in Ponta da Erva was also observed at the bottom of the core (22.5 cm depth). Higher Fe/Al ratio in Ponta da Erva was related with high Fe concentrations found in Ponta da Erva, which were higher than in Cala do Norte, evidencing the Fe content enrichment in this area of the estuary is possibly due to the proximity of a salt-marsh, which is known to have and export large quantities of iron (Vale *et al.*, 2003; Canário *et al.*, 2007).

In Cala do Norte, manganese concentrations normalized to Al (Figure 13) showed a different pattern compared to the vertical distribution of total Mn concentrations (see Figure 6). The Mn/Al vertical profile evidenced higher values in upper layers (0 – 13 cm), gradually decreasing. Below 13 cm depth, the ratio slightly increased downwards. In Ponta da Erva, Mn/Al profile was slightly different from the vertical distribution of Mn concentrations (Figure 6), conversely to the observed in Cala do Norte. Still, as the same observed for Fe, concentrations and ratios observed for Mn in Ponta da Erva core were higher than in Cala do Norte, which evidences the high enrichment on Mn, probably related with freshwater inputs from Sorraia river (Sundby *et al.*, 1981).

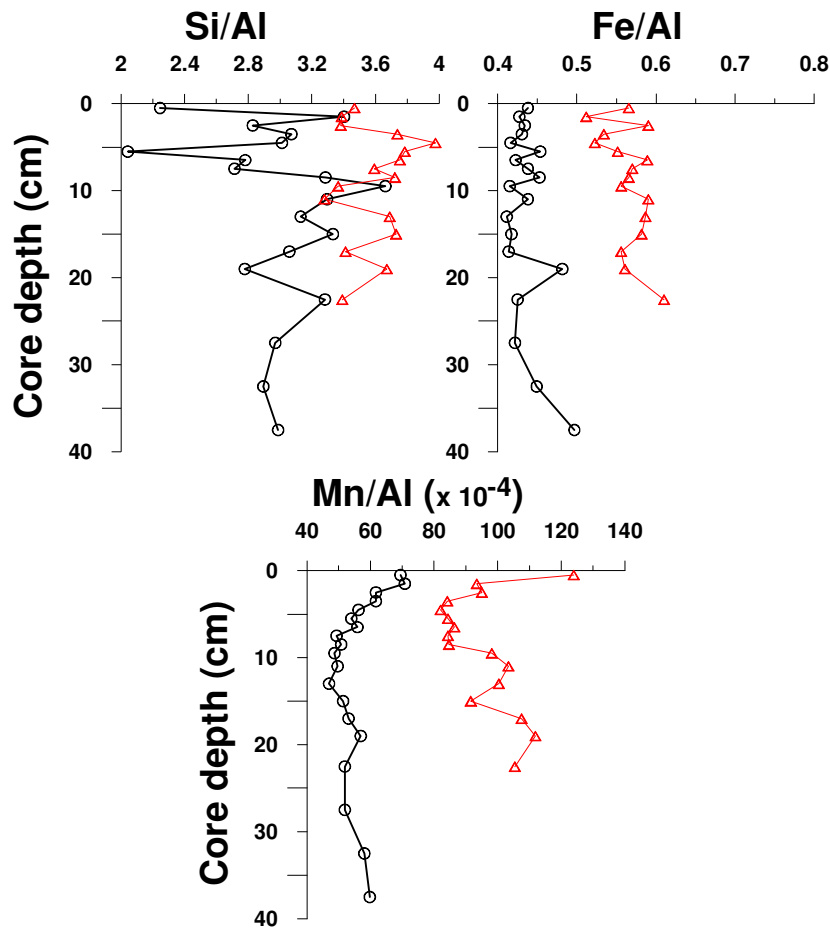


**Figure 13** – Vertical profiles of Si, Fe and Mn normalized to Al both in sediment cores collected in Cala do Norte and Ponta da Erva. The black circles correspond to Cala do Norte core and the red triangles to the core collected in Ponta da Erva.

#### 4.1.2. Pore waters

With respect to the concentrations of chloride anions in the pore waters it was possible to observe two different patterns. If by one hand the concentration in the first layer was considerably lower in Cala do Norte than the one observed in Ponta da Erva (see Figure 8), on the other hand the concentrations in the deepest layers, below approximately 15 cm depth, were significantly higher in Cala do Norte station. The density stratification and the presence of freshwater discharged from the industrial effluent nearby in Cala do Norte was observed by the high increment in the chloride concentrations of pore waters below the sediment/water interface. Chlorinity variations in depth pore waters from the core collected in Cala do Norte may be related with the mixture of the effluent discharges



and subsequent tidal oscillations (Fortunato *et al.*, 1997). These contrast with the linear decrease on  $\text{Cl}^-$  concentrations observed in Ponta da Erva.

Due to the strong anoxic conditions, microorganisms can use other electron acceptors than the preferential  $\text{O}_2$  in the first centimeters of the sediment, particularly Mn and Fe oxides/hydroxides, for the mineralization of organic matter (through bacterially mediated oxidation) leading to reductive dissolution of Mn(III and IV) into Mn(II) and Fe(III) into Fe(II) ions (Froelich *et al.*, 1979; Du Laing *et al.*, 2009; Lesven *et al.*, 2010). Dissolved Mn concentrations generally are good indicators of redox conditions prevailing in sediments (Gagnon *et al.*, 1997). The high dissolved Mn concentrations observed near the sediment/water interface (Figure 9) and its rapidly decrease in pore waters within the first layers of the sediment, both in Cala do Norte and Ponta da Erva, may reflect the oxic/sub-oxic conditions in the upper sedimentary column, where Mn oxyhydroxides may precipitate, thereby reducing the amount of other soluble trace metals in pore waters, such as Hg (Gagnon *et al.*, 1997; Du Laing *et al.*, 2009).

In Cala do Norte, the sequence of organic matter degradation does not appear to be changed, once it was observed high concentrations of dissolved Fe in pore waters at 2 cm depth, decreasing sharply below this depth. Due to oxic conditions at the sediment/water interface, relatively low dissolved Fe concentrations were observed, though, a rapid decrease in Eh may induced the solubility of precipitated Fe oxyhydroxides (reaction 3), therefore increasing the dissolved Fe concentrations at 2 cm depth (Figure 9). It is interesting to notice that below 6 cm depth Eh decreased, as well as pH decreased therefore increasing the acidity of the sediment. These observations reflected the solubility of Fe, being observed an increase on its concentrations due to dissolution of Fe oxyhydroxides. Moreover, as referred by Du Laing *et al.*, (2009), the stability of Fe(II) and Fe oxyhydroxides mainly depends on the combination of factors such as pH and Eh in sediments. The nearly amorphous  $\text{Fe}(\text{OH})_3$  minerals (ferrihydrite) are reduced at higher Eh, in relation to a given pH, than do the crystalline minerals of  $\text{FeOOH}$  (goethite) or  $\text{Fe}_2\text{O}_3$  (hematite) (Du Laing *et al.*, 2009).

In Ponta da Erva, dissolved Fe concentrations increased below the  $\text{SO}_4^{2-}$  reduction. The existence of different species used in the organic matter degradation is important to understand the different regions with redox conditions in sediments (Stumm and Morgan, 1996). Regarding the sequence proposed for the organic matter oxidation, it can

be changed due to the existence of Fe oxides with different physico-chemical stabilities that influence the preference for Fe(III) or  $\text{SO}_4^{2-}$  in diagenetic reactions (Postma and Jakobsen, 1996; Du Laing *et al.*, 2009). Consequently, organic matter can be degraded simultaneously by redox pairs Fe(III)/Fe(II) and  $\text{SO}_4^{2-}/\text{S}^{2-}$ , co-existing both reactions in the same sediment layers (Postma and Jakobsen, 1996), which could justify the increment on dissolved Fe concentrations below the sulphate reduction in Ponta da Erva.

Sulphate concentrations in both cores were higher in top layers, conversely to the lowest  $\text{HS}^-$  concentrations determined in the correspondent layers (Figure 14). Below the oxic/sub-oxic layer of the sedimentary column (first centimeters above 6 cm depth in Cala do Norte and 3 cm depth in Ponta da Erva), sulphate was being reduced forming  $\text{HS}^-$ . Depletion in dissolved  $\text{O}_2$  and after the reduction of Mn(IV) and Fe(III), degradation of organic matter proceeds to sulphate reduction (reaction 5), forming reduced sulphur compounds (Froelich *et al.*, 1979; Caetano, 1992), and explaining the increments on sulphide concentrations.

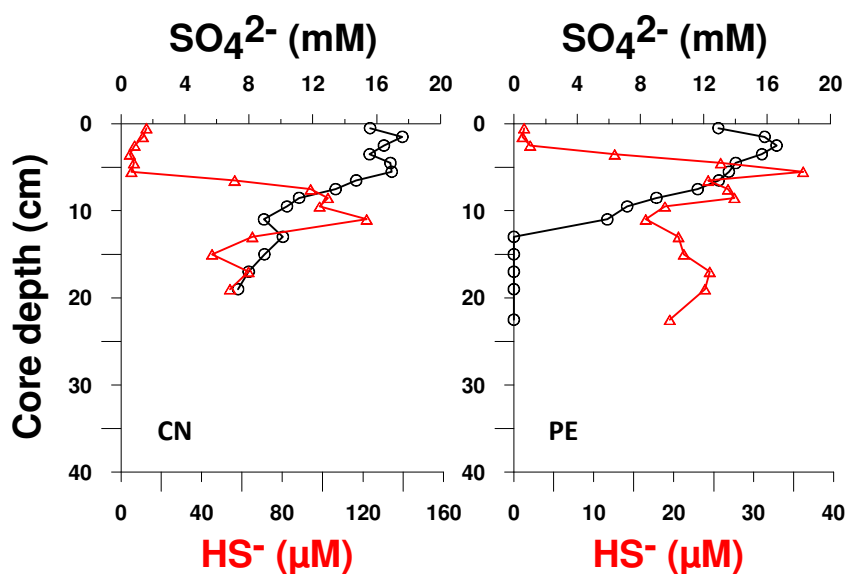


**Figure 14** - Vertical profiles of  $\text{SO}_4^{2-}$  (mM) and  $\text{HS}^-$  ( $\mu\text{M}$ ) both in pore waters of the sediment cores collected in Cala do Norte (CN) and Ponta da Erva (PE). The black circles correspond to  $\text{SO}_4^{2-}$  vertical distribution and the red triangles to  $\text{HS}^-$  vertical distribution.

If sulphate is determinant to enhance SRBs activity, it is important to assess if sulphate is in excess and therefore interfering in the microbial degradation of organic matter. Previous work from Canário *et al.* (2003b) reported high sulphate and sulphide

concentrations in pore waters from sediments nearby the industrial effluent in Cala do Norte, suggesting that these may derived from aluminum sulphate used as a coagulator in the plant sewage treatment. The excess of sulphate ( $\Delta \text{SO}_4^{2-}$ ) can be estimated by:

$$\Delta \text{SO}_4^{2-} = [\text{SO}_4^{2-}]_{\text{measured}} - [\text{Cl}^-] / 19.64 \quad (9)$$

where 19.64 represents the molar ratio of  $\text{Cl}^-$  to  $\text{SO}_4^{2-}$  in seawater (Culkin, 1965). Applying the same formulation based on sulphate and chlorinity data from this studied cores, no excess of sulphate was determined for both locations ( $\Delta \text{SO}_4^{2-}$  was lower than 0). In fact, the core collected in Cala do Norte presented the same range of concentrations for  $\text{SO}_4^{2-}$  as in Ponta da Erva. This may suggest that aluminum sulphate may no longer being added in sewage treatment, otherwise, sulphate and aluminum concentrations should be higher and probably sulphate would be in excess affecting the diagenetic mechanisms in the sedimentary column.

## 4.2. Mercury in sediments

The present study shows that mercury and MeHg concentrations in sediments were much higher in Cala do Norte than in Ponta da Erva (see Figure 11). Total mercury levels determined in Cala do Norte (up to 18  $\mu\text{g/g}$ ) were lower than the ones observed by Canário *et al.* (2005, 2007) for several contaminated sites in the Tagus Estuary, whereas in Ponta da Erva Hg concentrations (up to 0.5  $\mu\text{g/g}$ ) were one order of magnitude lower than in Cala do Norte. Comparing these results with other national coastal environments (Table 5), the Tagus Estuary can be considered moderately to highly Hg contaminated, contrasting with Ria de Aveiro, which presents the highest Portuguese Hg concentrations up to 343  $\mu\text{g/g}$  (Pereira *et al.*, 1998; Ramalhosa, 2002). Other Portuguese estuarine systems, such as the Mira Estuary, show by far the lowest total Hg levels (IPIMAR, 2010). On the other hand, MeHg concentrations were apparently higher than in Ria de Aveiro, despite Cala do Norte presented lower Hg concentrations in sediments. The assessment of MeHg concentrations in sediments of Portuguese estuarine systems is scarce and despite of Ria de Aveiro and Tagus, the other studied systems (e.g., Guadiana and Sado estuaries)

(Table 5) show a low degree of MeHg contamination compared with data from the present study.

**Table 5** – Comparison of total mercury (Hg) and methylmercury (MeHg) concentrations in sediments from Tagus Estuary with other national estuarine / coastal systems.

| Estuarine/coastal system | Hg <sub>T</sub> (µg/g) | MeHg (ng/g) | References                                    |
|--------------------------|------------------------|-------------|---|
| Tagus (Portugal)         | 0.4 – 18               | 0.1 – 87    | Present study                                 |
| Tagus (Portugal)         | 0.01 – 66.7            | 0.3 – 43    | Canário <i>et al.</i> (2005, 2007)            |
| Ria de Aveiro (Portugal) | 343                    | 12.4        | Pereira (1998)<br>Ramalhosa (2002)            |
| Guadiana (Portugal)      | 0.45 – 1.25            | 0.17 – 0.27 | Canário <i>et al.</i> (2007)<br>IPIMAR (2001) |
| Mira (Portugal)          | 0.005 – 0.081          |             | IPIMAR (2010)                                 |
| Sado (Portugal)          | 0.029-0.306            | 2.30-5.90   | Canário <i>et al.</i> (2007)                  |
| Douro (Portugal)         | 0.121-0.893            |             | IPIMAR (2010)                                 |

International coastal systems, generally, show lower Hg concentrations in sediments compared to data observed in the present study and contrasting with the worldwide case of Minamata Bay in Japan (over 4000 µg/g; Tomiyasu *et al.*, 2006). The Tagus Estuary mercury data (present study) has the same order of magnitude as Hg concentrations in the Wuli Estuary, China (up to 64 µg/g; Wang *et al.*, 2009).

Methylmercury concentrations were considerable higher in Cala do Norte (up to 87 ng/g) than in Ponta da Erva (up to 0.54 ng/g) (see Figure 11). On the other hand, MeHg concentrations were apparently higher than concentrations in sediments of the Wuli Estuary, China (up to 26 ng/g; Wang *et al.*, 2009). Other estuarine systems present much lower MeHg concentrations compared to the 87 ng/g obtained in the present study. Table 6 summarizes various data published in other works.

**Table 6** – Comparison of total mercury (Hg) and methylmercury (MeHg) concentrations in sediments from international estuarine / coastal systems (modified from Oh *et al.*, 2010).

| Estuarine/coastal system         | Hg <sub>T</sub> (µg/g) | MeHg (ng/g)   | References                    |
|----------------------------------|------------------------|---------------|-------------------------------|
| Minamata Bay (Japan)             | 1400 - 4300            |               | Tomiyasu <i>et al.</i> (2006) |
| Lake Shihwa (Korea)              | 0.02 – 0.28            | <0.026 – 0.67 | Oh <i>et al.</i> (2010)       |
| Oi island (Korea)                | 0.008 – 0.028          |               | Oh <i>et al.</i> (2010)       |
| Wuli (China)                     | 44 – 64                | 8.0 – 26      | Wang <i>et al.</i> (2009)     |
| Seine–Vasière Nord (France)      | 0.15 – 1.5             | 0.6 – 3.0     | Ouddane <i>et al.</i> (2008)  |
| Medway–Horrid Hill (UK)          | 0.02 – 1.2             | 0.02 – 4.3    | Ouddane <i>et al.</i> (2008)  |
| Medway (UK)                      | 0.02 – 1.30            |               | Spencer <i>et al.</i> (2006)  |
| Lot-Garonne (France)             | 0.06 – 0.5             |               | Schafer <i>et al.</i> (2006)  |
| Adour (France)                   | 0.004 – 1.46           | 0.1 – 1.6     | Stoichev <i>et al.</i> (2004) |
| Ore (Sweden)                     | 0.03 – 0.12            | 0.01 – 1.00   | Kwokal <i>et al.</i> (2002)   |
| Krka (Croatia)                   | 0.10 – 1.42            | 0.01 – 1.40   | Kwokal <i>et al.</i> (2002)   |
| Seine (France)                   | 0.3 – 1.0              | 0.1 – 6.0     | Mikac <i>et al.</i> (1999)    |
| Annapolis Harbor, Maryland (USA) | 0.498 ± 0.053          | 8.5 ± 1.5     | Mason and Lawrence (1999)     |
| Mainstem, Chesapeake Bay (USA)   | 0.08 – 0.18            | 1.0 – 1.5     | Mason <i>et al.</i> (1999)    |
| British estuaries (UK)           | 0.05 – 4.46            | 0.1 – 4.0     | Craig and Moreton (1986)      |

Some works have been devoted to study diagenetic processes and even the Hg mobility in contaminated sediments (Gobeil and Cossa, 1993; Gagnon *et al.*, 1997; Ramalhosa, 2002; Canário, 2004; Canário *et al.*, 2005, 2007; Válega *et al.*, 2008a). Normalization of Hg concentrations to Al content (Hg/Al ratios) (Figure 15) were made to assess Hg variability in relation with the mineral particles. Cala do Norte (ranged from 0.1 to 2.68) presented higher ratios than in Ponta da Erva (ranged from 0.05 to 0.06), evidencing relatively enhancements in Cala do Norte at 6 and 20 cm depth compared with Hg concentrations profile (see Figure 11).

Both, Cala do Norte and Ponta da Erva, Hg/Al profiles did not show significant variations in shape compared with Hg concentration profiles, which suggests that its vertical distribution is explained by Hg deposition over time.

Normalization of MeHg to Al (Figure 15) in Cala do Norte also did not show significant differences compared with MeHg concentrations profile, thereby reinforcing the idea of an increased methylation potential due to bioavailability of inorganic Hg (Ullrich *et al.*, 2001). As in Cala do Norte, Ponta da Erva MeHg/Al profile was not different from the MeHg concentrations profile, indicating that the presence of MeHg is related with methylation processes instead of a direct relation with the nature of particles.

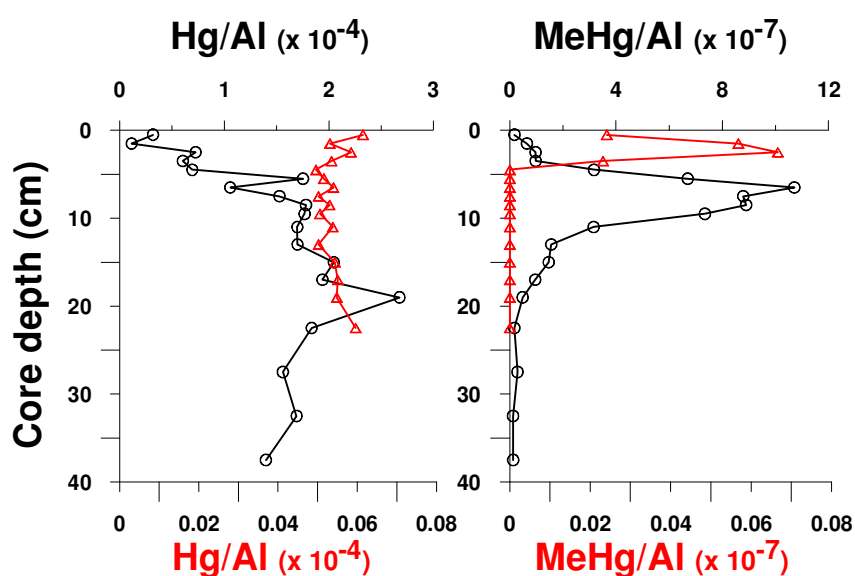


**Figure 15** – Vertical profiles of Hg and MeHg normalized to Al both in sediment cores collected in Cala do Norte and Ponta da Erva. The black circles correspond to Cala do Norte core and the red triangles to the core collected in Ponta da Erva.

Normalization of Hg to organic carbon ( $C_{org}$ ) (Figure 16), in Cala do Norte enhanced the peak concentrations but the Hg/ $C_{org}$  profile is similar to the one of Hg concentrations. This may suggest some relation with the organic matter content but reinforces that Hg in Cala do Norte is present due to anthropogenic contamination (Mason and Lawrence, 1999). In Ponta da Erva, the Hg/ $C_{org}$  profile is also similar to the Hg concentrations profile (Figure 11), which also suggests that the anthropogenic influence of Hg in Ponta da Erva

is probably related with agricultural activities and/or hydrological transport along the Tagus estuary (Fortunato *et al.*, 1997; Silva *et al.*, 2004).

The vertical profile of methylmercury normalization to  $C_{org}$  content (Figure 16) in Cala do Norte is similar compared with the MeHg one. In Ponta da Erva, the shape of the MeHg/ $C_{org}$  ratio is also comparable with the MeHg concentrations profile (Figure 11). These results suggest that MeHg distribution along the sediment cores were not influenced by the  $C_{org}$  distribution but were related to *in situ* MeHg production (Heyes *et al.*, 2006; Schafer *et al.*, 2010). Since there is no influence of this parameter, the results point for other environmental factors being the responsables for MeHg concentrations at each sediment layer, such as the availability of inorganic mercury or even bacterial activity (Merrit and Amirbahman, 2009; Schafer *et al.*, 2010).

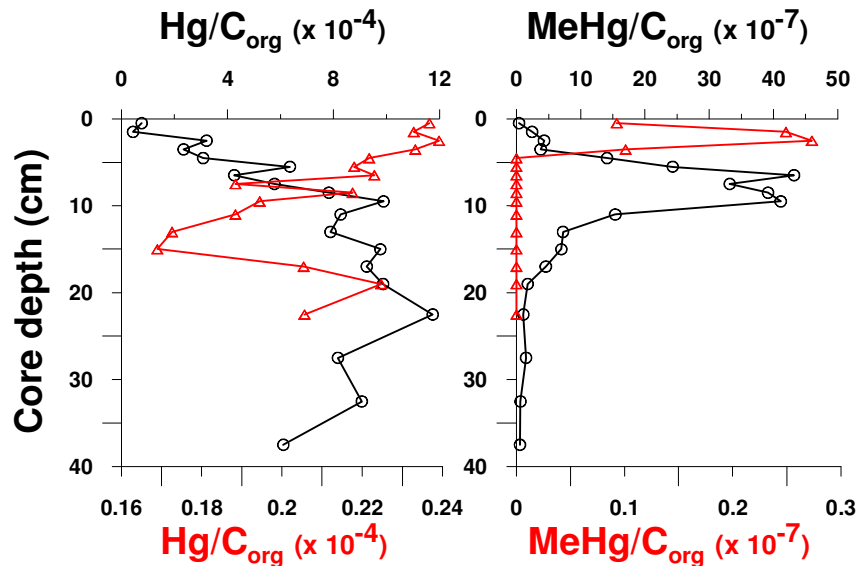


**Figure 16** - Vertical profiles of Hg and MeHg normalized to  $C_{org}$  both in sediment cores collected in Cala do Norte and Ponta da Erva. The black circles correspond to Cala do Norte core and the red triangles to the core collected in Ponta da Erva.

Despite the lack of significant correlations between Hg and MeHg in sediments, the distribution of MeHg in sediments of Cala do Norte increased with the increasing Hg concentrations, mostly until 10 cm depth (Figure 17). This may suggest that the existent MeHg was probably associated with the presence of bioavailable mercury in the solid fraction for methylation and this is also in line with previous works defending that besides inorganic mercury, MeHg also has a great affinity to particles (Ullrich *et al.*, 2001;

Hintelmann and Harris; 2004; Zhong and Wang, 2009). On the contrary, below 10 cm depth the same is not observed, whereas MeHg decreased as long as Hg concentrations remained constant. One explanation for this MeHg decrease may be hypothesized: the low Hg methylation below 10 cm depth and the consequently decrease of its concentration in solids and pore waters. This behavior was not observed in Ponta da Erva. In fact, MeHg increased while Hg concentrations slightly decreased in the first centimeters, reflecting in the solid fraction (sediments) the existent MeHg due to *in situ* Hg methylation (Schafer *et al.*, 2010).

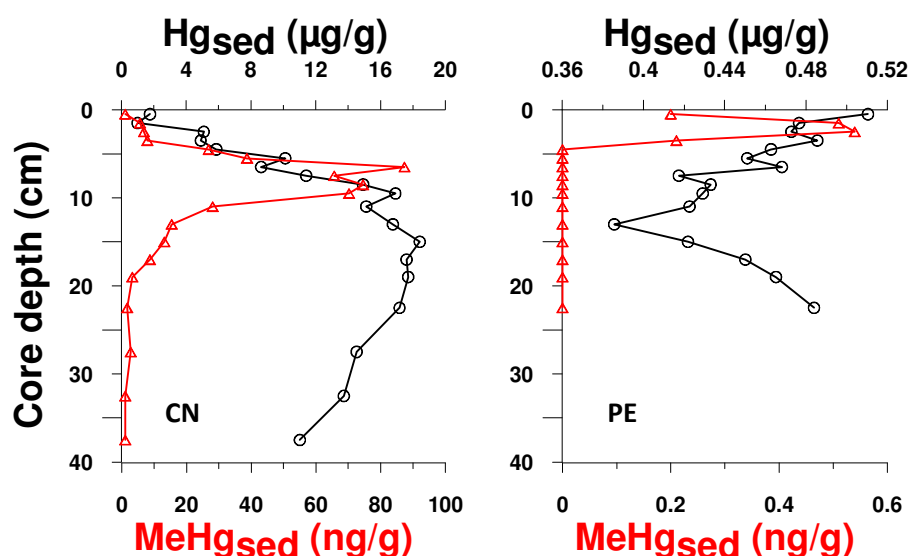


**Figure 17** – Vertical profiles of Hg concentrations ( $\mu\text{g/g}$ ) and MeHg ( $\text{ng/g}$ ) both in sediment cores collected in Cala do Norte (CN) and Ponta da Erva (PE). The black circles correspond to Hg vertical distribution and the red triangles to MeHg vertical distribution.

### 4.3. Mercury in pore waters

Regarding the reactive mercury concentrations, the results obtained in the present study are in agreement with previous works in the Tagus Estuary (1.86 – 15.3  $\text{ng/L}$ ; Canário, 2004). Total Hg concentrations (up to 166  $\text{ng/L}$ ), though, are lower than the ones reported by Canário (2004) (10 – 1160  $\text{ng/L}$ ) or Ramalhosa (2002) for Ria de Aveiro (60 – 884  $\text{ng/L}$ ) (Table 7). Despite these results, it is important to take into account the differences between these two systems as well as different environmental conditions, either hydrodynamic or sedimentation processes that affect diagenetic reactions and therefore Hg partitioning.



The present study is the first that quantifies MeHg concentrations in pore waters in a Portuguese estuarine system. Pore waters in Cala do Norte presented higher MeHg concentrations (up to 26 ng/L) compared with Ponta da Erva (< 3.4 ng/L). Concentrations in Cala do Norte show the same order of magnitude as in the Gulf of Trieste (up to 80 ng/L; Horvat *et al.*, 1999) but contrasting with Chesapeake Bay (up to 200 ng/L; Mason *et al.*, 1999) or San Francisco Bay, USA (up to 260 ng/L; Choe *et al.*, 2004) and especially with the Minamata Bay, Japan, which presents the highest dissolved MeHg levels (up to 5200 ng/L; Tomiyasu *et al.*, 2008).

**Table 7** - Comparison of total mercury (Hg<sub>T</sub>) and methylmercury (MeHg) concentrations in sediments from Tagus Estuary with other national and international estuarine / coastal systems (modified from Wang *et al.*, 2009).

| Estuarine /coastal system | Hg <sub>T</sub> (ng/L) | MeHg (ng/L) | Reference                          |
|---------------------------|------------------------|-------------|------------------------------------|
| Tagus Estuary, Portugal   | 6.8 - 165              | < 26.3      | Present study                      |
| Tagus Estuary, Portugal   | 10 - 1160              |             | Canário <i>et al.</i> (2005, 2008) |
| Ria de Aveiro, Portugal   | 60 - 884               |             | Ramalhosa (2002)                   |
| Gironde Estuary, France   |                        | 0.04 – 2.3  | Schafer <i>et al.</i> (2010)       |
| Wuli Estuary, China       | 2500                   | 640         | Wang <i>et al.</i> (2009)          |
| San Francisco Bay, USA    | 2 - 70                 | 0 - 260     | Choe <i>et al.</i> (2004)          |
| Minimata Bay, Japan       | 1.4 - 22               | 320 - 5200  | Tomiyasu <i>et al.</i> (2008)      |
| Chesapeake Bay, USA       | 0.2 - 5.5              | 5 - 200     | Mason <i>et al.</i> (1999)         |
| Gulf of Trieste           | 1 - 25                 | <5 - 80     | Horvat <i>et al.</i> (1999)        |

Usually, Hg concentrations in pore waters reflect the concentrations in sediments (Ullrich *et al.*, 2001). In Cala do Norte, Hg<sub>T</sub> and MeHg in pore waters (see Figure 12) were considerable higher than in Ponta da Erva; however the same was not observed for Hg<sub>R</sub> (see Figure 12), which was higher in Ponta da Erva, until 10 cm depth and below the 15 cm depth. This factor may increase methylation since Hg<sub>R</sub> is pointed as a preferential mercury species available for Hg methylation (Ullrich *et al.*, 2001). Between these depths, Hg<sub>R</sub> concentrations were higher in Cala do Norte than in Ponta da Erva.

Total Hg concentrations in both sediments and pore waters (Figure 18) showed that, in Cala do Norte, Hg<sub>T</sub> vertical distribution in pore waters was similar to the observed in sediments, whereas both profiles generally follow the same shape. This seems to be in

agreement with the observations of Muresan *et al.* (2007), who reported that  $Hg_T$  is in equilibrium between solid and solution fractions. On the contrary, in Ponta da Erva, this pathway was not evident, i.e. while sediment Hg increased,  $Hg_T$  in pore waters decreased. This is observed in top layers (0 – 6 cm depth) and at the bottom of the core. Between 10 and 17 cm depth, the similarity of both profiles suggests that dissolved and particulate Hg were in equilibrium.

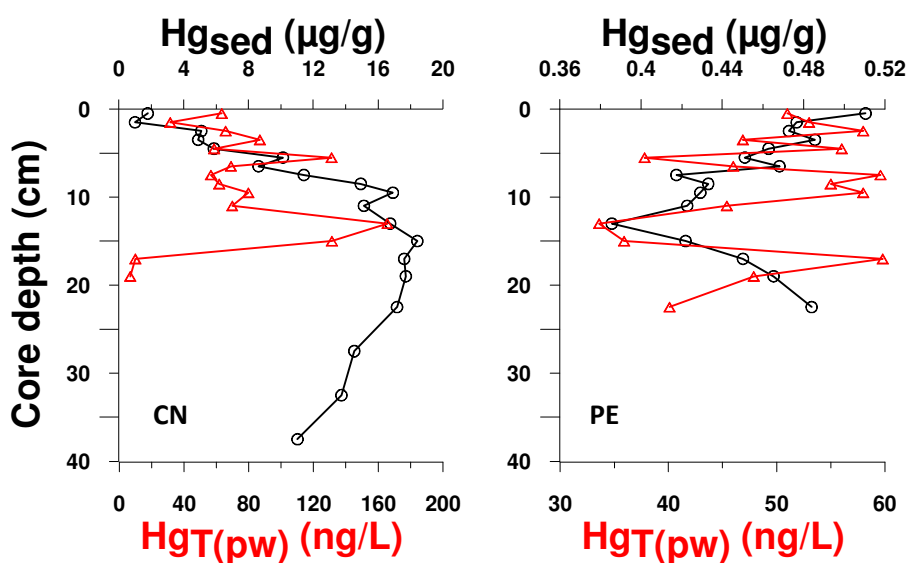


**Figure 18** – Vertical profiles of Hg concentrations in sediments ( $\mu\text{g/g}$ ) and  $Hg_T$  ( $\text{ng/L}$ ) in pore waters both in cores collected in Cala do Norte (CN) and Ponta da Erva (PE). The black circles correspond to Hg vertical distribution in sediments and the red triangles to  $Hg_T$  vertical distribution in pore waters.

Regarding MeHg vertical distribution, in Cala do Norte both sediment and pore waters profiles had similar shapes (Figure 19). The highest increments in solid fraction corresponded to the highest levels in dissolved MeHg. These results show that MeHg was in equilibrium between the two phases in Cala do Norte core and concentrations in solid sediment reflected the higher MeHg levels in pore waters. Conversely, in Ponta da Erva, MeHg profiles did not show the same pattern, whereas the solid phase increment was observed at 3 cm depth and the highest dissolved MeHg concentrations were found below this depth, at 5 cm depth. These profiles in Ponta da Erva do not reflect equilibrium conditions between MeHg in the solid sediments and the pore waters. In fact, dissolved

MeHg levels in Ponta da Erva were higher in pore waters than in the solid phase, contrary to the observed in Cala do Norte. Since methylmercuric cation ( $\text{CH}_3\text{Hg}^+$ ) has a high tendency to form complexes, in particular with soft ligands such as sulphur (Ullrich *et al.*, 2001), these MeHg increments in the dissolved form could be explained by the formation of soluble sulphide complexes, which could prevent MeHg sorption in solid sediments (Gagnon *et al.*, 1997).

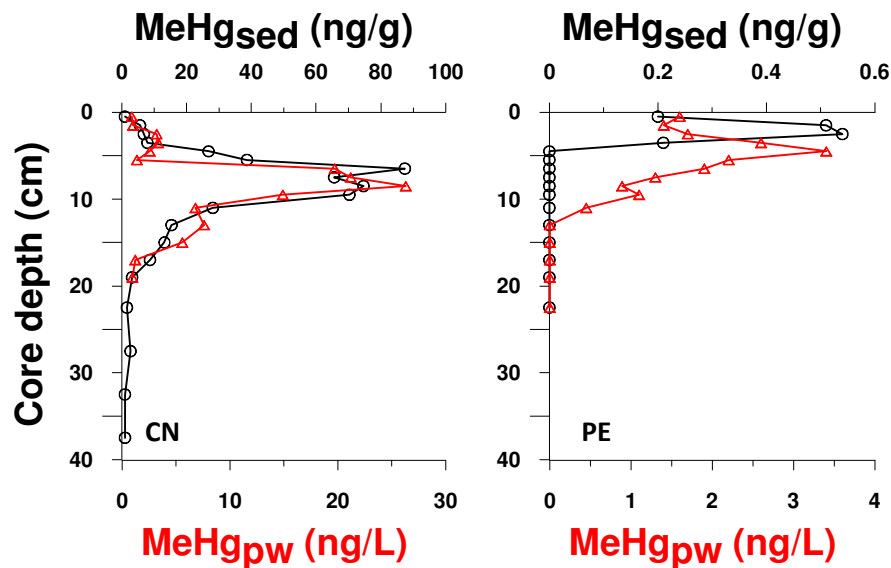


**Figure 19** – Vertical profiles of MeHg concentrations in sediments (ng/g) and dissolved MeHg (ng/L) in pore waters both in cores collected in Cala do Norte (CN) and Ponta da Erva (PE). The black circles correspond to MeHg vertical distribution in sediments and the red triangles to MeHg vertical distribution in pore waters.

Comparing  $\text{Hg}_T$  and  $\text{Hg}_R$  vertical distribution in pore waters, it was observed for both locations that  $\text{Hg}_R$  showed a similar profile to the  $\text{Hg}_T$  (Figure 20). In Cala do Norte is noticeable that the highest increment on  $\text{Hg}_R$  corresponded to the maximum  $\text{Hg}_T$  concentration. Identical profiles were observed in Ponta da Erva for the same Hg species. These results suggest that in both places the two dissolved Hg species ( $\text{Hg}_R$  and  $\text{Hg}_T$ ) are in equilibrium. Similar equilibriums were also found in a previous study in Cala do Norte (Canário, 2004).

Methylmercury in pore waters did not show a similar profile as well as the obtained for  $\text{Hg}_R$  concentrations in Cala do Norte pore waters (Figure 21). The increase in MeHg

concentrations was observed at 9 cm depth, above the  $Hg_R$  peak (12 cm depth) and right between the highest increments on  $Hg_T$  (between 6 and 12 cm depth) (see Figure 20). These data suggests that  $Hg_R$  was mobilized in the sedimentary column between those two depths and it is possible to be available for methylation. Either  $Hg_R$  was mobilized in the sedimentary column by downward diffusion or it was consumed during methylation, thereby decreasing its levels and consequently increasing MeHg levels. Conversely to the Cala do Norte, the processes affecting MeHg and  $Hg_R$  in Ponta da Erva appeared to be mediated by different factors. Reactive Hg concentrations generally accomplished the  $Hg_T$  levels (Figure 20) but the same was not observed for MeHg (Figure 21). In fact, the highest increment on MeHg concentrations was observed at 5 cm depth, at the same depth as it was observed increments on  $Hg_R$  and  $Hg_T$  concentrations. Below this depth, MeHg decreased while  $Hg_R$  increased (9 – 10 cm depth) suggesting that if conditions are favorable, Hg methylation may efficiently occur at this depth since  $Hg_R$  was bioavailable. On the other hand, the enhancement of  $Hg_R$  levels at this depth may be related with its increasing solubility due to the increment in sulphide concentrations (Figure 14) and the consequently formation of polysulphyde-mercury complexes, which are known to be quantified in the dissolved mercury fraction (Gagnon *et al.*, 1997; Ullrich *et al.*, 2001).

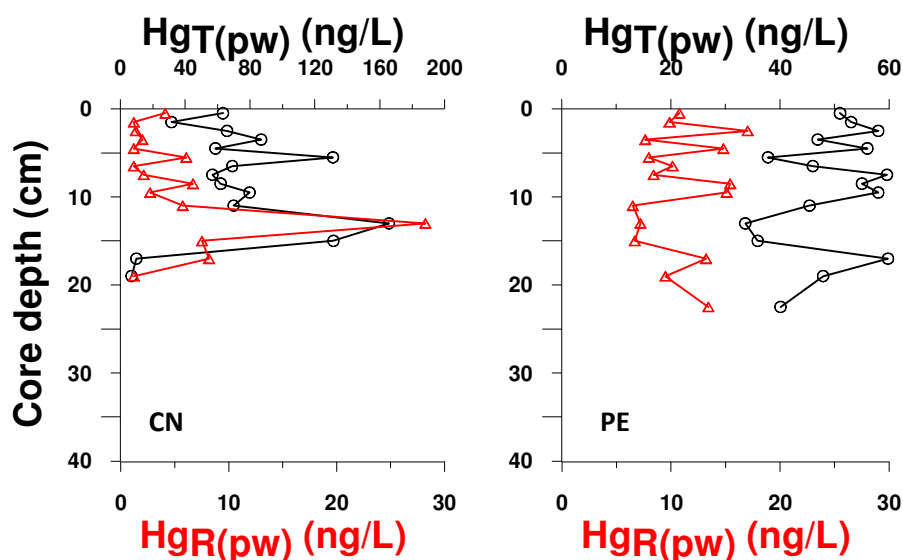


**Figure 20** – Vertical profiles of  $Hg_T$  and  $Hg_R$  (ng/L) in pore waters both in sediment cores collected in Cala do Norte (CN) and Ponta da Erva (PE). The black circles correspond to  $Hg_T$  vertical distribution and the red triangles to  $Hg_R$  vertical distributions in pore waters.

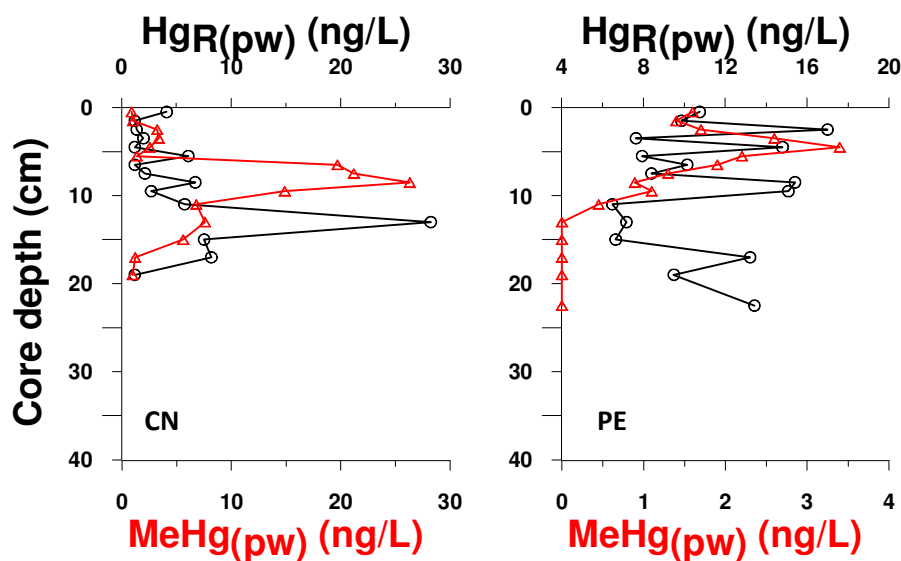


**Figure 21** – Vertical profiles of  $Hg_R$  and MeHg (ng/L) in pore waters both in sediment cores collected in Cala do Norte (**CN**) and Ponta da Erva (**PE**). The black circles correspond to  $Hg_R$  vertical distribution and the red triangles to MeHg vertical distributions in pore waters.

#### 4.4. Methylmercury diagenesis

In Cala do Norte, MeHg concentrations in sediments reflected the total Hg levels but the same was not observed in Ponta da Erva (see Figure 17). Despite showing identical distributions in the sediment/water interface and until 10 cm depth, MeHg only accounts for a maximum 1 % of total Hg concentrations in sediments at both locations. This is in agreement with values of the same order of magnitude reported in with other works (e.g., Ramalhosa, 2002) and is in line with the values described in literature (Gagnon *et al.*, 1997; Ullrich *et al.*, 2001; Benoit and Mason, 2003).

An opposite trend was observed for pore waters. In Ponta da Erva the highest increment on MeHg corresponded to an increment on  $Hg_T$  concentrations, at 5 cm depth (Figures 20 and 21). This only represents 6 % of total Hg present in Ponta da Erva while in Cala do Norte the maximum MeHg concentration accounts for 42.6 %. This may suggest that despite  $Hg_R$  levels are the same, both in Cala do Norte and Ponta da Erva, Hg methylation was more favorable in the environmental conditions in Cala do Norte than in Ponta da Erva. Moreover, this is probably related with the more anoxic sediment in Cala do Norte, as it was evidenced by larger variations in redox potential (see Figure 5). Some authors

(e.g., Ullrich *et al.*, 2001) reported that Hg methylation in estuarine sediments was strongly favored at low (-220 mV) Eh, whereas the same redox potential observed in Cala do Norte when sulphate started to decrease and sulphide increased.

While in Ponta da Erva no correlation was found between MeHg in solid sediments and pore waters, in Cala do Norte a significant correlation ( $R^2 = 0.799$ ;  $p < 0.05$ ) was observed (Figure 22). This observation clearly evidences that MeHg partition between these two phases may be related with Hg methylation occurring effectively in Cala do Norte sediments due to bioavailability of inorganic Hg (Ullrich *et al.*, 2001) or with the organic content and/or its nature (Ravichadran, 2004). Conversely, in Ponta da Erva, the equilibrium was not found, suggesting that MeHg was mobilized and diffusing to the upper layers, where it may be scavenged at the redox boundary (Mason and Lawrence, 1999). Other hypothesis is that methylation may occur in the pore waters, once solid sediment is not the only preferred substrate for the organic matter degradation (Mason and Lawrence, 1999).

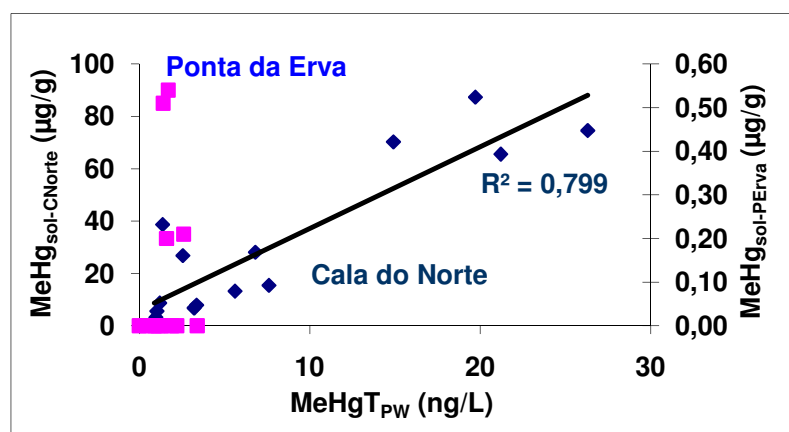


**Figure 22** - Correlation between total MeHg (ng/L) in pore waters (x axis) and MeHg (µg/g) in sediment cores (y axis) both in Cala do Norte and Ponta da Erva.

The affinity between MeHg and organic matter has been suggested for high increments on MeHg concentrations in sediments (Ravichadran, 2004). The negatively charged particles of the organic matter can adsorb positively charged MeHg evidencing this relation (Ravichandran, 2004). Yet, no correlation was found between the organic matter both in sediments and pore waters and the MeHg concentrations, suggesting that MeHg

levels in Cala do Norte and Ponta da Erva may not be explained by the organic matter content. Moreover, increments on MeHg concentrations appear to be related with availability of inorganic mercury for Hg methylation, as well as the availability of sulphate assuming that this process is mediated by sulphate reducing bacteria (Du Laing *et al.*, 2009). Other factor such as iron-reducing bacteria (Fleming *et al.*, 2006) and abiotic Hg methylation (Celo *et al.*, 2006) should not be excluded.

As previously mentioned, in Cala do Norte pore waters  $\text{SO}_4^{2-}$  reduction was observed at 6 cm depth, where  $\text{HS}^-$  concentrations increased below this depth (Figure 14). Methylmercury concentrations increased with the increasing  $\text{HS}^-$  concentrations in pore waters of Cala do Norte (Figure 23) while  $\text{Hg}_R$  concentrations increased with decreasing  $\text{HS}^-$  concentrations (compare with Figure 20). This points to SRBs activity and suggests that inorganic Hg is methylated by these bacteria at these depths. If  $\text{SO}_4^{2-}$  and  $\text{Hg}_R$  are necessary to SRBs methylate Hg,  $\text{HS}^-$  may contribute to diminish MeHg concentrations either controlling HgS precipitation (Ullrich *et al.*, 2001; Du Laing *et al.*, 2009), and thereby reducing the available  $\text{Hg}_R$  and/or originating dimethylmercury (reaction 2) (Gagnon *et al.*, 1996; King *et al.*, 2000). In fact, it was observed that MeHg concentrations generally accomplished  $\text{HS}^-$  concentrations (Figure 23), indicating that Hg available for methylation is not limited by HgS precipitation (Ullrich *et al.*, 2001). On the other hand,  $\text{Hg}_R$  concentrations increased when  $\text{HS}^-$  decreased at 11 cm depth, suggesting that lower  $\text{HS}^-$  concentrations increase  $\text{Hg}_R$  concentrations in pore waters (Du Laing *et al.*, 2009). Based on these results, mercury methylation seems to occur both with relatively high  $\text{HS}^-$  and  $\text{SO}_4^{2-}$  concentrations, which is in line with other works (e.g., Gilmour and Henry, 1991; King *et al.*, 2000).

Conversely to the Cala do Norte,  $\text{Hg}_R$  concentrations in Ponta da Erva pore waters showed an increment while  $\text{HS}^-$  concentrations increased at 5 cm depth (see Figures 12 and 14). At this depth  $\text{SO}_4^{2-}$  concentrations decreased, which is in line with SRBs activity reducing  $\text{SO}_4^{2-}$  to  $\text{HS}^-$  (Figure 14). Consequently, MeHg concentrations also increased at this depth (Figure 23). It appears that  $\text{HS}^-$  do not control inorganic Hg solubility in this layer, therefore increasing the availability of Hg for methylation.

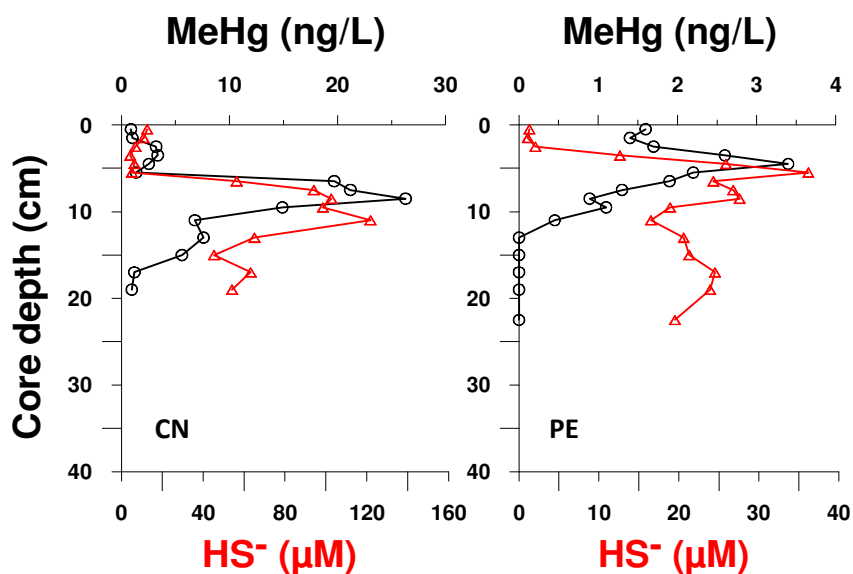


**Figure 23** – Vertical profiles of MeHg concentrations (ng/L) versus  $\text{HS}^-$  ( $\mu\text{M}$ ) both in pore waters of the sediment cores collected in Cala do Norte (CN) and Ponta da Erva (PE). The black circles correspond to MeHg vertical distribution, respectively, and the red triangles to  $\text{HS}^-$  vertical distribution.

#### 4.5. Mercury fluxes

In order to evaluate if diagenetic processes can lead to significant Hg and MeHg post depositional redistribution and/or diffusion to the overlying water an estimative of vertical diffusive fluxes were calculated applying Fick's first law of diffusion (Berner, 1980). The diffusion flux  $J$  is expressed as:

$$J = (-\Phi D_w / \theta^2)(dC/dz) \quad (10)$$

where  $J$  is the diffusion flux,  $\Phi$  is porosity,  $D_w$  is the whole-sediment diffusion coefficient and  $(dC/dz)$  is the concentration gradient,  $z$  being positive in the downward direction. According to Canário (2004), porosity was calculated using the expression:

$$\phi = \frac{m_w}{m_w + \frac{m_s}{2.65}} \quad (11)$$



where  $m_w$  is the pore water mass and  $m_s$  is the dried sediment mass.

According to Schafer *et al.* (2010),  $D_{w,25^\circ\text{C}} = 1.2 \times 10^{-5} \text{ cm}^2/\text{s}$  for dissolved MeHg and  $2 \times 10^{-6} \text{ cm}^2/\text{s}$  for  $\text{Hg}_R$  (assuming that inorganic Hg is bound to macromolecules in the colloidal size range) was used, corrected for temperature ( $T, ^\circ\text{C}$ ). Tortuosity was estimated from porosity using Boudreau's formulation (Boudreau, 1999; Muresan *et al.*, 2007):

$$\theta^2 = 1 - \ln(\Phi^2) \quad (12)$$

The estimated flux across sediment/water interface in Cala do Norte was  $0.30 \text{ ng}/\text{m}^2\text{d}$  for MeHg and  $0.50 \text{ ng}/\text{m}^2\text{d}$  for  $\text{Hg}_R$ . Conversely, in Ponta da Erva, MeHg flux was lower than in Cala do Norte,  $0.19 \text{ ng}/\text{m}^2\text{d}$ , while for  $\text{Hg}_R$  was higher,  $1.13 \text{ ng}/\text{m}^2\text{d}$ . These fluxes evidence the diffusive transport of Hg from the pore waters to the overlying water in both sites. These values are in line with other works in estuarine areas (e.g., Gill *et al.*, 1999; Schafer *et al.*, 2010).

These relatively low fluxes may indicate that, despite higher Hg concentrations in Cala do Norte, Hg is efficiently retained in sediments probably related with diagenetic processes near the sediment/water interface that scavenge Hg in solid sediments (Canário *et al.*, 2003b).

#### **4.6. Contamination impacts and legal figure**

Regarding the water quality criteria, concerning mercuric forms in natural environments, existing legislation considers only superficial freshwater for the production of drinking water, concerning dissolved mercury, with a maximum concentration recommended  $0.5 \text{ }\mu\text{g}/\text{L}$  and maximum limit of  $1.0 \text{ }\mu\text{g}/\text{L}$  ('D. L. 306/2007, 27 de Agosto'). There is no legislation concerning coastal waters used as fishery resources, although with the implementation of the European Framework Directive water quality guidelines should be expected in the near future for coastal waters.

Sediment quality criteria for Hg have been set in some countries but due to uncertainties regarding the bioavailability of Hg it has been suggested that these should be applied carefully and in concert with other site-specific data. Available legislation in Portugal

concerns the use and fate of dredged materials “Portaria nº 1450/2007, de 12 de Novembro”. The classification of sediments is made in classes from 1 to 5 regarding their degree of contamination, since the least contaminated with concentrations below 0.5 µg/g until the highest contaminations levels. Classification is presented in Table 8.

In Portugal, legislation regarding the contamination limits by discharges from chlor-alkali unit effluents, presents guidelines for controlling the use and emissions of mercury into the environment and monitoring the exposure to this contaminant, particularly from humans. According to European community directives (82/176/EEC) and the regulatory threshold value for mercury on chlor-alkali plants effluents, emission limit is 50 µg/L.

**Table 8** – Classification of Hg contamination levels in dredged sediment materials, according to “Portaria nº 1450/2007, de 12 de Novembro”.

| <i>Type of sediment</i> | <i>[Hg]<br/>(µg/g)</i> | <i>Classification</i>  |
|-------------------------|------------------------|--|
| <b>Class 1</b>          | < 0.5                  | Clean dredged material with no restrictions.   |
| <b>Class 2</b>          | 0.5 - 1.5              | Vestigial contamination and may be immersed taking into consideration the uses and characteristics of the environmental receptor.  |
| <b>Class 3</b>          | 1.5 - 3.0              | Slightly contaminated and may be used for landfill or immersed after detailed study of the receptor. Must be monitorized.  |
| <b>Class 4</b>          | 3.0 - 10               | Contaminated material with deposition only in impermeable sites.   |
| <b>Class 5</b>          | > 10                   | Contamination and no dredging operations are advised. If necessary, it requires treatment before deposition which must be made only in authorized landfills. No immersion is authorized. |

The cores collected in Cala do Norte were nearby an effluent of a chlor-alkali industrial plant. This plant discharges waste water directly into the estuary. Despite not clearly knowing the chemical composition of these discharges and attending to ancient effluent discharges in Cala do Norte containing high levels of Hg, it is clear that chemical characteristics of the sediment are altered due to continuous anthropogenic interferences. On the other hand, in Ponta da Erva, the sediments do not present high fluctuations in the upper layers with respect to its general characteristics such as pH, Eh, water content and *LOI*, conversely to the Cala do Norte, which may indicate that this area was not pressured by anthropogenic contamination as in Cala do Norte.

The lowest concentrations in Cala do Norte core were observed at sediment/water interface (1 µg/g), which accordingly with “Portaria nº 1450/2007, de 12 de Novembro”, surface sediments in Cala do Norte may be considered Class 2, with vestigial contamination. Although the highest Hg concentrations observed in deeper sediment (18 µg/g at 15 cm depth) may characterize the sediment as Class 5, highly contaminated. Based on these results, dredging activities are not advised on this part of the Estuary, considering that remobilization of the sediments will increase Hg concentrations in the water column, especially MeHg, which can be transported to the adjoining areas, with large implications to the estuarine/marine ecosystem.

Conversely, in Ponta da Erva the range of Hg concentrations was much smaller (0.4 – 0.5 µg/g), where sediment can be considered Class 1, not evidencing a high Hg contamination degree.

Considering that mercury and its compounds are very toxic, particularly to humans, and that can enter the food chain causing negative impacts in human health, due to biomagnification even at low concentrations, it is important to analyze the degree of contamination on both places. As referred by Wiener *et al.* (2003) the methylmercury concentration in fishes can exceed  $10^6$  to  $10^7$  fold the concentrations found in the water. Animals have the availability to regulate the metals content in their tissues; however mercury cannot be excreted from the organism at the same rate that it is accumulated, remaining in the body and being continually added over life. Since the primary route for humans exposure to mercury is through the consumption of contaminated fish and shellfish, the high levels of mercury in an ecosystem can have endangered the system ecologically and economically, particularly in areas highly dependent on fishery activities. Methylmercury concentrations in water is the major source for mercury concentrations in aquatic organisms (Morel *et al.*, 1998) and methylmercury in aquatic organisms corresponds to 85-90% of total mercury concentrations (Horvat, 1996).

Organic Hg concentrations were quantified in different organisms of Cala do Norte by Canário (2004) and the results clearly evidenced that the top predators are affected by Hg contamination. The organic Hg determined, mostly in the form of MeHg, indicated that fish and cephalopods species, such as *Pomatochistus minutes* (0.13 – 0.35 µg/g), *Liza ramada* (0.11 – 0.72 µg/g) and *Sepia officinalis* (0.50 µg/g), were the most Hg contaminated, showing organic Hg concentrations over 95 %. The species with lower levels in the food

web, such as shrimps (0.06 – 0.22 µg/g) and crabs (0.19 – 0.35 µg/g), presented lower organic Hg concentrations, below 95 % (Canário, 2004). The species *Liza ramada* and *Sepia officinalis* presented, by that time, concentrations exceeding the threshold levels (0.5 µg/g) established in the Portuguese law regarding the human consumption.

Evidences of Hg contamination and bioaccumulation in other species have also been reported in other areas of the Tagus Estuary (Raimundo *et al.*, 2010) or such as Ria de Aveiro (e.g., Válega *et al.*, 2008b,c; Coelho *et al.*, 2006, 2008, 2009), which reinforces the major concern regarding MeHg toxicity to the human health and therefore the major importance of Hg methylation in moderate to highly contaminated estuarine systems. Although Pato *et al.* (2008) suggested that the Ria de Aveiro does not export mercury to the coastal zone, is not clear whether the Tagus Estuary can export Hg to the adjacent coastal zone, because it has a different dynamics, putting the hypothesis if that happens, what are the effects of this metal (Hg or MeHg) entering the upwelling system on the western Iberian coast.

## **5. CONCLUSIONS**



The present study provides new Hg data and confirms that the Tagus Estuary is still one of the most contaminated estuaries of the Portuguese aquatic systems.

Previous works from Figuères *et al.* (1985) and Canário (2004) puts forward the major importance that contamination from this hazardous pollutant represents. Nowadays, and accordingly with the Portuguese law for dredging materials (“Portaria n° 1450/2007, de 12 de Novembro”), the sediments collected and analyzed in this study in Cala do Norte were classified as a Class 5 (highly contaminated) while in Ponta da Erva sediments were classified as Class 1 (clean material with no restrictions).

Mercury concentrations in sediments collected in Cala do Norte were higher compared to the ones collected in Ponta da Erva. Even so, Ponta da Erva presented levels of Hg contamination higher than the ones expected, regarding the baseline levels reported by Canário, 0.025 µg/g for Tagus coastal area (2000). The vertical distribution of Hg and MeHg reflects therefore the degree of contamination that the Tagus Estuary has been exposed to over the years, which was confirmed by the normalization of Hg and MeHg to Al and C<sub>org</sub>.

In Cala do Norte Hg and MeHg concentrations increased until 15 cm depth but in Ponta da Erva levels were found to be higher near the sediment/water. In pore waters, where for the first time MeHg concentrations were quantified, vertical distribution showed that in Cala do Norte dissolved MeHg was present in deeper layers (9 cm depth) right between the highest peaks of Hg<sub>T</sub> and Hg<sub>R</sub>. These results suggested the remobilization of these Hg species deeper in the sedimentary column. On the contrary, in Ponta da Erva the highest MeHg concentration was found at the same depth of Hg<sub>R</sub>. These observations are supported by the diagenetic processes affecting both locations, where the equilibrium between Hg in the solid phase and pore waters is important in respect with whether the different bounds that reactive Hg can establish and regarding the availability of Hg used in methylation processes or the preferred substrate used in Hg methylation, even related with the organic matter content and/or its nature. Methylmercury was mobilized and diffusing to the upper layers, where it may be scavenged at the redox boundary.

All these effects are most likely related with the different fluxes observed both in Hg<sub>R</sub> and MeHg concentrations between the sediment/water interfaces, which showed to be different in both places. Surprisingly, Hg<sub>R</sub> flux was higher in Ponta da Erva but the MeHg

transferred to the water column was superior in Cala do Norte, where the Hg methylation is potentiated.

From an ecotoxicological point of view and considering the complexity of factors that affect mercury methylation in estuarine environments, such as the Tagus Estuary, it is necessary to keep track of pollution levels in a perspective of environmental monitoring, taking into account the effects of bioaccumulation and biomagnification of this harmful metal, as previously observed in organisms of this system and concerning the MeHg toxicity to the human health.

Due to the dynamics of the Tagus Estuary, some questions should be posed: if dredging activities were done in highly contaminated areas of the estuary, such as in Cala do Norte and downstream areas, could Hg or MeHg increase its concentrations in the adjoining coastal area? What happens if these reach the known coastal upwelling system on the western Iberian margin? Even more, despite not being the aim of this study, for what concerns, Hg methylation processes in the water column are still unresolved and its potential, due to the higher surface of the particles than in sediments, may endanger the estuarine and marine environments.



## **6. REFERENCES**



Allen, G.P., Salomon, J.C., Bassoullet, P., Du Penhoat, Y., de Grandpré, C., 1980. Effects of tides on mixing and suspended sediment transport in macrotidal estuaries. *Sedimentary Geology* 26, Issues 1-3, 69 – 90.

Alvera-Azcárate, A., Ferreira, J. G., Nunes, J. P., 2003. Modelling eutrophication in mesotidal and macrotidal estuaries. The role of intertidal seaweeds. *Estuarine, Coastal and Shelf Science* 57, Issue 4, July, 715 – 724.

Amyot, M., Lean, D.R.S., Mierle, G., 1997. Production and loss of dissolved gaseous mercury in the coastal waters of the Gulf of Mexico. *Environ. Sci. Tech.* 31, 3606 – 3611.

APHA (American Public Health Association, American Water Works Association, and Water Environment Federation), *et al.*, 1995. Standard Methods for the Examination of Water and Wastewater, 19th ed. American Public Health Association, Washington, DC.

Baldi, F., 1997. Metal Ions in Biological Systems. Vol. 34 Marcel Dekker, Inc., N.Y., pp. 213 – 257.

Barkay, T. and Wagner-Dobler, I., 2005. Microbial Transformations of Mercury: Potentials, Challenges, and Achievements in Controlling Mercury Toxicity in the Environment. *Advances in Applied Microbiology* 57, 2005, Pages 1 – 52.

Benner, R., Strom, M., 1993. A critical evaluation of the analytical blank associated with DOC measurements by high-temperature catalytic oxidation. *Mar. Chem.* 41, Issues 1-3, 153 – 160.

Benoit J. M., Gilmour C. C., Mason R. P., Riedel G. S. and Riedel G. F., 1998. Behavior of mercury in the Patuxent River estuary. *Biogeochem.* 40, 249 – 265.

Benoit, J.M., Gilmour, C.C., Mason, R.P., Heyes, A., 1999. Sulfide controls on mercury speciation and bioavailability to methylating bacteria in sediment pore waters. *Environ. Sci. Technol.* 33, 951 – 957.

Benoit J. M., Mason R. P., Gilmour C. C. and Aiken G. R., 2001. Constants for mercury binding by dissolved organic matter isolates from the Florida Everglades. *Geochim. Cosmochim. Acta* 65, 4445 – 4451.

- Benoit J. M., Gilmour C. C., Heyes A., Mason R. P. and Miller C. L., 2003. Geochemical and biological controls over mercury production and degradation in aquatic systems. *ACS Symp. Ser.* 835, 262 – 297.
- Berner, R., 1980. Early Diagenesis. A Theoretical Approach. Princeton University Press, USA, 241 p.
- Bloom, N.S., 1992. On the chemical form of mercury in edible fish and marine invertebrate tissue. *Can. J. Fish. Aquat. Sci.* 49, 1010 – 1017.
- Bloom, N.S., Lasorsa, B.K., 1999. Changes in mercury speciation and the release of methyl mercury as a result of marine sediment dredging activities. *Sci. Tot. Environ.* 237/238, 379 – 385.
- Boudreau, B.P., 1999. Metals and models: diagenetic modelling in freshwater lacustrine sediments. *Journal of Paleolimnology* 22, 227 – 251.
- Brotas, V., Amorim-Ferreira, A., Vale, C., Catarino, F., 1990. Oxygen profiles in intertidal sediments of Ria Formosa (S. Portugal). *Hydrobiol.* 207, 123 – 129.
- Bufflap, S.E., Allen H.E., 1995. Sediment pore waters collection methods for trace metal analysis: a review. *Water Res.* 1, 165 – 177.
- Butcher, S.S., Charlson, R.J., Orians, G.H., Wolfe, G.V., 1992. Global Biogeochemical Cycles. Academic Press, N.Y., 377 pp.
- Burbacher, T. M., Rodier, P., Weiss, B., 1990. Methylmercury developmental neurotoxicity: a comparison of effects in humans and animals. *Neurotoxicology and Teratology* 12 (3), 191 – 202.
- Caetano, M., 1992. Distribuição de Organoclorados e Metais em Dois Sistemas de Aquacultura. Thesis, Science Faculty of the University of Lisbon, 166 p.
- Caetano M, Madureira MJ, Vale C., 2002. Metal remobilisation during resuspension of anoxic contaminated sediment: short-term laboratory study. *Water Air Soil Poll.* 143, 23 – 40.
- Canário, J., 2000. Mercúrio em Sedimentos Contaminados e Águas Intersticiais da Cala do Norte do Estuário do Tejo. Master thesis, New University of Lisboa, 98 pp.

Canário, J., Vale, C., Caetano, M., 2003a. Mercury in contaminated sediments and pore waters at a contaminated site of the Tagus Estuary. *Cienc. Mar.* 29 (4), 535 – 545.

Canário, J., Vale, C., Caetano, M., Madureira, M.J., 2003b. Mercury in contaminated sediments and pore waters enriched in sulphate (Tagus Estuary, Portugal). *Environ. Poll.* 126 (3), 425 – 433.

Canário, J., 2004. Mercúrio e monometilmercúrio na Cala do Norte do Estuário do Tejo – Diagénese, Trocas com a coluna de água e interações com o biota. Ph.D. Thesis. New University of Lisbon, Portugal.

Canário, J., Vale, C., 2004. Rapid release of mercury from intertidal sediments exposed to solar radiation: a field experiment. *Environ. Sci. Tech.* 38, 3901 – 3907.

Canário, J., Vale, C., Caetano, M., 2005. Distribution of monomethylmercury and mercury in surface sediments of the Tagus Estuary (Portugal). *Mar Pollut Bull.* 50, 1142 – 1145.

Canário, J., Caetano, M., Vale, C., Cesário, R., 2007. Evidence for elevated production of methylmercury in salt marsh. *Environ Sci Technol.* 41, 7376 – 7382.

Canário, J., Vale, C., Nogueira, M., 2008. The pathway of mercury in contaminated waters determined by association with organic carbon (Tagus Estuary, Portugal). *Applied Geochemistry* 23, Issue 3, Pages 519 – 528.

Cardoso, P.G., Lillebø, A.I., Lopes, C.B., Pereira, E., Duarte, A.C., Pardal, M.A., 2008. Influence of bioturbation by *Hediste diversicolor* on mercury fluxes from estuarine sediments: a mesocosms laboratory experiment. *Mar Poll Bull.* 56, 325–334.

Celo, V., Lean, David, R.S., Scott, S.L., 2006. Abiotic methylation of mercury in the aquatic environment. *Sci Total Environ.* 368 (1), 126 – 137.

Chiffolleau, J.F., Cossa, D., Auger, D., Truquet, I., 1994. Trace metal distribution, partition and fluxes in the Seine estuary (France) in low discharge regime. *Mar Chem.* 47, 145 – 158.

Choe, K.-Y., Gill, G.A., Lehman, R.D., Han, S., 2004. Sediment–water exchange of total mercury and monomethyl mercury in the San Francisco Bay-Delta. *Limnol. Oceanogr.* 49, 1512–1527.

Choi, S.C., Chase, T.J., Bartha, R., 1994. Metabolic pathways leading to mercury methylation in *Desulfovibrio desulfuricans* LS. *Appl. Environ. Microbiol.* 60, 4072–4077.

Clark, R.B., 2001. Marine Pollution fifth edition, Oxford University Press.

Coelho, J.P., Pereira, M.E., Duarte, A., Pardal, M.A., 2005. Macroalgae response to a mercury contamination gradient in a temperate coastal lagoon (Ria de Aveiro, Portugal). *Estuar Coast Shelf Sci.* 65, 492–500.

Coelho, J.P., Rosa, M., Pereira, E., Duarte, A., Pardal, M.A., 2006. Pattern and annual rates of *Scrobicularia plana* mercury bioaccumulation in a human induced mercury gradient (Ria de Aveiro, Portugal). *Estuar Coast Shelf Sci.* 69, 629–635.

Coelho, J.P., Reis, A. T., Ventura, S., Pereira, M.E., Duarte, A., Pardal, M.A., 2008. Pattern and pathways for mercury lifespan bioaccumulation in *Carcinus maenas*. *Mar Poll Bull.* 56, 1104–1110.

Coelho, J.P., Pereira, M.E., Duarte, A., Pardal, M.A., 2009. Contribution of primary producers to mercury trophic transfer in estuarine ecosystems: Possible effects of eutrophication. *Mar Poll Bull* 58, 358–365.

Compeau, G., Bartha, R., 1984. Methylation and demethylation of mercury under controlled redox, pH and salinity conditions. *Appl. Environ. Microbiol.* 48, 1203.

Costley, C., Mossop, K., Dean, J., Garden, L., Marshall, J., Carroll, J., 2000. Determination of mercury in environmental and biological samples using pyrolysis atomic absorption spectrometry with gold amalgamation. *Anal Chim Acta.* 405, 179–183.

Covelli, S., Faganeli, J., Horvat, M., Brambati, A., 1999. Pore waters distribution and benthic flux measurements of mercury and methylmercury in the Gulf of Trieste (Northern Adriatic Sea). *Estuar Coast Shelf Sci.* 48, 415–428.

Covelli, S., Faganeli, J., Horvat, M., Brambati, A., 2001. Mercury contamination of coastal sediments as the result of long-term cinnabar mining activity (Gulf of Trieste, northern Adriatic sea). *Applied Geochemistry* 16, Issue 5, 541–558.

Craig, P.J., Moreton, P.A., 1986. Total mercury, methylmercury and sulphide levels in British estuarine sediments-III. *Water Res* 20:1111–8.

Crespo-López, M.E., Sá, A., Herculano, A., Burbano, R., Nascimento, J.L., 2007. Methylmercury genotoxicity: a novel effect in human cell lines of the central nervous system. *Environ Inter.* 33 (2), 141 – 146.

Dias, M.D., Marques, J.M.S., 1999. Estuário do Tejo: O seu valor e um pouco da sua história. Ed. Reserva Natural do Estuário do Tejo, Instituto da Conservação da Natureza, Lisboa, 156 pp.

Driscoll, C.T., Holsapple, J., Schofield, C.L., Munson, R., 1998. The chemistry and transport of mercury in a small wetland in the Adirondack region of New York, USA. *Biogeochemistry* 40, 137–46.

Du Laing, G., Rinklebe, J., Vandecasteele, B., Meers, E., Tack, F.M.G., 2009. Trace metal behaviour in estuarine and riverine floodplain soils and sediments: A review. *Sci Tot Environ.* 407, Issue 13, 3972-3985.

Eggleton, J., Thomas, K.V., 2004. A review of factors affecting the release and bioavailability of contaminants during sediment disturbance events. *Environ Int* 30, 973–80.

EPA, 2001. Appendix to Method 1631: Total Mercury in Tissue, Sludge, Sediment, and Soil by Acid Digestion and BrCl Oxidation.

Falter, R., Wilken. R-D., 1998. Isotope experiments for the determination of the abiotic mercury methylation potential of a River Rhine sediment. *Vom Wasser* 90, 217–31.

Farago, M.E., 2000. Mercury in marine environments. In: Gianguzza, A., Pelizetti, E., Sammartano, S. (Eds). *Chemical Processes in Marine Environments*, Springer-Verlag, pp. 245-263.

Ferreira *et al.*, 1997. Nova travessia rodoviária sobre o Tejo em Lisboa. Monitorização da qualidade dos sedimentos de fundo. IPIMAR Technical Report, December, 62 pp.

Figuères, G., Martin, J.M., Meybeck, M., Seyler, P., 1985. A comparative study of mercury contamination in the Tagus Estuary (Portugal) and major French Estuaries (Gironde, Loire, Rhône). *Est. Coast. Shelf Sci.* 20, 183–203.

Fitzgerald, W.F., Mason, R.P., Vandal, G.M., Dulac, F., 1994. Air-water cycling of mercury in lakes. In: *Mercury Pollution: Integration and Synthesis*. Carl Watras and W. Hunckabee (Eds.), Lewis Publishers, California, 726 pp.

Fleming, E.J., Mack, E.E., Green, P.G., Nelson, D.C., 2006. Mercury methylation from unexpected sources: molybdate-inhibited freshwater sediments and an iron-reducing bacterium. *Appl. Environ. Microbiol.* 72, 457–464.

Forstner, U., Wittmann, G.T.W., 1981. *Metal pollution in aquatic environment*. Springer-Verlag, Berlin, 486 pp.

Fortunato, A.B., Baptista, A.M., Luettich Jr., R.A., 1997. A three-dimensional model of tidal currents in the mouth of the Tagus estuary. *Cont Shelf Res.* 17, Issue 14, 1689-1714.

Froelich, P.M., Klinkhammer, G.P., Bender, M.L., Lurdtko, N.A., Heath, G.R., Cullen, D., Dauphin, P., Hammond, D., Hartman, B., Maynard, V., 1979. Early oxidation of organic matter in pelagic sediments of the eastern equatorial Atlantic: suboxic diagenesis. *Geochim. Cosmochim. Acta* 43, 1075–1090.

Gagnon, C., Pelletier, E., Mucci, A., Fitzgerald, W.F., 1996. Diagenetic behavior of methylmercury in organic-rich coastal sediments. *Limnol. Oceanogr.* 41 (3), 428–434.

Gagnon, C., Pelletier, E., Mucci, A., 1997. Behaviour of anthropogenic mercury in coastal marine sediments. *Mar Chem.* 59, 159 - 176.

Gailer, J., 2007. Arsenic-selenium and mercury-selenium bonds in biology. *Coordin Chem Rev.* 251, 234-254.

Gambrell, P.R., 1994. Trace and Toxic Metals in Wetlands: A Review. *J. Environ Qual.* 23, 883-891.

Gilmour, C., Henry, E.A., 1991. Mercury methylation in aquatic systems affected by acid deposition. *Environ. Pollut.* 71, 131 – 169.

Gilmour, C.C., Henry, E.A., Mitchell, R., 1992. Sulfate simulation of mercury methylation in freshwater sediments. *Environ Sci Technol* 26, 2281–7.



Gilmour, C.C., Riedel, G.S., Ederington, M.C., Bell, J.T., Benoit, J.M., Gill, G., Stordal, M.C., 1998. Methylmercury concentrations and production rates across a trophic gradient in the northern Everglades. *Biogeochemistry* 40, 327–345.

Gobeil, C., Cossa, D., 1993. Mercury in sediments and sediment pore waters in the Laurentian Trough. *Can. J. Fish Aquat. Sci.* 50, 1794 – 1800.

Gonçalves, M.L.S., 1996. Métodos Experimentais para Análise de Soluções – Análise Quantitativa. Fundação Calouste Gulbenkian, Lisboa, 787 pp.

Goulet, R.R., Holmes, J., Page, B., Poissant, L., Siciliano, S.D., Lean, D.R.S., Wang, F., Amyot, M., Tessier, A., 2007. Mercury transformations and fluxes in sediments of a riverine wetland. *Geochim. Cosmochim. Ac.* 71, 3393-3406.

Hall, B., Bloom, N.S., Munthe, J., 1995. An experimental study of two potential methylation agents of mercury in the atmosphere: CH<sub>3</sub>I and DMS. *Water Air Soil Pollut* 80, 337– 41.

Hammerschmidt, C.R., Fitzgerald, W.F., 2004. Geochemical controls on the production and distribution of methylmercury in near-shore marine sediments. *Environ. Sci. Technol.* 38, 1487–1495.

Heyes, A., Miller, C., Mason, R.P., 2004. Mercury and methyl mercury in Hudson River sediment: impact of tidal resuspension on partitioning and methylation. *Mar Chem.* 90, 75-89.

Heyes, A., Mason, R.P., Kim, E.-H., Sunderland, E., 2006. Mercury methylation in estuaries: Insights from using measuring rates using stable mercury isotopes. *Mar Chem.* 102 (1-2), 134-147.

Hines, N.A., Brezonik, P.L., Engstrom, D.R., 2004. Sediment and pore water profiles and fluxes of mercury and methyl mercury in a small seepage lake in northern Minnesota. *Environ Sci Tech.* 38, 6610-6617.

Hintelmann, H., Harris, R., 2004. Application of multiple stable mercury isotopes to determine the adsorption and desorption dynamics of Hg(II) and MeHg to sediments. *Mar Chem.* 90, Issues 1-4, 165-173.

Holloway, J.M., Goldhaber, M.B., Scow, K.M., Drenovsky, R.E., 2009. Spatial and seasonal variations in mercury methylation and microbial community structure in a historic mercury mining area, Yolo County, California. *Chem Geo.* 267, Issues 1-2, 85-95.

Horvat, M., 1996. Mercury analysis and speciation in environmental samples. In: Regional and global mercury cycles: sources, fluxes and mass balances. Baeyens, W., Ebinghaus, R. and Vasiliev, O. (Eds.), Kluwer, Dordrecht, pp.1-31.

Horvat, M., 1999. Current status and future needs for biological and environmental reference materials certified for methylmercury compounds. *Chemosphere.* 39(7), 1167-1179.

IPIMAR, 2001. Caracterização química dos sedimentos do estuário do Guadiana, 35 pp.

IPIMAR, 2010. Caracterização química e ecológica dos estuários e zonas costeiras de Portugal. IPIMAR Reports, 325 pp.

Issaro, N., Abi-Ghanem, C., Bermond, A., 2009. Fractionation studies of mercury in soils and sediments: A review of the chemical reagents used for mercury extraction. *Analytica Chimica Acta* 631, Issue 1, 1-12.

Jackson, T.A., 1998. Mercury in aquatic ecosystems. In: Langston, W.J. and Bebianno, M.J. (Eds). Metal metabolism in the aquatic environment. Chapman and Hall, Lda Publishers, UK, pp. 77-138.

Jonnalagadda, S. B. and Rao, P. P., 1993. Toxicity, bioavailability and metal speciation. *Comparative Biochemistry and Physiology Part C: Pharmacology, Toxicology and Endocrinology* 106, Issue 3, 585-595.

Kehrig, H. A., Palermo, E. F. A., Seixas, T. G., Branco, C. W. C., Moreira, I. and Malm O., 2009. Trophic transfer of methylmercury and trace elements by tropical estuarine seston and plankton. *Estuarine, Coastal and Shelf Science* 85, Issue 1, 36-44.

Kim, E.-H., Mason, R.P., Porter, E.T., Soulen, H.L., 2004. The effect of resuspension on the fate of total mercury and methyl mercury in a shallow estuarine ecosystem: a mesocosm study. *Mar Chem* 86, 121-137.

- Kim, E.-H., Mason, R.P., Porter, E.T., Soulen, H.L., 2006. The impact of resuspension on sediment mercury dynamics, and methyl mercury production and fate: a mesocosm study. *Mar Chem* 102, 300-315.
- King, J. K., Saunders, F. M., Lee, R. F., Jahnke, R. A., 1999. Coupling mercury methylation rates to sulfate reduction rates in marine sediments. *Environ. Toxicol. Chem.* 18, 1362–1369.
- King, J.K., Kostka, J.E., Frischer, M.E., Saunders, F.M., 2000. Sulfate-reducing bacteria methylate mercury at variable rates in pure culture and marine sediments. *Appl Environ Microbiol.* 66, 2430–7.
- King, J.K., Kostka, J.E., Frischer, M.E., Saunders, F.M., Jahnke, R.A., 2001. A quantitative relationship that demonstrates mercury methylation rates in marine sediments are based on the community composition and activity of sulfate-reducing bacteria. *Environ Sci Technol* 35, 2491–6.
- Kwokal, Z., Franciskovic-Biliniski, S., Bilinski, H., Branica, M., 2002. A comparison of anthropogenic mercury pollution in Kastela Bay (Croatia) with pristine estuaries in Ore (Sweden) and Krka (Croatia). *Mar Pollut Bull* 44, 1152–7.
- Krishnamurthy S., 1992. Biomethylation and environmental transport of metals. *Chem Environ.* 69, 347– 50.
- Lamborg, C.H., Hoyer, M.E., Keeler, G.J., Olmez, I., Huang, X., 1994. Particulate-phase mercury in the atmosphere: collection/analysis method development and applications. In: *Mercury Pollution: Integration and Synthesis*. Carl Watras and W. Hunckabee (Eds.), Lewis Publishers, California, 726 pp.
- Laurier, F.J.G., Cossa, D., Gonzalez, J.L., Breviere, E., Sarazin, G., 2003. Mercury transformations and exchanges in a high turbidity estuary: the role of organic matter and amorphous oxyhydroxides. *Geochimica et Cosmochimica Acta* 67, 3329-3345.
- Leermakers, M., Meuleman, C., Baeyens, W., 1995. Mercury speciation in the Scheldt Estuary. *Water, Air, and Soil Pollution* 80, 641-652.
- Lesven, L., Lourino-Cabana, B., Billon, G., Recourt, P., Ouddane, B., Mikkelsen, O., Boughriet, A., 2010. On metal diagenesis in contaminated sediments of the Deûle river (northern France). *App Geochem.* 25, Issue 9, 1361-1373.

- Lépine, L., Chamberland, A., 1995. Field sampling and analytical intercomparison for mercury and methylmercury determination in natural water. *Water, Air, & Soil Pollution* 80, 1-4, 1247-1256.
- Louis, VLS, Rudd, JWM, Kelly, CA, Beaty, KG, Flett, RJ, Roulet, NT., 1996. Production and loss of methylmercury and loss of total mercury from boreal forest catchments containing different types of wetlands. *Environ Sci Technol.* 30, 2719– 29.
- Loring, D. H., 1991. Normalization Of Heavy-Metal Data From Estuarine And Coastal Sediments. *ICES Journal of Marine Science* 48, 101-115.
- Lu, X., Jaffe, R., 2001. Interaction between Hg(II) and natural dissolved organic matter: a fluorescence spectroscopy based study. *Water Research* 35, Issue 7, 1793-1803.
- Mason, R. P., Fitzgerald, W. F., Hurley, J., Hanson, A. K., Donaghay, P. L., Sieburth, J. M., 1993. Mercury biogeochemical cycling in a stratified estuary. *Limnol. Oceanogr.* 38, 1227–1241.
- Mason, R.P., Morel, F.M.M., Hermond, H.F., 1995. The role of microorganisms in elemental mercury formation in natural waters. *Water, Air, Soil Pollut.* 80, 775 – 787.
- Mason, R.P., Lawrence, A.L., 1999. Concentration distribution and bioavailability of mercury and methylmercury in sediments of Baltimore Harbour and Chesapeake Bay, Maryland, USA. *Environ. Toxicol. Chem.* 18 (11), 2438–2447.
- Mason, R. P., Lawson, N. M., Lawrence, A. L., Leaner, J. J., Lee, J. G., Sheu, G.-R., 1999. Mercury in the Chesapeake Bay. *Mar. Chem.* 65, 77–96.
- Mason, R.P., Benoit, J.M., 2003. Organomercury compounds in the environment. In: Graig, P. (Ed.), *Organometallic Compounds in the Environment*. Wiley, West Sussex, UK, pp. 57–99.
- Mason, R.P., Kim, E-H., Cornwell, J., Heyes, D., 2006. An examination of the factors influencing the flux of mercury, methylmercury and other constituents from estuarine sediment. *Mar Chem.* 102, Issues 1-2, 96-110.

Merritt, K.A., Amirbahman, A., 2009. Mercury methylation dynamics in estuarine and coastal marine environments, a critical review. *Earth-Science Reviews* 96, 54-66.

Mikac, N., Niessen, S., Ouddane, B., Wartel, M., 1999. Speciation of mercury in sediments of the Seine estuary (France). *Appl Organomet Chem* 13, 715-25.

Miller, C.L., 2006. The role of organic matter in the dissolved phase speciation and solid phase partitioning of mercury. PhD thesis. University of Maryland, College Park, MD, USA.

Morel, F.M.M., Kraepiel, A.M.L., Amyot, M. 1998. The chemical cycle and bioaccumulation of mercury. *Annu Rev Ecol Syst.* 29, 543-566.

Monterroso, P., Abreu, S. N., Pereira, E., Vale, C., Duarte, A. C., 2003. Estimation of Cu, Cd and Hg transported by plankton from a contaminated area (Ria de Aveiro). *Acta Oecologica* 24, Supplement 1, S351-S357.

Munthe, J., Hultberg, H., Iverfeldt, A., 1995. Mechanism of deposition of methylmercury and mercury to coniferous forests. *Water Air Soil Pollut.* 80, 363-71.

Muresan, B., Cossa, D., Jezequel, D., Prevot, F., Kerbellec, S., 2007. The biogeochemistry of mercury at the sediment-water interface in the Thau lagoon. 1. Partition and speciation. *Estuar Coast Shelf Sci.* 72, 472-484.

NOAA, 1996. Contaminants in aquatic habitats at hazardous waste sites: Mercury. Technical Memorandum NOS ORCA 100, 64 pp.

Oh, S., Kim, M-K., Yi, S-M., Zoh, K-D., 2010. Distributions of total mercury and methylmercury in surface sediments and fishes in Lake Shihwa, Korea. *Sci Tot Environ.* 408, Issue 5, 1059-1068.

Ouddane, B., Mikac, N., Cundy, A.B., Quillet, L., Fischer, J.C., 2008. A comparative study of mercury distribution and methylation in mudflats from two macrotidal estuaries: the Seine (France) and the Medway (United Kingdom). *Appl Geochem.* 23, 618-31.

Pato, P., Lopes, C., Válega, M., Lillebø, A.I., Dias, J.M., Pereira, E., Duarte, A.C., 2008. Mercury fluxes between an impacted coastal lagoon and the Atlantic Ocean. *Estuar Coast Shelf S.* 76, 4, 787-796.

Pato, P., Otero, M., Válega, M., Lopes, C.B., Pereira, M.E., Duarte, A.C., 2010. Mercury partition in the interface between a contaminated lagoon and the ocean: The role of particulate load and composition. *Mar Poll Bull.* 60, Issue 10, 1658-1666.

Pereira, M.E.C., 1996. Distribuição, reactividade e transporte do mercúrio na Ria de Aveiro. PhD Thesis. Chemistry Dept., University of Aveiro. Aveiro, Portugal.

Pereira, M.E., Duarte, A.C., Millward, G.E., Vale, C., Abreu, S.N. 1998. Tidal export of particulate mercury from the most contaminated area of Aveiro's lagoon, Portugal. *Sci Total Environ.* 213, 157-163.

Poissant, L., Zhang, H. H., Canário, J., Constant, P., 2008. Critical review of mercury fates and contamination in the arctic tundra ecosystem. *Sci Tot Environ.* 400, Issues 1-3, 1 173-211.

Postma, D., Jakobsen, R., 1996. Redox zonation: Equilibrium constraints on the Fe(III)/SO<sub>4</sub><sup>-</sup> reduction interface. *Geochimica et Cosmochimica Acta* 60, Issue 17, 3169-3175.

Raimundo, J., Vale, C., Canário, J., Branco, V. and Moura, I., 2010. Relations between mercury, methyl-mercury and selenium in tissues of *Octopus vulgaris* from the Portuguese Coast. *Environ Poll* 158, 2094 – 2100.

Ramalhosa, E., 2002. Mercúrio na Ria de Aveiro: associações, reactividade e especiação. PhD thesis. University of Aveiro, Portugal.

Rantala, R.T.T., Loring, D.H., 1975. Multi-element analysis of silicate rocks and marine sediments by atomic absorption spectrophotometry. *At. Absorp. Newsl.* 14, 117–120.

Ravichadran, M., 2004. Interactions between mercury and dissolved organic matter—a review. *Chemosphere* 55, 319–331.

Schafer, J., Blanc, G., Cossa, D., Audry, S., Bossy, C., 2006. Mercury in the Lot-Garonne river system (France): sources, fluxes and anthropogenic component. *Appl Geochem.* 21, 515–27.

Schafer, J., Castelle, S., Blanc, G., Dabrin, A., Masson, M., Lanceleur, L., Bossy, C., 2010. Mercury methylation in the sediments of a macrotidal estuary (Gironde Estuary, south-west France). *Est Coast Shelf Sci.* 90, Issue 2, 80-92.

Spencer, K.L., MacLeod, C.L., Tuckett, A., Johnson, S.M., 2006. Source and distribution of trace metals in the Medway and Swale estuaries, Kent, UK. *Mar Pollut Bull.* 52, 226–30.

Stoichev, T., Amouroux, D., Wasserman, J.C., Point, D., De Diego, A., Bareille, G., *et al.*, 2004. Dynamics of mercury species in surface sediments of a macrotidal estuarine–coastal system (Adour River, Bay of Biscay). *Estuar Coast Shelf Sci.* 59, 511–21.

Strobal, M.C., Gill, G.A., Wen, L-S., Santschi, P.H., 1996. Mercury phase speciation in the surface waters of three Texas estuaries: importance of the colloidal forms. *Limnol. Oceanogr.* 41, 52 – 61.

Silva, S., Ré, A., Pestana, P., Rodrigues, A., Quintino, V., 2004. Sediment disturbance off the Tagus Estuary, Western Portugal: chronic contamination, sewage outfall operation and runoff events. *Mar Poll Bull.* 49, Issue 3, 154-162.

Stumm, W., Morgan, J.J., 1996. *Aquatic Chemistry*. John Wiley & Sons, Inc., New York.

Sunderland, E.M., Gobas, F.A.P.C., Branfireun, B.A., Heyes, A., 2006. Environmental controls on the speciation and distribution of mercury in coastal sediments. *Mar Chem.* 102, 111– 123.

Sundby, B., Silverberg, N., & Chesselet, R., 1981. Pathways of manganese in an open estuarine system. *Geochimica Cosmochimica Acta* 45(3), 293–307.

Tomiyasu, T., Matsuyama, A., Eguchi, T., Fuchigami, Y., Oki, K., Horvat, M., Rajar, R., Akagi, H., 2006. Spatial variations of mercury in sediment of Minamata Bay, Japan. *Sci Tot Environ.* 368, Issue 1, 283-290.

Tomiyasu, T., Matsuyama, A., Eguchi, T., Marumoto, K., Oki, K., Akagi, H., 2008. Speciation of mercury in water at the bottom of Minamata Bay, Japan. *Mar. Chem.* 112, 102–106.

Turner, A., Millward, G.E., Le Roux, S.M., 2004. Significance of oxides and particulate organic matter in controlling trace metal partitioning in a contaminated estuary. *Mar Chem.* 88, 179-192.

Ullrich, S.M., Tanton, T.W., Abdrashitova, S.A., 2001. Mercury in the aquatic environment: a review of factors affecting methylation. *Crit Rev Env Sci Tec.* 31(3), 241-293.

Vale, C., Caetano, M., Raimundo J. (2003). Incorporation of trace elements on iron-rich concretions around plant roots of Tagus estuary salt marshes (Portugal). *J. Soils Sed.* 3(3), 208-212.

Válega, M., 2003. Efeito das plantas na acumulação de mercúrio em sedimentos de sapais. MSc. Thesis. Chemistry Dept., University of Aveiro, Portugal.

Válega, M., Lillebø, A.I., Pereira, M.E., Corns, W.T., Stockwell, P.B., Duarte, A.C., Pardal, M.A., 2008a. Assessment of methylmercury production in a temperate salt marsh (Ria de Aveiro Lagoon, Portugal). *Mar Poll Bull.* 56, Issue 1, 153-158.

Válega, M., Lillebø, A.I., Pereira, M.E., Caçador, I., Duarte, A.C., Pardal, M.A., 2008b. Mercury in salt marshes ecosystems: *Halimione portulacoides* as biomonitor. *Chemosphere* 73, Issue 8, 1224-1229.

Válega, M., Lillebø, A.I., Pereira, M.E., Duarte, A.C., Pardal, M.A., 2008c. Long-term effects of mercury in a salt marsh: Hysteresis in the distribution of vegetation following recovery from contamination. *Chemosphere* 71, Issue 4, 765-772.

Wang, S., Jia, Y., Wang, S., Wang, X., Wang, H., Zhao, Z., Liu, B., 2009. Total mercury and monomethylmercury in water, sediments, and hydrophytes from the rivers, estuary, and bay along the Bohai Sea coast, northeastern China. *App Geochem.* 24, Issue 9, 1702-1711.

Weber, JH., 1993. Review of possible paths for abiotic methylation of mercury in the aquatic environment. *Chemosphere* 26, 2063-77.

Wiener, J.G., Krabbenhoft, D.P., Heinza, G.H., Scheuhammer, A.M., 2003. Ecotoxicology of mercury. In: Hoffman, D.J. et al. (Eds). *Handbook of Ecotoxicology*. CRC Press, Boca Raton-Florida, pp. 409-463.

Zhong, H., Wang, W-X., 2009. The role of sorption and bacteria in mercury partitioning and bioavailability in artificial sediments. *Environ Poll.* 157, Issue 3, 981-986.